This is to certify that the

dissertation entitled

CIRCADIAN MODULATION OF BRAIN AREAS THAT CONTROL THE SLEEP-WAKE CYCLE IN DIURNAL AND NOCTURNAL ANIMALS

presented by

Colleen M. Novak

has been accepted towards fulfillment
of the requirements for
Ph.D. degree in Psychology/Neuroscience

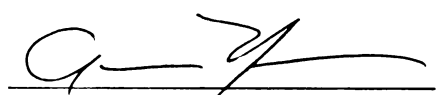

Major professor

Date 8/13/99

CIRCADIAN MODULATION OF BRAIN AREAS THAT CONTROL THE SLEEP-WAKE CYCLE IN DIURNAL AND NOCTURNAL RODENTS

By

Colleen M. Novak

A DISSERTATION

Submitted to
Michigan State University
In partial fulfillment of the requirements
For the degree of

DOCTOR OF PHILOSOPHY

Department of Psychology and Neuroscience Program

1999

ABSTRACT

CIRCADIAN MODULATION OF BRAIN AREAS THAT CONTROL THE SLEEP-WAKE CYCLE IN DIURNAL AND NOCTURNAL RODENTS

By

Colleen M. Novak

The sleep wake cycle follows a circadian pattern that depends upon a signal from the suprachiasmatic nucleus (SCN), the primary circadian pacemaker in mammals, regardless of whether the animal is active during the day (diurnal) or night (nocturnal). The work presented in this dissertation investigated how the SCN differentially modulates brain areas known to be important in the control of sleep or wakefulness in nocturnal and diurnal animals, using the immediate-early gene product Fos as an index of neuronal activity. The daily patterns of Fos expression in these brain regions were monitored in the nocturnal murid rodent, *Rattus norvegicus,* and in a diurnal murid rodent, *Arvicanthis niloticus*.

In both the diurnal and nocturnal species, Fos expression in the ventrolateral preoptic area (VLPO) showed a significant daily rhythm that peaked during the inactive phase of the cycle, when sleep episodes are frequent. The VLPO was found to receive only a minor

direct input from the SCN. Therefore, the circadian regulation of VLPO neural activity is likely to involve multisynaptic pathways or the effects of humoral outputs of SCN neurons.

Rhythms of Fos activity were also detected in the paraventricular thalamic nucleus (PVT) and in the centromedial thalamic nucleus (CMT) in the rat. Further, Fos expression in the PVT and CMT was negatively correlated with Fos expression in the VLPO. In the PVT of both species, significant peaks of neural activity were associated with times of peak behavioral activity. In both species, the PVT receives projections from the SCN, some of which are vasopressinergic. Therefore, circadian regulation of PVT neural activity is likely to be mediated by direct inputs from the SCN. In *A. niloticus*, but not in the rat, neuronal activity in the histaminergic cells of the ventral tuberomammillary nucleus was associated with behavioral activity and wakefulness at dawn and dusk. This species difference suggests that the support of wakefulness may involve different neural systems in nocturnal and diurnal mammals.

In summary, the interactions between the SCN and regions of the brain that control vigilance and sleep differ between species and may be responsible for the emergence of a diurnal or nocturnal pattern of behavior.

This dissertation is dedicated to my family for their unconditional love and understanding, and to my friends for their support over the last few years.

ACKNOWLEDGEMENTS

I wish to express my gratitude to the members of my committee, Drs. Laura Smale, Juli Wade, Lynwood Clemens, and Tony Nunez, for their guidance and suggestions. Special appreciation goes to Tony not only for the laboratory resources, but for his patience and direction, as well as to Laura for the extra time and effort she expended for me, and especially for access to the *Arvicanthis*.

Many graduate students and postdoctoral scientists also lent technical knowledge and support that made many of these projects possible. Thanks to Megan Mahoney, Terri McElhinny, Julie Blanchong, Abel Bult, Alan Elliott, David Parfitt, and especially to Kris Krajnak for patiently training me. I also appreciate the friendship and support of Erin O'Bryant, Russ Romeo, Heather Richardson.

Many undergraduate assistants were involved in these projects, including Sandra Rose, Jen Mirich, Todd Adams, and Lesz Pathak. Special thanks go to Julie Harris for her help in many of these projects. Thanks also for the valuable technical assistance of David McFarland. Scott Stevens and Constance Montville are also appreciated.

These studies were supported by NIMH MH11232 to C.M.N., NSF IBN9514374 to A.A.N., and NIMH 2R01.MH53433-04 to L.S.

TABLE OF CONTENTS

LIST OF TABLES

LIST OF FIGURES

KEY TO ABBREVIATIONS

BRAIN REGIONS:

3V	third ventricle
AHA	anterior hypothalamic area
Arc	arcuate nucleus
BF	basal forebrain
BST	bed nucleus of the stria terminalis
ceA	central amygdala
CMT	centromedial thalamic nucleus
DMN	dorsomedial hypothalamic nucleus
DTM	dorsal tuberomammillary nucleus
f	fornix
HDB	nucleus of the horizontal limb of the diagonal band
IGL	intergeniculate leaflet
LC	locus coeruleus
LD	laterodorsal thalamic nucleus
LH	lateral hypothalamic nucleus
LPO	lateral preoptic area
LS	lateral septum
meA	medial amygdala
MnPO	median preoptic nucleus
MPO	medial preoptic area
mPON	medial preoptic nucleus
MRF	midbrain reticular formation
mt	mammillothalamic tract
NAC	nucleus accumbens
oc	optic chiasm
ot	optic tract
PAG	periaqueductal gray
PeF	perifornical area
PeV	periventricular hypothalamic nucleus
PH	posterior hypothalamus
PLH	posterior lateral hypothalamus
PMN	premammillary nucleus
POA	preoptic area
PO/AH	preoptic area/anterior hyothalamus
PVN	paraventricular hypothalamic nucleus

PVT	paraventricular thalamic nucleus
Rt	reticular thalamic nucleus
SCN	suprachiasmatic nucleus
SCNdm	dorsomedial subdivision of the suprachiasmatic nucleus
SCNvl	ventrolateral subdivision of the suprachiasmatic nucleus
SON	supraoptic nucleus of the hypothalamus
sPVHz	sub paraventricular hypothalamic zone
SUM	supramammillary nucleus
TMN	tuberomammillary nucleus
TC	tuber cinerum
VLPO	ventrolateral preoptic area
VMH	ventromedial hypothalamic nucleus
VTA	ventral tegmental area
VTM	ventral tuberomammillary nucleus

NEUROTRANSMITTERS, ENZYMES, METHODS:

ABC	avidin biotin complex
AVP	arginine vasopressin
CSF	cerebrospinal fluid
CT	circadian time
CTβ	cholera toxin, beta subunit
DAB	3, 3'- diaminobenzidine
DAB-Ni	DAB with nickel intensification
DMSO	dimethyl sulfoxide
EEG	electroencephalogram
GABA	gamma amino buteric acid
GAL	galanin
GAD	glutamic acid decarboxylase
GRP	gastrin releasing peptide
ICC	immunocytochemistry
i.c.v.	introcerebroventricular
i.p.	intraperitoneal
L:D	light:dark
MUA	mutiple unit activity
NGS	normal goat serum
NHS	normal horse serum
PBS	phosphate buffered saline

PLP	4% paraformaldehyde with 0.2% sodium periodate and 1.3% lysine
REM	rapid eye movement sleep
SEM	standard error of the mean
SWS	slow wave sleep
tx	Triton X-100, 0.3%
VIP	vasoactive intestinal polypeptide
ZT	zeitgeber time

INTRODUCTION

Circadian and Homeostatic Control of Sleep.

Most organisms show daily rhythms in physiology and behavior. These rhythms are endogenous, and environmental cues regulate the phase and period of the rhythms (Klein *et al.*, 1991). The suprachiasmatic nucleus (SCN) is the principal generator of these circadian rhythms in mammals, as well as in many non-mammalian species (Klein *et al.*, 1991). Although the SCN has been intensely studied (Klein *et al.*, 1991), little is known about how the SCN affects specific brain regions to produce hormonal and behavioral rhythms. The sleep-wake cycle is a salient behavioral rhythm controlled by the circadian clock of the SCN. Thus, the activity of brain areas that control the sleep-wake cycle are likely to be modulated by the SCN.

Sleep and arousal are not unitary (single, inseparable) phenomena, and many brain areas and pathways are important in the coordination of the sleep/wake cycle. One group of cells important for the induction of sleep has been localized in the basal forebrain (BF) and preoptic area/anterior hypothalamus (PO/AH). Large lesions of the preoptic area (POA) in the cat cause long-term reductions in sleep with only partial recovery over time (Lucas and Sterman, 1975; McGinty and Sterman, 1968), indicating that this

brain region is important in sleep induction. The loss of sleep is accompanied by increased wakefulness, not increased drowsiness (Lucas and Sterman, 1975). Chemical lesions of the BF produce similar deficits (Szymusiak and McGinty, 1986a). In rats, lesions of the POA also cause suppression of slow wave sleep (SWS), and this decrease in sleep is potentiated by low ambient temperatures (Szymusiak and Satinoff, 1984). Consistent with results of lesion studies, bilateral stimulation of the PO/AH induces sleep (Sterman and Clemente, 1962b), and stimulation of the BF results in EEG synchrony (Sterman and Clemente, 1962a), a hallmark of SWS. Warming of the BF also hastens sleep onset (Krilowicz *et al.*, 1994; Roberts and Robinson, 1969).

The results of electrophysiological studies also reveal the importance of neural activity in the POA/BF in sleep control. In the POA, activity of 84% of single cells sampled displayed increased firing during sleep (Kaitin, 1984), and a subset of BF neurons displayed maximal firing in sleep as well as in the transition into SWS (Szymusiak and McGinty, 1986b). Multiple unit activity (MUA) in the POA also increased during SWS (Ogawa and Kawamura, 1988). Preoptic cells show changes in activity correlated with the transition from EEG desynchrony to the synchronous EEG pattern typical of SWS (Mallick *et al.*, 1983). Following an arousing stimulus that induced

cortical desynchrony, many of these neurons decreased their activity (Nuñez, 1996). Taken together, these data indicate that increased neuronal activity in the POA/BF is closely associated with both electrophysiological (EEG) and behavioral indicators of sleep.

Whereas cell populations in the POA/BF are involved in sleep onset and maintenance, brain structures in the posterior lateral hypothalamus are critical for waking and vigilance (Kinomura *et al.*, 1996; Lin *et al.*, 1989). Lesions of the posterior lateral hypothalamus (PLH) in rats leads to the lateral hypothalamic syndrome, with symptoms that include decreased arousal and vigilance and with increased somnolence (Danguir and Nicolaidis, 1980; Shoham and Teitelbaum, 1982; Szymusiak *et al.*, 1989). It has been suggested that the lateral hypothalamus influences activity in the brainstem and midbrain reticular formation (Paré *et al.*, 1989; Steriade *et al.*, 1982b), and damage to this circuit results in somnolence. However, lesions of the lateral or posterior lateral hypothalamus that produce the lateral hypothalamic syndrome cover a large area of the brain and affect behaviors other than sleep (Danguir and Nicolaidis, 1980; Kolb *et al.*, 1979). Therefore, it is more useful to describe this area of the hypothalamus in terms of specific connections and pathways. More restricted lesions of the posterior portion of the lateral hypothalamus result in behavioral somnolence and EEG synchrony

(Szymusiak *et al.*, 1989), and cells in the posterior lateral hypothalamus have been associated with behavioral activation (Krilowicz *et al.*, 1994). Specifically, histaminergic cells in the tuberomammillary nuclei (TMN) in the posterior hypothalamus, which project throughout the brain including the cerebral cortex, are critical for behavioral arousal in rats (Kalivas, 1982; Kiyono *et al.*, 1985; Monti, 1993; Monti *et al.*, 1988; Panula *et al.*, 1989). It is therefore important to determine the relationship between the TMN and the POA/BF since these areas appear to play opposing roles in the control of sleep and wakefulness. Tract tracing studies have shown that GABAergic cells in the POA project to the PLH in rats (Gritti *et al.*, 1994) and electron microscopy has revealed that GABAergic terminals contact TMN neurons (Ericson *et al.*, 1991b). Microinjections of muscimol, a GABA agonist, into the posterior hypothalamus induce sleep, whether the POA is damaged or intact (Lin *et al.*, 1989; Sallanon *et al.*, 1989), and warming of the POA decreases firing in the PLH and induces sleep (Krilowicz *et al.*, 1994). Therefore, the forebrain areas important in the sleep wake cycle can influence sleep by affecting neurons in the PLH, and specifically histaminergic neurons in the TMN. Activation of POA/BF sleep areas induces the onset of SWS at least partially by inhibiting the PLH and

TMN via GABAergic projections, thereby decreasing cortical and behavioral activation (Lin *et al.*, 1989; Szymusiak *et al.*, 1989).

Specific cell groups within the preoptic area may modulate sleep onset and maintenance. In the rat ventrolateral preoptic area (VLPO), there is a cluster of cells that shows increased activity during sleep, as evidenced by greater numbers of cells immunoreactive for Fos (Fos+), the product of the early-immediate gene c-*fos* (Sherin *et al.*, 1996). This increase in VLPO Fos expression is associated with recent sleep experience rather than time of day; after sleep deprivation uncouples the display of sleep states from the circadian cycle, Fos expression in the VLPO still increases during sleep. This supports the claim that VLPO cells are involved in regulating homeostatic aspects of sleep (Sherin *et al.*, 1998; Sherin *et al.*, 1996). Recent electrophysiological experiments have shown that increases in firing rate of sleep-active VLPO cells occurs before changes in EEG indicated sleep onset (i.e., EEG delta activity) (McGinty *et al.*, 1997). Tract tracing experiments show that VLPO cells project to the TMN, locus coeruleus (LC), and the raphe nuclei (Sherin *et al.*, 1998). The VLPO may be one source of inhibitory inputs to the histaminergic neurons of the TMN that regulate vigilance, as well as to other regions important in inducing arousal and wakefulness.

The thalamus is also an important component of circuits that control sleep and vigilance. The intralaminar thalamus relays information from the midbrain reticular formation (MRF) to the cerebral cortex, a pathway important in the regulation of attention and vigilance (Steriade and Glenn, 1982) and EEG desynchronization (Kinomura *et al.*, 1996). The intralaminar and midline thalamic nuclei, such as the centromedial thalamic nucleus (CMT) and the paraventricular thalamic nucleus (PVT), respectively, also play a role in the sleep-wake cycle. In rats, the PVT shows more Fos activity (greater number of Fos+ cells) in the dark (active) phase of the cycle, after the rats had spent at least 70% of their last 2 hours awake (Peng *et al.*, 1995). In humans, the intralaminar nuclei have been shown to be active during states of vigilance and attention (Kinomura *et al.*, 1996). In both the PVT and CMT, neural activation is seen while animals engage in functions that are incompatible with sleep. Afferent and efferent projections of these thalamic nuclei further support the claim that these nuclei modulate the daily activity cycle. The PVT has reciprocal connections with the SCN (Moga *et al.*, 1995; Watts and Swanson, 1987; Watts *et al.*, 1987), and receives input from both the intergeniculate leaflet (IGL) as well as the retina (Moga *et al.*, 1995). Both the retina and IGL provide input to the SCN important for entrainment of circadian rhythms (Johnson *et al.*,

1988a; Rusak *et al.*, 1989). The PVT relays information to regions of the basal forebrain involved in motivation and reward, and may provide the SCN with feedback about the general arousal and motivational state of the organism. Projections from the CMT terminate in the frontal cortex (Berendse and Groenewegen, 1991) and serve to modulate general cortical excitability and hence attention. These areas are likely to play important roles in the expression of the sleep-wake cycle.

The need for sleep is regulated by homeostatic mechanisms; for example, sleep deprivation results in sleep rebound, which is the enhancement of sleep seen after deprivation (Trachsel *et al.*, 1986). In addition to this homeostatic regulation, circadian mechanisms have a profound influence on sleep timing, even after sleep deprivation (Mistlberger *et al.*, 1983). Various mathematical models have been proposed to explain and predict circadian/homeostatic interactions in the control of sleep. A model proposed by Borbély *et al.* (1979) aims to explain how the timing of sleep onset and termination are modulated by circadian influences on homeostatic mechanisms: the circadian pacemaker modulates the threshold to fall asleep throughout the day (for example, lowering the threshold for sleep during the night in humans). Other models (Strogatz, 1987) address how the desire and ability to initiate sleep in humans is

influenced by two circadian oscillators, one controlling the sleep wake cycle *per se*, and the other controlling the rhythm in body temperature. Although these models combine circadian and homeostatic factors to make accurate predictions about parameters of the sleep cycle, they provide no information about the relevant neural circuits. Research on the brain circuitry involved in circadian/homeostatic interactions is needed for the development of functional anatomical models of sleep cycle regulation.

A necessary component of any neuroanatomical model of circadian sleep regulation is the SCN, which serves as the generator of the circadian signals. Lesions of the rat SCN eliminate the circadian rhythm of sleep without affecting the homeostatic aspects of sleep (Mistlberger *et al.*, 1983; Tobler *et al.*, 1983). Following SCN lesions in rats, the animals show sleep rebounds after sleep deprivation (Tobler *et al.*, 1983), and the ultradian sleep rhythm (cycle of sleep stages) remains intact (Mistlberger *et al*, 1983). One difference between animals with SCN lesions and intact animals lies in the timing of sleep recovery after sleep deprivation: circadian influences on sleep recovery are evident in the intact animals, but area absent after SCN lesions (Mistlberger *et al.*, 1983). After sleep deprivation in intact rats, an episode of SWS rebound that begins in the light phase occurs in a single stage, whereas recovery that begins

in the dark phase occurs in two stages. The two-stage pattern seen in the dark seems to be due to the fact that under those conditions, the rats initiate the sleep rebound episode at a time coincident with their active phase. As a result of this coincidence, the sleep episode in the dark is relatively short. Later, the animals initiate a second rebound sleep episode in the light phase (Borbély and Neuhaus, 1979). A circadian modulation of rebound sleep is not seen in SCN-lesioned rats (Mistlberger *et al.*, 1983). Together, these data imply that a circadian signal inhibiting sleep or promoting wakefulness is present during the dark phase in nocturnal animals.

The claim that the SCN is not directly involved in the homeostatic regulation of sleep is challenged by the results of a lesion experiment on squirrel monkeys, a diurnal primate (Edgar *et al.*, 1993). In that study, monkeys with SCN lesions showed a significant increase in total sleep time. The authors attributed this change to a deficit in "wakefulness initiation" after SCN lesions (Edgar *et al.*, 1993), suggesting that the SCN normally induces wakefulness or inhibits sleep in this species, and suggested that this homeostatic function of the SCN may be a feature of diurnal (day-active) species. However, it is possible that this effect of SCN lesions is unique to monkeys (or primates in general) and not related to diurnality *per se*, especially considering the highly consolidated sleep patterns of

primates when compared to rodents. Alternatively, the reduced wakefulness of monkeys with SCN lesions may be secondary to the reduction in general activity seen after damage to the anterior hypothalamic / SCN regions, which has been documented in other species (Brown and Nunez, 1986). Additional comparative research is needed to investigate the possible differences in the circadian regulation in diurnal and nocturnal mammals, as well as the possible influence of the SCN on sleep homeostasis.

Sleep and Circadian Rhythms in Diurnal and Nocturnal Mammals.

Although physiological and behavioral variables follow predictable circadian patterns, animals differ in how their daily activity relates to the light-dark cycle; namely, some animals are active during the dark phase (nocturnal), some during the light phase (diurnal), and still others during dawn and dusk (crepuscular). Little is known about the differences between neural structures controlling the circadian systems of diurnal and nocturnal species, and much of what we know about circadian physiology comes from studies using nocturnal rodents, with a few notable exceptions discussed below.

Light, phase shifts, and Fos expression in the SCN. One possible difference between rhythms in diurnal and nocturnal animals is their response to light. Exposure to light will shift the phase of a free-

running rhythm depending upon the circadian time (CT, where CT 12 is the onset of activity in nocturnal animals) at which the animal sees light; these data (the number of hours phase advanced or delayed) can be plotted to yield a phase-response curve. In nocturnal rodents, only light pulses during the subjective night (CT 12-24) phase shift the animals' rhythms (Klein *et al.*, 1991). However, in one species of diurnal rodent, the *Octodon degus*, light pulses at CT 4 induce phase shifts in the activity cycle (Krajnak *et al.*, 1997). Therefore, light pulses a the same time relative to peak SCN activity have different phase shifting effects in rats and degus. These data imply that species differences in daily rhythms may be partially due to differential responsiveness of the SCN to light.

In nocturnal rodents, light pulses presented at times when phase shifts are induced also result in increased Fos expression in the SCN (Klein *et al.*, 1991). However, in the diurnal chipmunk, light pulses presented in both the subjective day and the subjective night induce Fos expression in the SCN (Abe *et al.*, 1995). Unlike other rodents, light pulses failed to induce noticeable phase shifts in chipmunks, regardless of the phase of the rhythms at which they were presented. Thus, the effects of light on the SCN and behavioral rhythms may be different between diurnal and nocturnal rodents. Moreover, the sensitivity of subregions within the SCN may also

differ between diurnal and nocturnal animals. In nocturnal rats and hamsters, light pulses induce Fos expression mostly in the ventrolateral portion of the SCN (SCNvl) (Klein *et al.*, 1991; Rea, 1992), but a measurable increase in Fos expression can be found throughout the rat SCN after light pulses at CT 16 (Krajnak *et al.*, 1997). In diurnal degus, it was found that light pulses at CT 16 increased Fos expression only in the SCNvl, and light pulses presented at CT 4 decreased the amount of Fos expression in the dorsomedial part of the SCN (SCNdm) (Krajnak *et al.*, 1997). Additional observations indicate that Fos activity induced by light is expressed in different peptidergic groups of the SCN of rats (Earnest and Olschowka, 1993; Earnest*et al.*, 1993; Romijn *et al.*, 1996) and the diurnal *Arvicanthis niloticus* (Katona and Smale, 1997). For example, Fos expression in vasopressin-immunoreactive (AVP+) cells in the SCN increases during the light phase in *A. niloticus* housed on a 12:12 light:dark cycle, whereas very few Fos+ AVP-containing cells are ever found in the SCN of rats (Rose *et al.*, 1999). Thus, differences in activity patterns throughout the day may be due in part to species differences in how light affects distinct neuronal populations of the SCN, which may in turn serve different functions in diurnal and nocturnal animals.

Similarities in SCN activity patterns across species. Although species differences exist in how light pulses affect the SCN of nocturnal and diurnal animals (see above), other observations have identified similarities in SCN function across species that show very different activity patterns with respect to the light/dark cycle. For example, taken as a whole, the SCN is metabolically more active during the light phase of the cycle in both nocturnal and diurnal mammals (Schwartz *et al.*, 1980; Schwartz *et al.*, 1983). Similarly, when animals are kept on a 12:12 light-dark cycle, the temporal pattern of Fos expression in the SCN in *Arvicanthis* is similar to that seen in the rat (Katona and Smale, 1997; Nunez *et al.*, in press). In both species, Fos immunoreactivity is high in the light and low during darkness (Nunez *et al.*, in press). Lastly, the SCN neuronal firing rates peak in the light phase regardless of the phase in which the animals are active (Kurumiya and Kawamura, 1988; Sato and Kawamura, 1984a). Given these common features, it is possible that differences in the phase of behavioral rhythms across species result from the differential responsiveness of SCN targets to clock signals received via axonal projections of the SCN (Watts and Swanson, 1987; Watts *et al.*, 1987), although the possibility remains that SCN targets respond to a diffusible product of SCN neurons (Lehman *et al.*, 1995;

Silver *et al.*, 1996). These questions have yet to be answered in a suitable diurnal animal model.

The presence of apparent common patterns of neural activity in the whole SCN of diurnal and nocturnal mammals does not rule out possible species differences within specific neuronal groups of the SCN. Neuronal subpopulations within the SCN may send different signals to target brain regions. In this manner, neurons controlling the rhythm of AVP concentration in the cerebrospinal fluid (CSF) and those controlling melatonin secretion, rhythms that are similar in diurnal and nocturnal animals (Illnerova, 1991; Reppert *et al.*, 1987), should have similar activity patterns in all species. Contrary to this, neurons controlling rhythms that differ between species should have different activity profiles across the light:dark cycle in different species.

Progress in the understanding of the workings of the circadian clock in diurnal mammals has been slowed by the lack of a convenient animal model. The *Arvicanthis niloticus* (unstriped Nile grass rat, see Figure 1), a diurnal rodent indigenous to Africa, represents an attractive animal model to investigate the workings of the circadian system in diurnal mammals and to study the differences and similarities between diurnal and nocturnal species (Katona and Smale, 1997; McElhinny *et al.*, 1997). Using *Arvicanthis* and *Rattus*

Figure 1. Photograph of the diurnal murid rodent, *Arvicanthis niloticus*, in captivity

norvegicus, the differences between nocturnal and diurnal animals' SCN, as well as differences in targets of the SCN, can be investigated.

The following experiments were designed to investigate how the activity patterns of selected regions of the brain differ between species with divergent activity and sleep patterns across the day-night cycle. The experiments in this dissertation were designed to test the following hypothesis: differences in daily sleep-wake patterns between species can be explained by differences in the temporal pattern of neural activity in specific brain regions important for sleep and wakefulness. Alternatively, these brain regions may function differently in diurnal and nocturnal animals. A testable prediction from this hypothesis is that brain regions that differentially support sleep and wakefulness in nocturnal animals should display rhythms in Fos expression consistent with the overt display of sleep and wakefulness of the species (see Experiments 1 and 5). Further, since the SCN imposes a circadian rhythm on sleep, brain regions important in sleep that display rhythms in Fos expression should receive direct neural input from the SCN (Experiments 2 and 6). Before testing these predictions, however, preliminary experiments had to be conducted to determine (1) the sleep/wake pattern in the diurnal animal used in these studies, the Nile grass rat, and (2) the precise location and characteristics of the

sleep-active cell group of the VLPO in diurnal grass rats (Experiments 3 and 4).

EXPERIMENT 1: Daily Rhythms in Fos expression in Brain Areas Related to the Sleep-Wake Cycle in the Nocturnal Rat (*Rattus norvegigus*).

It is hypothesized that species differences in the timing of the sleep/wake cycle are the result of different daily patterns of activity in brain regions that control sleep and wakefulness. As a first step towards a test of that hypothesis, the presence of rhythms in Fos expression in the brain of the nocturnal laboratory rat was determined. In the rat, brain areas important for the onset and maintenance of sleep are likely to be more active during the light than the dark phase of the cycle. The VLPO is one brain area that has been shown to increase in activity during sleep in rats (Lu *et al.*, 1998; McGinty *et al.*, 1997; Sherin *et al.*, 1998; Sherin *et al.*, 1996). Conversely, brain areas such as the PVT, CMT, and TMN, which are important in maintaining wakefulness and arousal, are expected to increase Fos expression during the dark phase of the cycle, when rats are active. This experiment was designed to document the occurrence of daily rhythms in Fos expression across the day-night cycle in brain areas previously shown to be critical in the control of sleep and arousal in rats.

In this study, animals were taken at four different times of day in order to obtain information about Fos expression at the beginning and middle of each the light and dark phase of the cycle. The areas examined for Fos expression were the VLPO, PVT, CMT, and two subdivisions of the TMN.

Method:

Animals. Thirty-two adult male rats were individually housed on a 12:12 Light:dark (L:D) cycle, with lights on at zeitgeber time (ZT; hours after lights-on) 0; a dim red was on all the time. Animals were fed and watered *ad libitum* with Harlan 8640 Teklad 2215 rodent diet and tap water.

Tissue Collection. Animals (n=8/sampling time) were perfused at ZT 1, ZT 5, ZT 12.5, and ZT 17. The rats were injected with the Equithesin (1.5 ml) in the animal room; at ZT 12.5 and 17, a light-tight hood (tin foil) was placed over their heads in order to prevent light from reaching the retina and to avoid light-induced Fos expression in the SCN. The animals were then perfused with 0.01M phosphase buffered saline (PBS) followed by 4% paraformaldehyde mixed with 0.2% sodium periodate and 1.3% lysine (PLP) in PBS. Brains were postfixed for 24 hours and then transferred to 20% sucrose in PBS. The brains were sectioned at 30μm using a freezing

microtome. The sections were divided into three sets and stored in cryoprotectant for later use.

Fos Immunocytochemistry. Every third section was processed for Fos immunocytochemistry (ICC) using a rabbit anti-fos primary antibody (Santa Cruz); all incubations and rinses were done with rotation at room temperature unless otherwise noted. The tissue was rinsed in 0.1M PBS for 2 hours and 40 min, then incubated in NGS (5%; Vector Laboratories) in PBS-tx for 1 hr, 45 min. The tissue was then washed (3X10 min) and incubated in the primary antibody (1:1000) with 3% NGS in PBS-tx overnight at 4°C. The sections were then rinsed and incubated in the biotinylated secondary antibody (goat anti-rabbit; Vector Laboratories) 1:250, with 3% NGS, in PBS-tx overnight at 4 C. Sections were washed and incubated in avidin-biotin solution (7.5 µl/ml A and B PBS; ABC elite kit, Vector Laboratories), for 2 hours, 10 min. After rinsing, the chromagen, 3,3'-diaminobenzidine (DAB), was added to Trizma buffer, and the sections were pre-incubated for 2.5 min; hydrogen peroxide (2%) was added, and the sections were incubated for 6 min. The tissue was then mounted onto gelatin-coated slides and the number of Fos+ cells was counted using a Zeiss microscope.

Microscopic Analysis. The VLPO was identified in the rat following the description in Sherin et al. (1996). An area $(190\mu m)^2$ in the VLPO was counted bilaterally at 250X. In each brain region, the data were averaged to give a mean number of Fos+ cells per section. The number of Fos+ cells in the PVT was also counted. The PVT was divided into anterior, middle, and posterior, using the landmarks described in Peng, *et al.* (1995): the anterior PVT was bounded by the stria medullaris and the third ventricle dorsally; the middle and posterior PVT were located ventral to the habenula; the posterior PVT was also more distinctly bilateral (two nuclei as opposed to one midline nucleus) than the middle PVT. The CMT was identified using the Paxinos and Watson rat brain atlas (Paxinos and Watson, 1997) and an area of $(300\mu m)^2$ was counted 250X with the aid of an optical grid. The TMN was located in the posterior hypothalamus (Ericson *et al.*, 1987; Paxinos and Watson, 1997) and was separated into two subdivisions. The ventral TMN (VTM) is located on the lateral edge of the posterior hypothalamus, and was quantified at 400X magnification using an optical grid; an area $(150\mu m)^2$ was counted. The dorsal TMN (DTM) was located lateral to the dorsal portion of the third ventricle in the posterior hypothalamus, and an area $(120\ \mu m)^2$ was counted.

All data were analyzed using a one-way analysis of variance (ANOVA) for each brain region, with the number of Fos+ cells per section as the dependent variable and the ZT as the independent variable; Fisher's PLSD was used for pairwise analyses. The numbers of sections used for the analysis of each region were counted and subjected to an ANOVA to determine if there were group differences in the number of sections analyzed which may bias the analyses; no differences were found. Correlation coefficients were also calculated for each brain area combination.

Results:

Zeitgeber time significantly affected the number of Fos+ cells (p=0.0001) in the VLPO of rats (see Figures 2 and 3). There were more Fos+ cells in the VLPO of animals taken at ZT 5 and ZT 12.5 than at ZT 1 and ZT 17 (p<0.001).

Figure 2 shows the significant (p<0.0001) rhythm in Fos activity in the whole PVT over the light-dark cycle. Fos expression in the PVT at ZT 1 was significantly different from all other time points (p<0.01). Fos+ cell number from animals at ZT 17 was also significantly different from ZT 5 and ZT 12.5 (p<0.001). All regions of the rat PVT (anterior, middle, posterior) showed the same pattern (except that for the middle PVT, ZT1 and ZT 17 were not significantly

Figure 2. Rhythms in Fos+ cells in the ventrolateral preoptic area (VLPO), paraventricular thalamic nucleus (PVT), and centromedial thalamic nucleus (CMT), but not in the ventral or dorsal tuberomammillary nuclei (VTM, DTM) over the 12:12 light:dark cycle in rats. Yellow bars represent daytime, and dark bars represent nighttime. a. different from zeitgeber time (ZT, hours after lights-on) 5 and ZT 12.5, b. different from ZT 17 ($p < 0.05$).

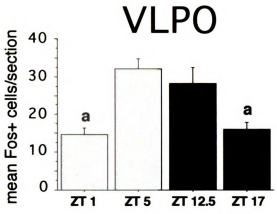
VLPO
mean Fos+ cells/section
40
30
20
10
0
a
a
ZT 1
ZT 5
ZT 12.5
ZT 17

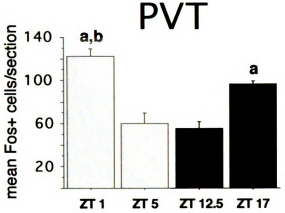
PVT
mean Fos+ cells/section
140
100
60
20
a,b
a
ZT 1
ZT 5
ZT 12.5
ZT 17

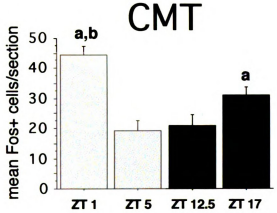
CMT
mean Fos+ cells/section
50
40
30
20
10
0
a,b
a
ZT 1
ZT 5
ZT 12.5
ZT 17

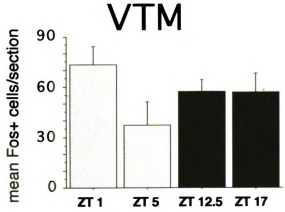
VTM
mean Fos+ cells/section
90
60
30
0
ZT 1
ZT 5
ZT 12.5
ZT 17

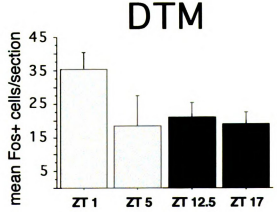
DTM
mean Fos+ cells/section
45
35
25
15
5
ZT 1
ZT 5
ZT 12.5
ZT 17

Figure 3. Photomicrographs of Fos+ cells in coronal sections taken through the (top) ventrolateral preoptic area (VLPO), (middle) paraventricular thalamic nucleus (PVT), and (bottom) centromedial thalamic nucleus (CMT) of rats. Fos+ cell number increased in the PVT and CMT at night, but increased in the VLPO during the light phase. ZT= zeitgeber time.

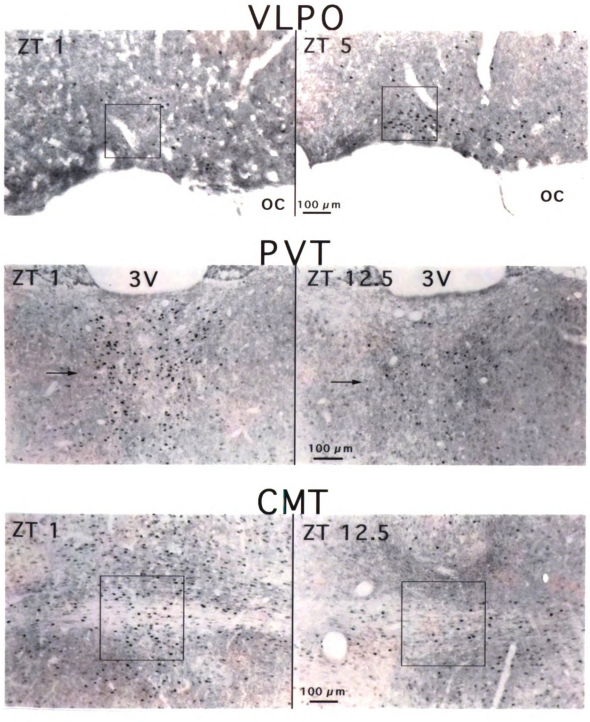
VLPO
ZT 1
ZT 5
OC
100 μm
OC
PVT
ZT 1
3V
ZT 12.5
3V
100 μm
CMT
ZT 1
ZT 12.5
100 μm

different); Figure 3 illustrates the difference found in the middle PVT. The pattern of Fos expression in the PVT was the opposite as the VLPO; as shown in Table 1, a significant negative correlation was found between the number of Fos+ cells in the VLPO and the PVT (r=-0.527, $p<0.01$). This statistically significant ($p<0.05$) negative correlation with Fos expression in the VLPO held for all regions of the PVT.

Fos expression in the rat CMT also showed a rhythm over the L:D cycle similar to that of the PVT (Figure 2; $p<0.0001$). The CMT contained more Fos+ cells in the animals taken at ZT 1 and ZT 17 than in the animals taken at ZT5 and ZT 12.5; ZT 1 and ZT 17 were also significantly different from each other in Fos+ cell number ($p<0.05$). Shown in Table 1, there was a significant negative correlation between Fos+ cell number in the VLPO and the CMT in rats (r=-0.401), and a significant positive correlation between the number of Fos+ cells in the CMT and PVT (r=0.894).

No significant rhythms were found in either one of the TMN subdivisions (VTM and DTM; Figure 2). However, Fos+ cell numbers in the TMN showed significant correlations with other brain areas (see Table 1). First, the Fos+ cell numbers in the TMN subdivisions were highly correlated with each other (r= 0.749, $p<0.0001$). Further, there was a significant negative correlation between the VLPO and

Table 1

Correlations between Fos+ cell number in brain regions in rats

	VLPO	PVT	CMT	VTM	DTM
VLPO	---	-0.527**	-0.401*	-0.363*	-0.272
PVT	---	---	0.894***	0.441*	0.537**
CMT	---	---	---	0.443*	0.503**
VTM	---	---	---	---	0.749***
DTM	---	---	---	---	---

VLPO, ventrolateral preoptic area; PVT, paraventricular thalamic nucleus; CMT, centromedial thalamic nucleus; VTM, ventral tuberomammillary nucleus; DTM, dorsal tuberomammillary nucleus. *$p<0.05$, **$p<0.01$, ***$p<0.0001$

VTM (r=-0.363, $p<0.05$), and significant positive correlations between both the VTM and DTM and both the CMT and PVT ($p<0.05$).

Discussion:

This study demonstrated that the VLPO shows a rhythm of Fos expression over the light-dark cycle. More Fos+ cells were found in the VLPO in the middle and just at the end of the light period, when rats are (or recently have been) inactive and frequently show sleep (Brown and Nunez, 1989b; Stephan and Nunez, 1977). Fos expression remained high into the beginning of the dark phase; this residual Fos expression in the VLPO at the beginning of the dark phase (ZT 12.5) reflects the production of Fos protein an hour earlier, during the light phase of the cycle. These data imply that Fos expression in the VLPO continues throughout the sleep (light) phase of the cycle and decreases during the active phase of the cycle. It has been shown previously that the VLPO becomes active during sleep, regardless of the time of day (Sherin *et al.*, 1996). These data showing that the VLPO is important in the homeostatic regulation of sleep, taken together with the present data indicating that the VLPO shows a daily rhythm in Fos expression, suggest that the VLPO may integrate circadian and homeostatic influences on sleep onset and maintenance.

The integration of circadian and homeostatic sleep demands by the VLPO necessitates neural input to the VLPO from brain areas important in regulating both sleep homeostasis and circadian rhythmicity. Studies have already demonstrated that the VLPO has reciprocal connections with brain regions important in wakefulness and arousal, such as the TMN, LC, raphe nuclei, and ventral tegmental area (VTA) (Chou *et al.*, 1998; Sherin *et al.*, 1998). The daily rhythm in the VLPO Fos expression may be due to afferent input from the SCN, which may serve to modulate VLPO neuronal activity. Efferent projections from the SCN have been traced to the POA as a whole (Watts *et al.*, 1987). If some of these fibers terminate specifically in the VLPO, they could provide direct circadian information to the sleep-active cells of the VLPO.

The rhythm of Fos expression in the VLPO may also be influenced by retinal inputs to that area (Lu *et al.*, 1997). Experiments with animals kept in constant darkness are needed to differentiate between true circadian modulation of the VLPO from effects due to direct retinal inputs. Therefore, the conclusion that the 24-hour pattern of Fos expression seen in the VLPO is due to SCN input has to remain tentative at this time. The same qualification applies to the rhythm seen in the PVT, since retinal projections also reach this structure in the rat (Speh and Moore, 1992).

In contrast to the pattern seen in the VLPO, the two thalamic nuclei investigated here showed enhanced Fos expression during and immediately following the active period. Cellular Fos activation in the PVT and CMT showed a remarkably strong positive correlation and a pattern that was 180° out of phase with the VLPO rhythm. Previous work indicates that both thalamic regions become active during situations incompatible with the onset and maintenance of sleep. For example, neuronal activity in the PVT is associated with consummatory behaviors (Robinson and Mishkin, 1968) and increased dopamine utilization in the nucleus accumbens (NAC) (Jones *et al.*, 1989), which is associated with reward attainment (Pennartz *et al.*, 1994). Activity in the intralaminar nuclei increases during wakefulness, enhanced vigilance (Allingham *et al.*, 1998; Glenn and Steriade, 1982; Steriade *et al.*, 1982a), and, in humans, during tasks that require attention (Kinomura *et al.*, 1996). In addition, enhanced activity in both the PVT and CMT is associated with stress (Chastrette *et al.*, 1991; Cullinan *et al.*, 1995; Senba *et al.*, 1993). Since increased arousal and wakefulness in general are associated with stimuli that increase activity in these thalamic nuclei (e.g., intralaminar thalamic neural activity increases during cortical desynchronization), stress alone cannot account for the patterns of Fos expression seen in the CMT and PVT. The rhythms in Fos

expression described here for the PVT and CMT are consistent with previous reports showing that Fos expression in the PVT decreases after sleep, and that neural activity in the intralaminar nuclei increase during wakefulness (Glenn and Steriade, 1982; Peng *et al.*, 1995). Therefore, the circadian system may modulate motivation, attention, and vigilance by acting on these thalamic areas. Although the circadian influence on the PVT can easily be attributed to direct projections from the SCN, the possible neural circuit responsible for rhythms in the CMT is not as evident, given that the SCN efferent fibers seen in the CMT do not appear to terminate there (Watts *et al.*, 1987). One possibility is that the CMT neurons may respond to a diffusable factor, first identified in fetal SCN neural transplants, that exerts a rhythmic influence on behavior after SCN lesions (Lehman *et al.*, 1995; LeSauter *et al.*, 1996; LeSauter and Silver, 1994; Silver *et al.*, 1996). Alternatively, the SCN may project to POA hypnogenic areas (Watts *et al.*, 1987), which in turn inhibit MRF neurons that send excitatory input to the intralaminar nuclei (Bremer, 1975; Lineberry and Seigel, 1971; Szymusiak and McGinty, 1989). For example, a study using transynaptic tract tracers has demonstrated that the pontine reticular formation receives indirect input from the SCN (Mintz *et al.*, 1998). In this way, the SCN could indirectly affect activity in the intralaminar nuclei, as well as the display of sleep.

Although a trend was evident, no significant rhythm of Fos expression was found in the rat TMN. Because of the well known importance of the histamine-containing cells of the TMN and histamine in arousal and wakefulness (Itowi *et al.*, 1991; Kalivas, 1982; Kiyono *et al.*, 1985; Lin *et al.*, 1996; Lin *et al.*, 1994; Monti, 1993; Monti *et al.*, 1988; Monti *et al.*, 1994; Monti *et al.*, 1996), and the presence of SCN projections to the posterior hypothalamus (Morin *et al.*, 1994; Watts *et al.*, 1987), the lack of a salient rhythm of Fos in these cells was surprising. If this lack of a rhythm in Fos reflects on the overall neuronal activity of the TMN, then it follows that neuronal activity in the TMN is not tonically higher in the dark phase (when rats are awake and active). This does not preclude the idea that momentary changes in TMN neuronal activity are critical for transitory changes in arousal. For example, the TMN may be important in transitions from a less aroused to a more aroused state at any time of day, as opposed to setting the gain on wakefulness in general, as is true for the midbrain reticular formation and intralaminar thalamus, for example. In this case, the neuronal activity of the TMN would be predicted more by transitory alterations in the animal's activity than by general activity levels over the light:dark cycle. This proposition is supported by data demonstrating that, in cats, neuronal discharge rates of cells in the

posterior lateral hypothalamus peaked during phasic, exploratory movements, as well as during phasic events during REM sleep. Further, discharge rates in these cells were similar during quiet wakefulness and slow-wave sleep; tonic EEG activation did not predict neuronal activity in the posterior lateral hypothalamus (Szymusiak *et al.*, 1989).

Previous studies have been somewhat inconsistent with respect to the pattern of histamine concentration or release within the brain. Some studies find that histamine content or release in the blood or brain regions (striatum, hypothalamus) peaks at the beginning of or during the dark (active) phase of the cycle in rats (Friedman and Walker, 1968; Friedman and Walker, 1969; Mochizuki *et al.*, 1992; Wada *et al.*, 1985); histamine release in cats also increased at night (Philippu and Prast, 1991). However, other studies have found no rhythm in whole brain (Oishi *et al.*, 1987) or hypothalamic (Kobayashi and Hopin, 1974) histamine content, or have found that it peaks during the light phase of the cycle in rats (Orr and Quay, 1975a; Orr and Quay, 1975b). Together, these data suggest that there is no salient or consistent circadian release of histamine in rats. In the current experiment, the lack of a salient daily rhythm in Fos in the TMN may be due to the presence of only very few inputs to this area from the SCN (Ericson *et al.*, 1991a). The lack of a daily

rhythm in TMN Fos expression is consistent with the idea that cells in the TMN do not play an important role in tonic or rhythmic arousal. Rather, in rats, histamaminergic cells in the posterior hypothalamus seem to play a role in short-term, phasic aspects of arousal, wakefulness, and REM sleep.

The possibility remains that not all of the Fos+ cells in the TMN regions counted in this study were histaminergic. For example, a rhythm of Fos in histaminergic cells may have been masked by nonrhythmic activity of nearby, nonhistaminergic cells. In order to answer this question, TMN cells expressing Fos would need to be double-labeled for histamine or a colocalized enzyme (Ericson *et al.*, 1987; Sherin *et al.*, 1998).

The coordination of the daily sleep-wake cycle requires the integration of homeostatic and circadian inputs. The VLPO shows a daily rhythm in neural activity, but also increases activity during sleep regardless of the time of day (Sherin *et al.*, 1996). Therefore, the VLPO is likely to receive both circadian and homeostatic information, and this area may serve to coordinate the activity of brain circuits important in sleep regulation. It has been demonstrated that the VLPO is reciprocally connected to brain regions critical for arousal (TMN, raphe nuclei, locus coeruleus, and the VTA) (Sherin *et al.*, 1998). However, the presence of a significant

input from the circadian clock, the SCN, has yet to be demonstrated. The next study therefore examines the afferent connections of the VLPO in rats, with specific interest on the SCN projections to the VLPO.

EXPERIMENT 2: Projections from the Suprachiasmatic Nucleus to the Sleep-Active Ventrolateral Preoptic Area in the Rat

Experiment 1 established that brain regions important for the control of the sleep-wake cycle show daily rhythms of Fos expression in rats. This indicates that these brain regions (VLPO, PVT, and CMT) are influenced by the circadian pacemaker, which suggests that they receive axonal or humoral inputs from the SCN. Although the SCN sends projections to the lateral preoptic area in general (Watts *et al.*, 1987), the extent of projections from the SCN to the VLPO sleep-active cell group have yet to be positively documented. Further, two sets of unpublished data from a single laboratory have reported disparate results on this question: one reported that a substantial number of vasopressinergic SCN cells project to the VLPO in rats (Gaus and Saper, 1998), while the other reported very few SCN projections to the VLPO, which receives more projections from areas surrounding the SCN (Chou *et al.*, 1998).

The aim of this study was to describe the afferent projections to the VLPO in rats using cholera toxin (β subunit, CTβ; see Appendix) as a retrograde tracer. Specifically, the presence of SCN projections to the VLPO was examined in order to determine the potential for a

direct circadian input to the VLPO in rats, as well as to explain contradicting results from previous reports. The aim of this study was to test the claim that the VLPO receives direct axonal input from the circadian clock of the SCN.

Method:

Animals: Fifty-four adult male Sprague-Dawley rats (250-350g) were used in the following studies. Animals were initially housed in groups of 2 or 3 on a 12:12 light:dark cycle, with lights on at ZT 0, as described in Experiment 1.

CTβ injections: Each animal was subjected to a unilateral microinjection of the retrograde tract tracer CTβ into the VLPO. Animals were first weighed and injected with the anesthetic Nembutal (pentobarbital sodium, Abbott Laboratories; 40 mg/kg i.p.), and the top of the head was shaved. The rat was then placed in the stereotaxic apparatus (Stoelting) with the incisor bar at –3.3. The following coordinates were used for the VLPO, with respect to bregma: anterior-posterior (AP) =-0.4-0.0 (most accurate injections at -0.2-0.0), medial-lateral (ML) ±1.0, dorsal ventral (DV) –7.5 from dura mater. A small hole was drilled in the skull using a dental drill (Dremel). Then, using a 500 nl Hamilon syringe, 10 nl of CTβ (List

Biological Laboratories) was injected into the VLPO over 5 min., and the needle was left in the brain for 15 min following injection in order to reduce leakage from the site of the injection. After the injection, the syringe was slowly removed from the brain, gelfoam (Upjohn) was used to seal the hole in the skull, and the wound was closed using autoclips (Clay Adams). Each animal was then individually housed and returned to the animal room after recovery. All injections were done during the light phase of the cycle.

Perfusion and tissue processing. Two days after CTβ injection, animals were perfused. Each animal received an injection of Nembutal (1 ml) in the animal room at either ZT 5 or ZT 17 (at which time, light-tight hoods were placed over the heads of the rats). Animals were transported to another room and transcardially perfused with 0.1 M PBS (300 ml) followed by 4% paraformaldehyde in 0.1 M PBS (300 ml). The brains were then removed and placed into 4% paraformaldehyde for 12 hours, followed by saturation in 20% sucrose solution in 0.1 M PBS. Brains were sectioned at 30 μm using a freezing sliding microtome, and sections were stored in cryoprotectant for later use. Because the brain region of interest was the SCN, brain sections were taken only through the preoptic area

and hypothalamus, including the posterior hypothalamus and the most rostral end of the midbrain.

Every fourth section was processed using ICC for CTβ. First, sections were rinsed for 1 hr in 0.1 M PBS. Tissue was then incubated in normal horse serum (NHS; 5%) for 1-2 hr. After a brief rinse, tissue sections were incubated in the primary antiserum (1:10,000 goat anti CTβ, List Biological Laboratories) with 3% NHS in PBS-tx overnight (about 15 hours) at 4°C. Brain sections were then rinsed (3 times, 10 min each in PBS) and incubated in the secondary antibody (1:200 horse anti-goat; Vector Laboratories) with 3% NHS in PBS-tx for 1-2 hr. After rinsing, tissue was placed in the ABC solution (Vector ABC elite kit) for about 2 hr. The sections were rinsed and placed in the chromagen, DAB (Vector DAB kit) with nickel intensification for 90 sec.; this short incubation time decreased the background staining significantly. Sections were then rinsed and mounted onto gelatin-coated slides, dehydrated and delipidated, stained with pyronin Y, and affixed with a cover slip using DPX mounting medium.

Microscopy: The placement of the injection was determined in each brain at low magnification (40X to 100X). The SCN of each animal was examined for cells containing immunostaining for CTβ

(CTβ+) at a high magnification (400X); the TMN of each brain was also analyzed because the TMN is known to have reciprocal connections with the VLPO (Chou *et al.*, 1998). For the brain with the best VLPO injection placement (case #269), every section processed (i.e., every fourth section) was examined for CTβ+ cells in brain areas other than the SCN and TMN.

Results:

Very few SCN cells contained CTβ immunostaining in cases in which the injection was restricted to the VLPO (n=2; 4 labeled cells found in SCN in #269), or included at least a portion of the VLPO but not the SON (n=16 total). However, cells surrounding the SCN on all sides were found to be CTβ+ after a successful injection of the VLPO. In contrast, many CTβ+ cells were found in the SCN in animals in which the supraoptic nucleus (SON; n=2) was included in the injection site (see Figures 4-7). More specifically, when the tracer was injected into the SON, cells located in the dorsomedial portion of the SCN contained CTβ (see Figure 7). No such bias in the location of CTβ+ cells in the SCN was seen after a successful injection restricted to the VLPO. Further, numerous CTβ+ neurons were found in the median preoptic nucleus (MnPO) of animals after injections that included

Figure 4. Injection site of cholera toxin-β (CTβ) into the ventrolateral preoptic area (VLPO) of rat #269 is marked in black. The sections are ordered from rostral (upper left) to caudal (lower right). mPON = medial preoptic nucleus, 3v = third ventricle, oc = optic chiasm, ac = anterior commissure. Compare to Figure 3, top. *injection path.

Figure 5. Retrogradely-labeled CTβ-immunoreactive cells in and around the suprachiasmatic nucleus (SCN) after a successful injection of the tracer into the right ventrolateral preoptic area (VLPO; rat #269). The sections are ordered from rostral (upper left) to caudal (lower right). 3V = third ventricle, oc = optic chiasm, AHA = anterior hypothalamic area.

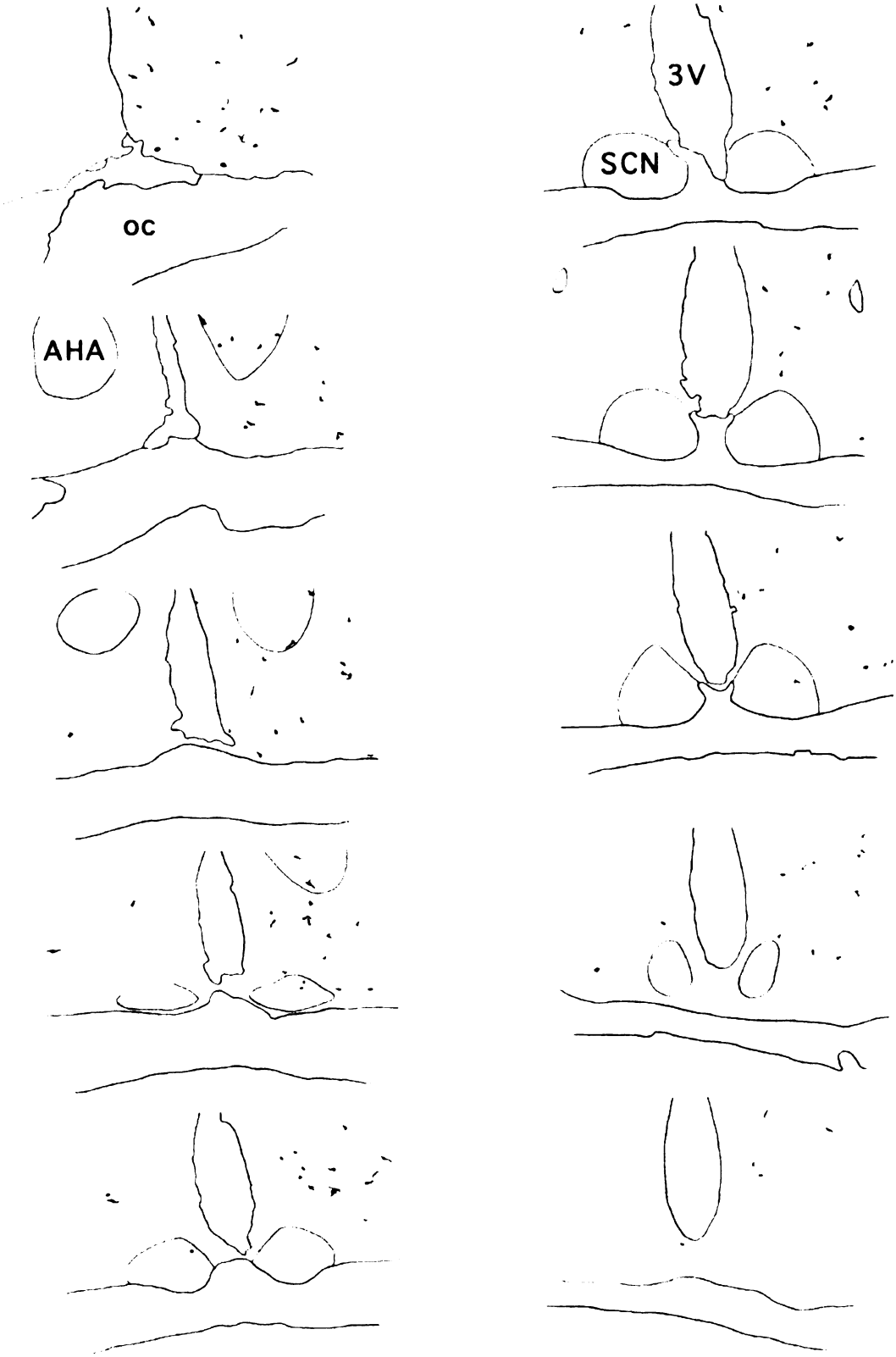
OC
AHA
3V
SCN

Figure 6. Injection site of CTβ into the ventrolateral preoptic area (VLPO) and the supraoptic nucleus (SON) of rat #159 is marked in black. The sections are ordered from rostral (upper left) to caudal (lower right). mPON = medial preoptic nucleus, 3v = third ventricle, oc = optic chiasm. *injection path.

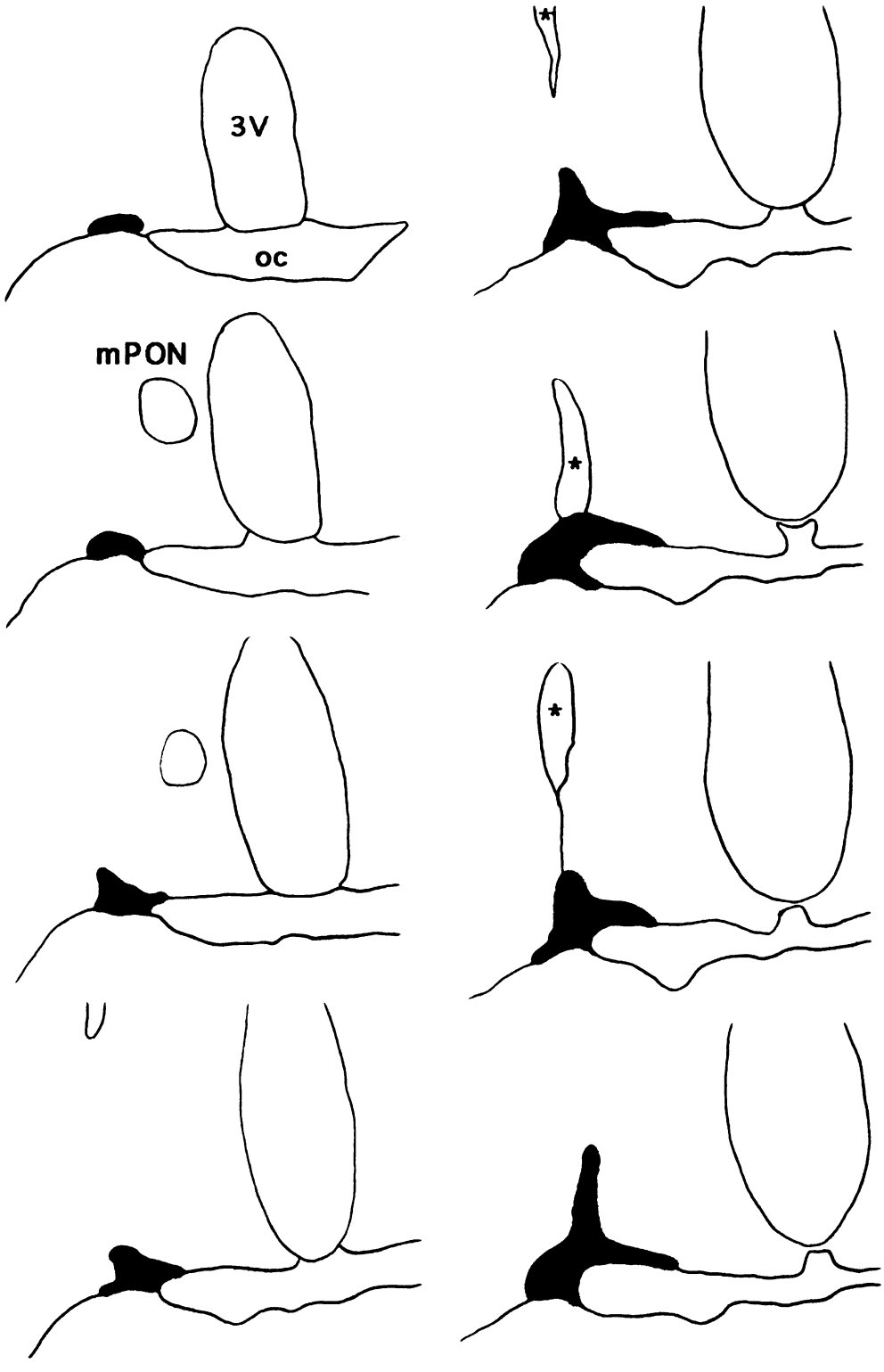
3V
oc
mPON
*
*
*

Figure 7. Many retrogradely-labeled CTβ-immunoreactive cells were found in and around the suprachiasmatic nucleus (SCN) after a injection of the tracer into the ventrolateral preoptic area (VLPO) that included a portion of the supraoptic nucleus (SON). The sections are ordered from rostral (upper left) to caudal (lower right). 3V = third ventricle, oc = optic chiasm, AHA = anterior hypothalamic area.

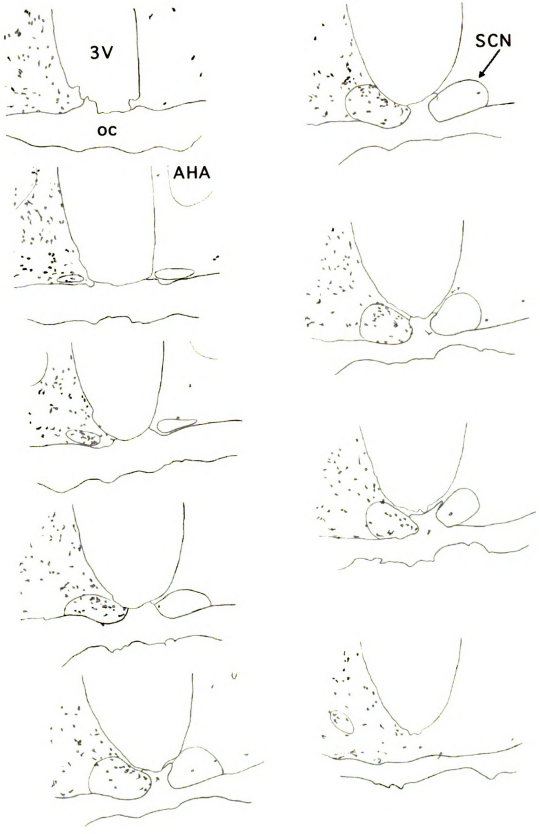
3V
oc
AHA
SCN

portions of the SON, but few labeled cells were found in the MnPO if the injection included the VLPO but not the SON (see Chou *et al.*, 1998; Armstrong, 1995).

Brains in which microinjections included the VLPO contained CTβ+ cells in the dorsal and ventral TMN, as well as CTβ+ cells in other nuclei in the posterior hypothalamus, including the premammillary nuclei, supramammillary nuclei (SUM), and infundibular nucleus (see Figure 8). When the injection included but was not restricted to the VLPO, CTβ+ cells were also found in these posterior hypothalamic nuclei. In the case shown in Figures 6 and 7, the injection site contained both the VLPO and the SON, and many CTβ+ cells were found in the TMN and surrounding hypothalamic nuclei. However, when the VLPO was missed, CTβ+ cells within the boundaries of the TMN were less numerous than when the injection included the VLPO.

In the brain containing the best VLPO injection (Case #269), few CTβ+ cells were found in the SCN, with more labeled cells found outside the SCN (Figure 5, Table 2). Additionally, neurons containing CTβ were found in the PVT as well as many hypothalamic sites, including the anterior hypothalamic area (AHA), lateral hypothalamus (LH), ventromedial nucleus (VMH), dorsomedial

Figure 8. Retrogradely labeled CTβ+ cells were found in the tuberomammillary nuclei (TMN), as well as other areas in the posterior hypothalamus, after a successful injection of the tracer into the ventrolateral preoptic area (VLPO). The sections are ordered from rostral (upper left) to caudal (lower right). Shading on the right side of each section indicates regions where histaminergic neurons are concentrated (Ericson, *et al.*, 1987). 3V = third ventricle, mt = mammillothalamic tract, f = fornix, DTM = dorsal tuberomammillary nucleus, PMN = premammillary nucleus.

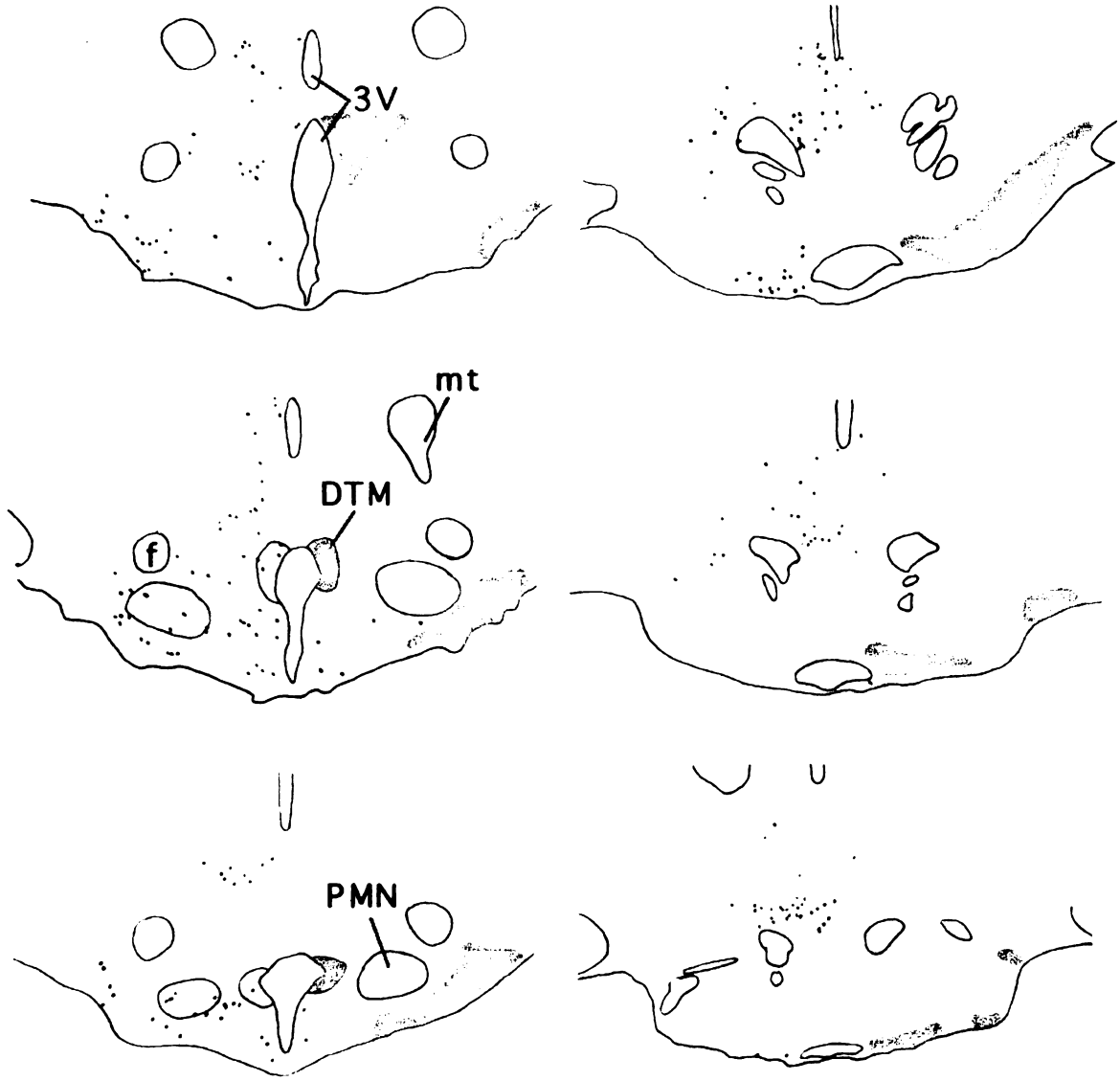
3V
mt
DTM
f
PMN

Table 2
Brain regions containing CTβ+ neurons following microinjection in the ventrolateral preoptic area of rat #269.

General Brain Region			
Anterior to Hypothalamus	Hypothalamus and Thalamus	Amygdala and Associated areas	Posterior to Hypothalamus
near substantia inominata	perifornical region	anterior amygdaloid area, dorsal, ventral	periaqueductal gray
lateral septum	periventricular n.	cortical amygdala	raphe, caudal-linear, medial, dorsal
medial preoptic area	suprachiasmatic n.(4)	intercalated amygdala	
lateral preoptic area	subparaventricular region	medial amygdala	
median preoptic n.	anterior hypothalamic area	basolateral amygdala	
horizontal diagonal band(1)	lateral hypothalamic area	basomedial amygdala	ventral tegmental area
endopiriform n., ventral(2), dorsal	ventromedial n.	bed n. of the stria terminalis	
anterior dorsal preoptic n.	dorsomedial n.	piriform cortex	interpeduncular n.
	posterior hypothalamus		
	arcuate n.		
	tuber cinerum area		
	tuberomammillary n.		
	premammillary n.		
	supramammillary n.		
	paraventricular thalamic n.		

Numbers in parentheses indicate number of labeled cells found in brain regions containing very few labeled cells.

nucleus (DMN), periventricular nucleus (PeV), perifornical nucleus (PeF) as well as near the fornix throughout the extent of the hypothalamus, and in the tuber cinerum (TC) and arcuate nucleus. Cells labeled with CTβ were also found throughout the amygdala, including the basomedial, anterior cortical, and intercallated nucleus, but the medial nucleus of the amygdala (meA) was the most densely labeled nucleus in this structure. Labeled cells were also found in the lateral septum (LS), bed nucleus of the stria terminalis (BST), and medial and lateral preoptic areas (MPA and LPO); a few labeled neurons were found in the piriform cortex, nucleus of the horizontal limb of the diagonal band (HDB), the median preoptic nucleus (MnPO), and paraventricular hypothalamic nucleus (PVN). Labeled neurons were seen in the posterior hypothalamus as well (Table 2). In the most caudal sections taken, labeled neurons were found in the periaqueductal gray (PAG).

Discussion:

The data from this study indicate that very few SCN cells project to the VLPO in rats. However, the SCN may send circadian information to the VLPO indirectly through relay neurons. After injections restricted to the VLPO, CTβ+ cells were seen in the sub-

paraventricular region (sPVHz) which receives heavy SCN input (Morin *et al.*, 1994; Watts *et al.*, 1987). Therefore, neurons in the SCN may send circadian information to the sPVHz, which then send projections to the VLPO, imposing a circadian rhythmicity to VLPO neurons. Since the PVT projects to the VLPO (Sherin *et al.*, 1998, present data), and receives SCN input, this thalamic nucleus may also function as a relay of circadian signals to the sleep-active cells. However, the lack of substantial direct SCN projections to the VLPO may also reflect the importance of a diffusible signal from the SCN (Silver *et al.*, 1996) in the control of the VLPO by the circadian pacemaker.

These data help to account for conflicting reports of the presence of abundant SCN projections to the VLPO (Chou *et al.*, 1998; Gaus and Saper, 1998). In animals with injections of the VLPO which also encompassed the SON, numerous CTβ+ neurons were found in the SCN. When only coronal sections through the VLPO (anterior to the rostral edge of the SON) were examined for spread of the tracer, these injection sites resembled the successful VLPO injections in which the tracer did not invade the SON (see Figures 4-7). However, examination of the sections posterior to the VLPO made it easy to differentiate between successful containment of the tracer in the

VLPO and cases in which the tracer invaded the SON. This implies that the AVP+ SCN neurons previously reported to project to the VLPO are likely to terminate in the SON. The SCN sends projections to the SON (Cui *et al.*, 1997; Stephan *et al*, 1981), and the peptide content of these projections can be investigated by microinjecting a retrograde tracer in the SON only and comparing the pattern of labeled cells in the SCN with the VLPO+SON injections. Further, the AVP+ fibers identified in the VLPO (Gaus and Saper, 1998) could actually be dendrites of SON neurons rather than axons emanating from the SCN. If indeed the VLPO does not receive abundant AVP+ projections from the SCN, then this argues that AVP is not the neurotransmitter responsible for communicating circadian information to the VLPO, and therefore imposing a circadian pattern on sleep. This conclusion is strengthened by evidence showing that AVP is not needed for the sleep-wake cycle to show circadian rhythmicity (Brown and Nunez, 1989a).

In general, the findings in this experiment agree with previous data on the projections patterns to the VLPO in rats (Chou *et al.*, 1998). Monoaminergic cell groups such as the TMN, raphe nuclei, and ventral tegmental area were found to project to the VLPO. In the neural model proposed in Sherin, *et al.* (1996; 1998;Chou *et al.*, 1998), these brain regions have mutual inhibitory connections with

the VLPO and the VLPO coordinates the sleep/wake cycle by inhibiting all of these brain regions concurrently.

EXPERIMENT 3: Observations of the Sleep/Wake Cycle in the Nile Grass Rat (*Arvicanthis Niloticus*)

The hypothesis behind the experiments presented in this dissertation work seeks to explain species differences in the sleep/wake cycle by demonstrating differences in the daily patterns of activity in brain regions important in sleep and arousal. Before any species comparison can be made involving the brain regions investigated in rats (VLPO, PVT, CMT, and TMN), these areas must be identified in the *Arvicanthis niloticus*. The VLPO is a newly described region in the rat (Sherin *et al.*, 1996) and therefore has not been identified in many species. Further, in order to identify the sleep-active VLPO in *A. niloticus*, the animals must be taken while they are asleep. Accordingly, the following experiments document the daily pattern of behavioral indices of sleep in Nile grass rats, then proceed to use these data to identify the pattern of Fos expression in the VLPO of grass rats.

The circadian sleep-wake cycle of the nocturnal rat has been well documented (for example, see Trachsel *et al.*, 1986). This rich set of behavioral data facilitates the investigation of brain areas that control sleep and wakefulness in laboratory rats. Contrary to this, the features of the sleep/wake cycle of the Nile grass rat are not

known. Although rhythms in temperature, activity, and mating indicate that this species is diurnal (Katona and Smale, 1997; McElhinny *et al.*, 1997) and therefore likely to sleep at night, the sleep patterns of *A. niloticus* have not been established. Because these animals are likely to resist traditional methods for measuring sleep (i.e., using chronic electrophsyiological recording approaches), behavioral correlates of sleep were monitored around the clock for 2 days to document the daily display of these behavioral correlates of sleep in these rodents.

Methods:

Animals: Four adult female *A. niloticus* were used (see Figure 1). All of the grass rats used in this and subsequent studies were born in the lab and descended from the original group of animals captured in Kenya in 1993 (Katona and Smale, 1997). Animals were fed and watered *ad libitum*. The animals were housed in a 12:12 light:dark cycle with a dim red light (< 5 lux) that was kept on at all times.

Behavioral correlates of sleep across the 12:12 light dark cycle. Four animals were individually placed in a 30.5 cm deep 25.5x51 cm glass terrarium with 5 Kimwipes (Kimberly-Clark) for bedding and allowed to acclimate for at least 4 days. Each animal was videotaped

for 24-25 hours. Within 16 days, each animal was videotaped a second time under the same conditions, except that a small piece (13 cm long, 5 cm diameter) of PVC tubing was placed in the terrarium. For the videotaping, a Panasonic camera (WV-BP310), with a 6mm Panasonic TV lens (WV-LA6B2), was attached to a Sony time lapse videotape recorder (VCR; SVT-5000). A Sony black and white monitor (SSM 121) served to center and focus the camera, and 3M T120 and Quantegy T180 professional videotapes were used.

The videotapes were evaluated using an RCA XL 100 XS Stereo commercial skip television and a Panasonic PV-7400 VCR plus. The first 20-40 min of the videotaped data were not analyzed to allow for acclimation. Each hour was divided into 12 5-min bins, and the vigilance state of the animal was determined for each bin over each 24-hour period. The animals were considered awake if they were locomoting, eating, drinking, grooming, or if their eyes were open and they were scanning the environment. The animals were considered asleep if they were sedentary, with eyes closed, or laying on their sides. For each 5-min. bin, the sleep or wake state of each animal was recorded. The number of 5-min bins containing sleep without wakefulness was totaled for each hour, as well as for the light period (ZT 0-12) and the dark period (ZT 12-24) for each animal for each day of videotaping. Student's paired t-tests (2-tailed, dependent

samples) were used to compare the amount of sleep (sleep-only and wake-only bins) shown during the day and compared to the night. The number of bins containing sleep and wake were compared between the 2 days of videotaping to determine if animals slept more on one of the test days compared to the other.

Results:

A.niloticus displayed sleep bouts throughout the 24-hour light-dark cycle; however, sleep was concentrated in the dark phase of the cycle. The number of 5-min bins containing sleep without wakefulness did not differ significantly between the two days of videotaping for both the light and the dark period ($p>0.40$ for both comparisons). Therefore, the data were averaged across the two days for each animal.

There were significantly more sleep-only bins in the night (mean±SEM = 47.75±2.93) than the day (mean±SEM = 9.00±1.50; $t_{(1,3)}=-16.369$, $p<0.0005$, 2-tailed). Figure 9 (top) shows the average distribution of sleep-only bins over the 12:12 light-dark cycle. The number of sleep-only bins peaked at ZT 19-21; by ZT 23, few bins contained only sleep. Wakefulness, however, shows a bimodal pattern (Figure 9, bottom), with the number of wake-only bins high at the transitions between light at dark. Further, the number of

Figure 9. The number of 5-min bins that contained behavioral indices of sleep without wakefulness (A; sleep-only bins), or bins containing wake without any indications of sleep (B; wake-only bins) throughout the 12:12 light:dark cycle in *Arvicanthis niloticus*. The number of bins are listed on the vertical axis, and zeitgeber times (ZT; hours after lights-on) are listed on the horizontal axis. The light-dark bar illustrates that lights came on at ZT 0 and were turned off at ZT 12. The number of sleep-only bins peaked in the hour starting at ZT 19, and behavioral indices of sleep decreased prior to lights-on. The number of wake-only bins had a bimodal distribution, with peaks at lights-on and lights-off.

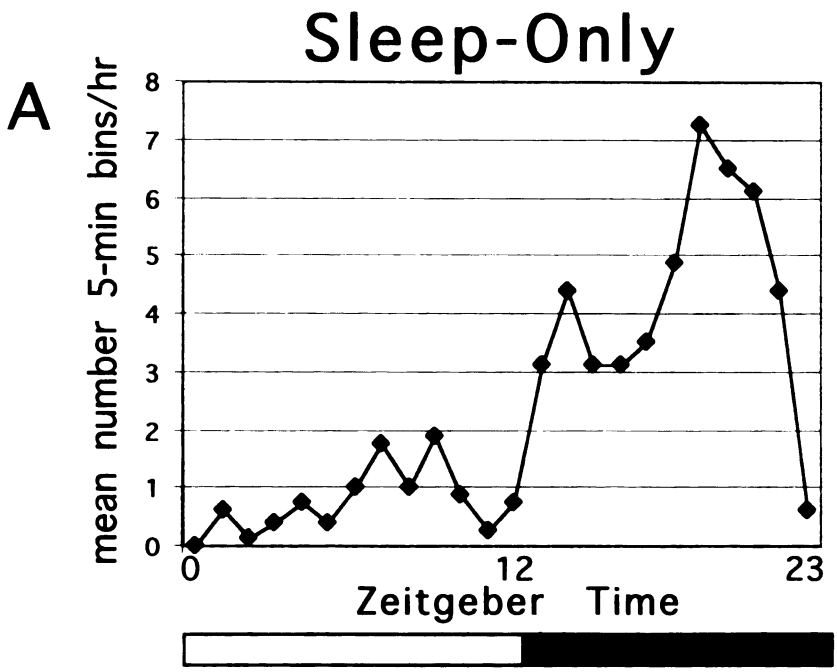
A
Sleep-Only
mean number 5-min bins/hr
0
1
2
3
4
5
6
7
8
0
12
23
Zeitgeber Time

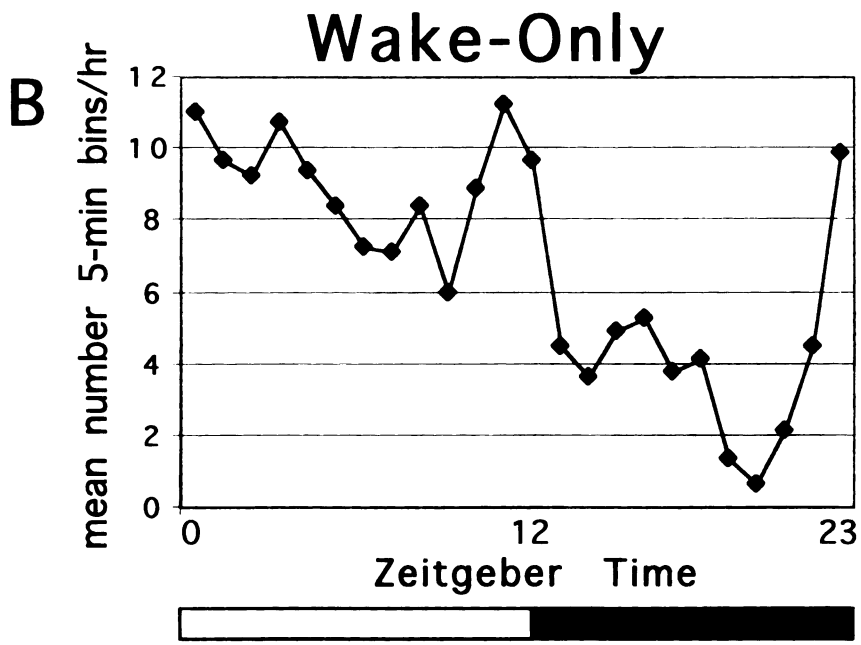
B
Wake-Only
mean number 5-min bins/hr
0
2
4
6
8
10
12
0
12
23
Zeitgeber Time

wake-only bins was significantly greater in the day (ZT 0-12) than at night (ZT 12-24; $t_{(1,3)}$= 10.534, p<0.01, 2-tailed).

Discussion:

The results clearly show that behavioral correlates of sleep in *Arvicanthis* are more frequent in the dark phase of the illumination cycle, as demonstrated by the increased number of 5-min bins devoid of wakefulness at night in this species (see Figure 9A). These data, taken together with other studies (Blanchong and Smale, in press; Katona and Smale, 1997; McElhinny *et al.*, 1997), strongly support the claim that *A. niloticus* is a diurnal species.

Other aspects of the *Arvicanthis* sleep pattern are also notable. First, the behavioral indices of sleep peaked during the hour beginning at ZT 19 (7 hours after lights-off), in the middle of the dark phase. Therefore, brain areas where activity is important for sleep are predicted to be active at this time. Second, although sleep was concentrated in the dark phase, sleep bouts occurred throughout the light-dark cycle. This unconsolidated aspect of grass rats' sleep pattern resembles sleep in other rodents, including rats, which also show numerous sleep bouts throughout their cycle (Trachsel *et al.*, 1986). This fragmented sleep pattern differs from the consolidated sleep pattern seen in primates such as squirrel monkeys (Edgar *et al.*,

1993) as well as humans (Dijk and Czeisler, 1995). This difference in the length of sleep bouts between rodents and primates (i.e. minutes vs. hours) suggests species differences in brain mechanisms responsible for the circadian rhythm of sleep, regardless of whether the animals are nocturnal or diurnal. In diurnal species with highly consolidated sleep patterns (i.e. primates), the circadian signal inducing wakefulness during the day, or the response to the circadian signal, needs to be stronger or more sustained throughout the day compared to a diurnal rodent, such as *A. niloticus*, that has a fragmented sleep/wake pattern. This may explain why SCN lesions change the total amount of sleep in primates (Edgar *et al.*, 1993) but not rodents (Mistlberger *et al.*, 1983).

Third, in addition to differences in the light:dark distribution of sleep, rats and *Arvicanthis* differ in the display of sleep and wakefulness at light-dark transitions (dawn and dusk). In grass rats, sleep decreases in anticipation of lights-on, and wakefulness peaks at dawn and dusk (Figure 9B). In nocturnal rats, however, very little activity is seen in anticipation of transitions to lights-on or lights-off (Trachsel *et al.*, 1986). These data, together with other observations (Katona and Smale, 1997; McElhinny *et al.*, 1997), serve to document the crepuscular tendencies of *Arvicanthis* which are absent in rats (Trachsel *et al.*, 1986). Further, this activity pattern must be

considered when predictions are made regarding when brain regions important in sleep will be most active in *A. niloticus*. Lastly, this salient crepuscular component of the *Arvicanthis* activity cycle in the laboratory (Katona and Smale, 1997) is not present in animals trapped in the field, where most animals are trapped outside the burrow in the middle of the day (Blanchong and Smale, in press). However, grass rats may be active in the burrow system at dawn and dusk, in which case the activity pattern seen in the laboratory would reflect activity of *Arvicanthis* in their natural habitat both above ground (diurnal pattern of trapping) and underground (possible crepuscular pattern).

In the future, with the development of new technology, valuable data would be attained by investigating the EEG patterns of this diurnal species, *Arvicanthis niloticus*. Smaller monitoring devices that do not disturb these animals' activity patterns may accurately measure the sleep-wake cycle in *Arvicanthis*. However, for the current purposes, the assessment of the behavioral indices of sleep was sufficient to demonstrate the sleep patterns in this species. The following experiments can therefore correlate activity in brain areas important in sleep and wakefulness with the pattern of sleep in *A. niloticus*. Before this can be done, however, the VLPO must be identified in *Arvicanthis*. The next study describes the sleep-active

VLPO in Nile grass rats making use of ICC for GAL and histological techniques in addition to quantification of Fos expression at different ZTs.

EXPERIMENT 4: Identification and Characterization of the Ventrolateral Preoptic Area in the Nile Grass Rat

The previous study demonstrated that behavioral correlates of sleep in *A. niloticus* are preferentially displayed at night, while wakefulness dominates the daytime and the transitions of the light:dark cycle. This pattern differs considerably from that of laboratory rats. Very little is known about the neural mechanisms responsible for these species differences in the distribution of sleep and wakefulness throughout the day. In diurnal and nocturnal species, brain areas related to sleep onset and maintenance should exhibit different patterns of neural activity over the light-dark cycle. One region believed to be important in the regulation of sleep in rats is the VLPO (Lu *et al.*, 1998; Sherin *et al.*, 1998; Sherin *et al.*, 1996). Fos expression in neurons within the VLPO of rats is elevated following a sleep episode (Sherin *et al.*, 1996) as well as during the rest phase of the cycle (Experiment 1). Neurons of the VLPO have been shown to contain GABA as well as the neuropeptide GAL (Sherin *et al.*, 1998), which is thought to inhibit the firing of histaminergic neurons in the tuberomammillary nuclei (TMN) in the posterior hypothalamus (Schonrock *et al.*, 1991). Direct retinal

projections reach the VLPO of the rat and may mediate some effects of light on the quality and distribution of sleep (Lu *et al.*, 1997).

In contrast to the rat, nothing is known about the functional anatomy of the VLPO in diurnal mammals. Consequently, the goals of the studies described below were to identify the sleep-active cells of the VLPO in the diurnal *A. niloticus*, to determine if these cells contain GAL, and to examine the sleep-active area for retinal projections. Additionally, the number of Fos+ cells in the CMT and PVT was assessed in order to correlate Fos expression in these areas with the VLPO.

Methods:

The *A. niloticus* used in the following studies were individualy housed as described in Experiment 3; standard housing conditions did not include terrariums used for videotaping.

Giemsa stain. Five female *A. niloticus* were injected with 1 ml Nembutal and perfused transcardially with 125 ml 0.01 M phosphate buffered saline (PBS), followed by 125 ml PLP. Brains were postfixed in PLP for 2 hours then saturated in 20% sucrose (in 0.1 M PBS) overnight. The next day, four brains were sectioned into 3 sets of 30μm frozen sections; one brain was sectioned at 40μm, and every section was used. Sections were stored in cryoprotectant for

later use, or in PBS for use the same day. Tissue was mounted onto gelatin coated slides, dehydrated, and stained with giemsa stain (1mg/ml, Sigma; (Iniguez *et al.*, 1985; Sherin *et al.*, 1998)) in potassium dihydrogen sulfate (11.5 mg/ml) at 60°C for 10 min, followed by an aqueous rinse, dehydration, Hemo-De (Fisher), and coverslipping with DPX (Fluka). Using the microscope, the ventral and lateral preoptic area were examined.

Galanin immunostaining. Two female *A. niloticus* injected with Nembutal (9 ml/kg i.p., pentobarbital sodium, Abbott Laboratories) and placed in the stereotaxic device and a local anaesthetic was given under the skin on the skull (0.01 ml 2% Lidocaine, 1:1 with saline, Elkins-Sinn, Inc.). Colchicine (5µl volume, 0.0025 mg; Sigma) was injected bilaterally into the lateral ventricles to block axonal transport in order to facilitate the detection of the peptide in cell bodies. The following coordinates were used: AP +1.0 from bregma, ML ±2.3, DV –4.3 from skull, with the bite bar set at –5.0. Colchicine was injected over 5 min using a 10 µl Hamilton syringe; the syringe was removed 5 min after completion of the injection. Each animal was then removed from the stereotaxic apparatus and the wound was closed using autoclips. The animal was given 1 ml saline, 0.3 ml (0.03 mg/ml) Buprenex (10% in saline; Bergen Brunswic), the head was treated with Novalsan antiseptic ointment (Fort Dodge

Laboratories, Inc.), and the cage was placed on a heating pad until the animal began moving.

Twenty-four hours after surgery, animals were perfused. Each animal was injected with 0.5 ml Nembutal and perfused transcardially with 125 ml 0.01 M PBS followed by 125 ml PLP. Brains were removed, postfixed for 4 hours, allowed to saturate in a 20% sucrose solution (in 0.1 M PBS), and sectioned into 3 sets of 30μm frozen sections that were stored in cryoprotectant for later use.

One set of sections (every third section) was processed using ICC for GAL. Sections were rinsed for an hour in 0.01 M PBS before incubation in the primary antiserum, rabbit anti GAL (Cambridge) at a 1:10,000 dilution in 5% normal goat serum (NGS) and 3% Triton X-100 (tx) for 18 h at 4°C. Sections were then rinsed (3 times, 10 min each) and incubated in the secondary antiserum (biotinylated goat anti-rabbit, 1:200; Vector Laboratories) in PBS-tx for 1 h. After rinsing, tissue was placed in the avidin-biotin complex (ABC; Vector Laboratories) for 2.25h. Sections were then reacted with DAB with 0.3% hydrogen peroxide for 2 min, then rinsed, mounted onto gelatin-coated slides, coverslipped, and observed under the microscope. The area assessed is shown in Figure 10; a grid (190 $\mu m)^2$ was placed over the VLPO, and GAL+ cells within this area

were counted on each side of the brain in four sections at 400X magnification. The number of GAL+ cells in each VLPO (unilateral) was averaged across sections.

Fos expression. Fourteen female *A. niloticus* used in this study were individually housed as described in Experiment 3. Animals were entrained to the 12:12 light:dark cycle for 12 days, and perfused at ZT 20 (n=7) or ZT 23 (n=7). These times were chosen because videotapes of similar animals (see Experiment 3) demonstrated that this species is most likely to be sleeping at ZT 19 (Figure 2), but awake and active 1-2 hours before lights come on. These time points also permit the sampling of Fos expression in the VLPO over time independently of the possible acute effects of light. At the time of perfusion, each animal was injected with 0.3 ml Nembutal (i.p.) in the colony room. A light-tight hood was placed over the head and the animals were transported to a different room where they were perfused transcardially with 125 ml 0.01 M PBS, followed by 125 ml 4% PLP. The brains were removed and postfixed for 4 h, and then placed in 20% sucrose in 0.1 M PBS overnight. Three sets of frozen sections (30 μm) were obtained through the preoptic/anterior hypothalamic region and stored in cryoprotectant.

The sections were then processed for Fos ICC. One set of sections was rinsed (3 times in 0.1 M PBS), and then incubated in 5%

NGS in 0.1 M PBS for 90 min. The tissue was then rinsed once and incubated in the primary antiserum, rabbit anti-Fos at 1:2000, in PBS-tx at 4°C for 19 h. Sections were then rinsed and incubated in the secondary antiserum (biotinylated goat anti-rabbit) at 1:200 in PBS-tx for 2 h. After rinsing, the tissue was incubated in the avidin-biotin complex (ABC, Vector Laboratories) for 90 min, and then exposed to the DAB chromagen with 0.3% hydrogen peroxide for 3 min. The sections were then rinsed, mounted onto gelatin-coated slides, and coverslipped.

Using a grid, the number of Fos+ cells in the VLPO was counted bilaterally in two sections at 400X from each animal by an investigator unaware of the time at which the animals were perfused. For each section, the middle of the grid was placed at the lateral edge of the optic chiasm. The number of Fos+ cells per VLPO section (bilateral) was averaged for each animal, and the data were subjected to a Student's *t*-test (two-tailed, independent samples), with the number of Fos+ cells as the dependent variable and ZT as the independent variable. The number of Fos+ cells in the area directly dorsal to the VLPO was also quantified using the same grid and served as a control area. Again, the number of Fos+ cells per section were averaged and subjected to a Student's *t*-test.

Lastly, the number of Fos+ cells was also counted in the CMT as well as the PVT, which was divided up into three regions (anterior, middle, and posterior) using the landmarks described in Peng, *et al.* (1995): the anterior PVT was bounded by the stria medullaris and the third ventricle dorsally; the middle and posterior PVT were located ventral to the habenula; the posterior PVT was also more distinctly bilateral (two nuclei as opposed to one midline nucleus) than the middle PVT. The CMT was identified using the Paxinos and Watson rat brain atlas (Paxinos and Watson, 1997) and an area of $(300\mu m)^2$ was counted at 250X with the aid of an optical grid. The number of Fos+ cells per section in the PVT and CMT were averaged and subjected to Student's *t*-tests; correlation analyses were perfomed comparing Fos+ cell number in the VLPO with each the PVT, middle PVT (see results), and CMT; the PVT and middle PVT were each compared to the CMT.

Retinal afferents. To determine if retinal ganglion cells send projections to the VLPO, two female *A. niloticus* were given unilateral intraocular injections of CTβ (Johnson *et al.*, 1988b). Cholera toxin was reconstituted and diluted (1:1) with 4% DMSO and 1.8% saline; 10 µl of the CTβ solution was injected into one eye using a 10 µl Hamilton syringe while the animal was under metofane

(Methoxyflurane, Pitman-Moore) anesthesia. After 2 days, the animals were perfused, as described above, at ZT 20.

The brains were cut into three sets of 30 μm frozen sections. The tissue was processed for CTβ-ICC, using the protocol described above, with the following modifications: after nonspecific binding was blocked with 5% NHS, the tissue was incubated in the goat anti-CTβ primary antiserum at a 1:10,000 dilution with PBS-tx with 3% NHS, and incubated about 45 h; the secondary antibody used was horse anti-goat, diluted 1:200 with 3% NHS in PBS-tx, and incubated for about 90 min; sections were incubated in ABC for 2 h; the chromagen used was DAB with nickel intensification, and the incubation lasted 3 min. The VLPO area, the SON, the PVT, and the SCN were microscopically examined (100-500X) to determine the presence of labeled fibers.

ICC controls. For each ICC procedure, sections were processed deleting the primary antibody to control for nonspecific staining. Deletion of the primary antibody resulted in the absence of any labeling of cells or fibers for CTβ, Fos, or GAL; additionally, preabsorbtion of the primary antiserum for GAL with GAL peptide (Sigma; 50 μg GAL peptide in 500 μl PBS, with 5 μl anti-GAL primary antibody) also resulted in tissue devoid of immunostaining.

Results:

Giemsa stain. A small cluster of cells was found in the area of the VLPO in tissue sections of *A. niloticus*. Figure 10 illustrates the region identified as the VLPO in this species. The location of the cluster of cells (Figure 11) is similar to that of the rat. This area is found just dorsal to the lateral edge of the optic chiasm and medial to the HDB, with the caudal end of the VLPO in the same section as the rostral pole of the SCN. The cluster of cells is pyramidal in shape, with the base near the edge of the optic chiasm and flaring out dorsally and laterally. Also, a blood vessel near the base of the brain often marks the lateral edge of the VLPO, depending on the angle at which the brains are sectioned.

Galanin. As shown in Figure 11 (bottom), many GAL+ cells were found in the area identified as the VLPO in *Arvicanthis*. A mean of 34.625 (SEM=3.63) GAL+ cells per section (unilateral) was found in the VLPO. Galanin+ cells were concentrated in a cluster in the VLPO, with scattered GAL+ cells in the POA (see Figure 12). Cells heavily labeled for GAL were also seen in the paraventricular hypothalamic nucleus (PVN) and SON, regions where GAL-immunoreactive cell bodies have previously been described (Melander *et al.*, 1986; Merchenthalter *et al.*, 1993).

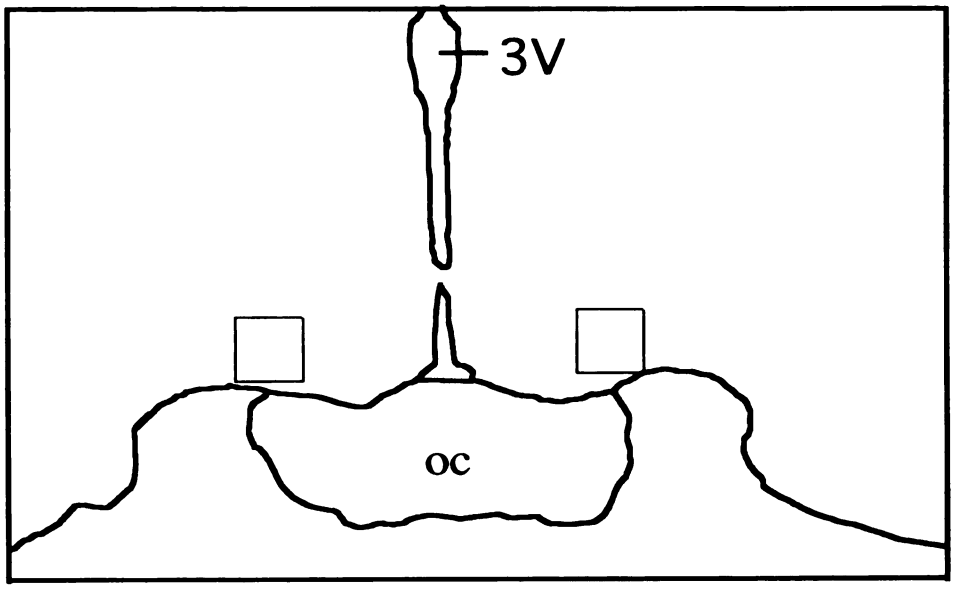

Figure 10. The ventrolateral preoptic area (VLPO) in the diurnal rodent *Arvicanthis niloticus*. The drawing shows the (190 μm)^2 area counted in Experiment 4. 3V = third ventricle, oc = optic chiasm.

Figure 11. The top photomicrograph identifies the ventrolateral preoptic area (VLPO) of *Arvicanthis niloticus* with giemsa stain. The photomicrograph on the bottom shows the VLPO immunostained for galanin (GAL). oc = optic chiasm, HDB = nucleus of the horizontal limb of the diagonal band.

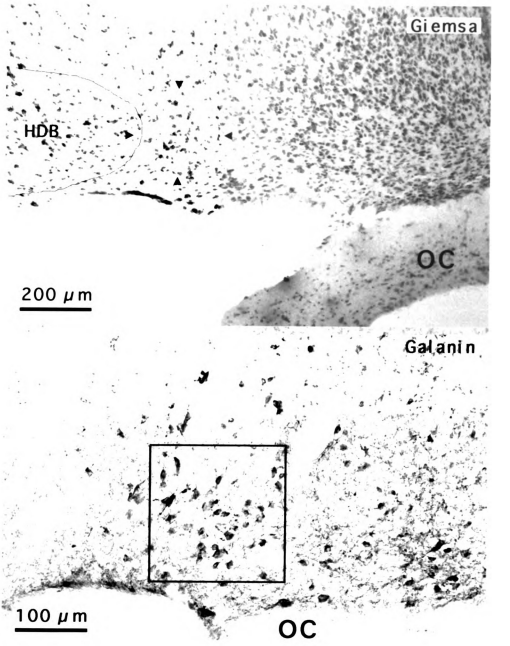
Giemsa
HDB
OC
200 μm
Galanin
100 μm
OC

Figure 12. Profiles of the ventrolateral preoptic area (VLPO) of *Arvicanthis niloticus* from rostral (top) to caudal (bottom). Drawings on the left show the pattern of Fos+ cells in the VLPO. The region inside of the (190 μm)^2 box was counted in Experiments 3 and 4. The right drawings illustrate the pattern of immunostaining for galanin (GAL) in the VLPO. 3V = third ventricle, oc = optic chiasm.

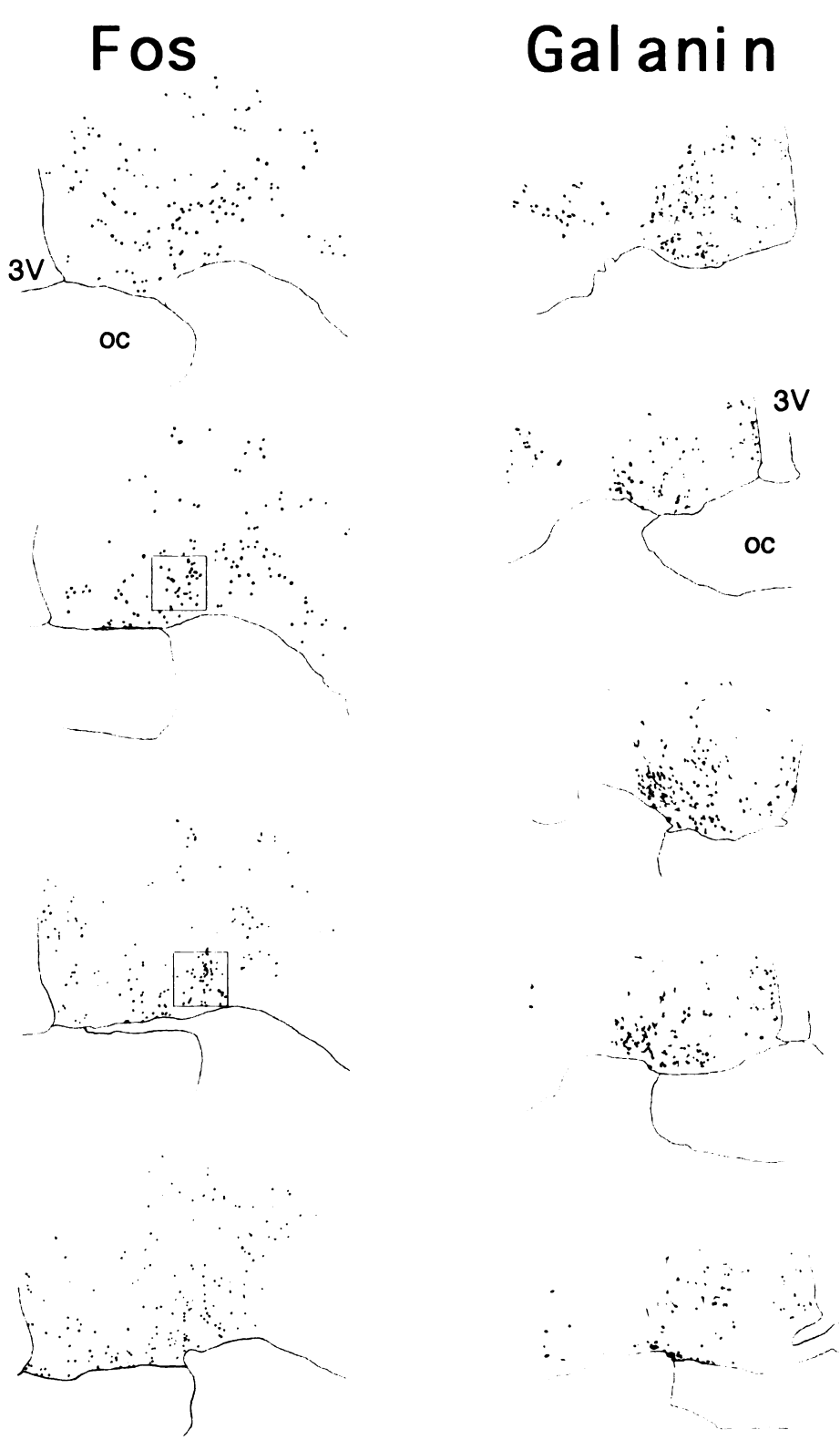
Fos
Galanin
3V
oc
3V
oc

Fos expression in the VLPO. The Fos+ cells in the VLPO were seen in locations similar to those reported for the rat (Sherin *et al.*, 1996), in the same area shown to contain GAL+ cells (see Figure 12); Fos+ VLPO cells began dorsal and rostral to the SCN and extended caudally to the level of the rostral SCN (see Figure 12). As shown in Figure 13, more Fos+ cells were found in the VLPO of animals perfused at ZT 20 than ZT 23 ($t_{(1,12)}$=2.337, p=0.038). Figure 14 shows photomicrographs of the VLPO from animals at each ZT. No difference in Fos+ cell number was found in the control area directly dorsal to the VLPO ($t_{(1,12)}$=0.182, p=0.859).

Fos expression in the thalamus. In the thalamus, a significant effect of time of perfusion on Fos expression was found only in the middle region of the PVT ($F_{(1, 12)}$=8.620, p=0.013), where there were more Fos+ cells at ZT 23 than at ZT 20. No differences were found in the anterior PVT ($F_{(1, 12)}$=4.122, p=0.065), posterior PVT ($F_{(1, 12)}$=0.367, p=0.556), the PVT as a whole ($F_{(1, 12)}$=2.333, p=0.153), or in the CMT($F_{(1, 12)}$= 1.187, p= 0.294). No correlations were significant (at $p<0.05$); however, trends were observed between Fos+ cell numbers in the PVT and VLPO (r=-0.460, p=0.0992), as well as between the middle PVT and CMT (r=0.483, p=0.086).

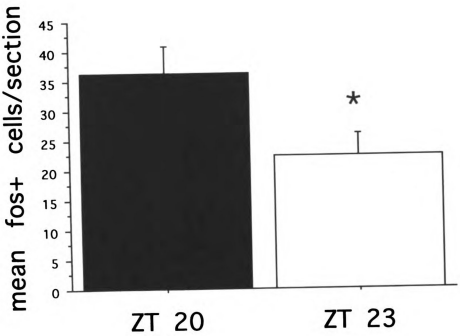

Figure 13. Fos+ cell number in the ventrolateral preoptic area (VLPO) of *Arvicanthis niloticus* at different zeitgeber times (ZT, hours after lights-on). More Fos+ cells were found in the VLPO at ZT 20 than ZT 23. *$p<0.05$.

Figure 14. Photomicrographs of the ventrolateral preoptic area (VLPO) of *Arvicanthis niloticus*. More Fos+ cells were found in the VLPO at zeitgeber time (ZT) 20 (top) than ZT 23 (bottom). Box = $(190\ \mu m)^2$, oc = optic chiasm.

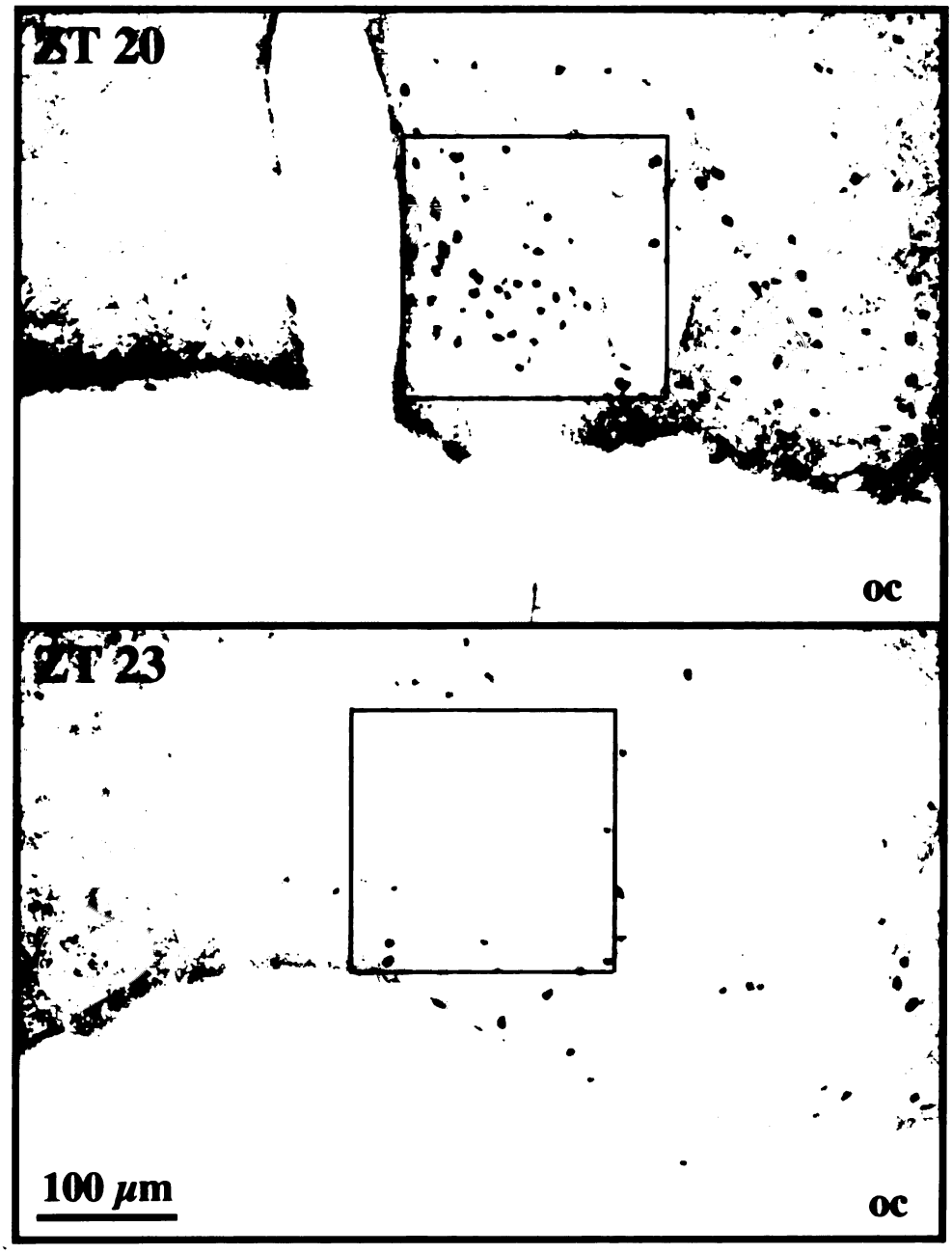
ZT 20
oc
ZT 23
100 μm
oc

Retinal afferents. A shown in Figure 15, very sparse retinal projections were seen in and around the VLPO. This very light retinal input to the VLPO was seen in both animals, and contrasts with the presence of a substantial number of labeled fibers seen caudal to the VLPO around the borders of the SON, as well as the very strong labeling seen in the SCN. No labeled fibers were seen in the PVT.

Discussion.

The studies described in this section of the dissertation are the first to document and describe the sleep-active VLPO in a diurnal species. The *Arvicanthis* VLPO resembles the region first described in the rat (Sherin *et al.*, 1996) in many aspects. First, the VLPO in grass rats, identified by giemsa staining (see Figure 11, top), is located in the ventral most part of the lateral preoptic area, medial to the HDB; the shape is slightly different than in rats, flaring out dorsally and laterally, rather than having a more triangular shape (see Figures 11, 12, and 14). The *Arvicanthis* VLPO appears to be located more medial than in rats, this is a consequence of the enlarged size of the optic chiasm relative to the rest of the brain in *Arvicanthis*, a diurnal animal. Second, VLPO cells in both rats and *Arvicanthis* contain the inhibitory neuropeptide GAL. It is

Figure 15. Photomicrographs of cholera toxin-β (CTβ)-labeled retinal projections to the hypothalamus and preoptic area of *Arvicanthis niloticus*. (A) Very few retinal projections were found in the ventrolateral preoptic area (VLPO) of *A. niloticus*. The box represents the 190 μm^2 area counted in experiments 4 and 5. Many projections were found near the supraoptic nucleus (SON, B) and suprachiasmatic nucleus (SCN, C), indicating successful transport of the tracer. 3V = third ventricle, ot = optic tract, oc = optic chiasm.

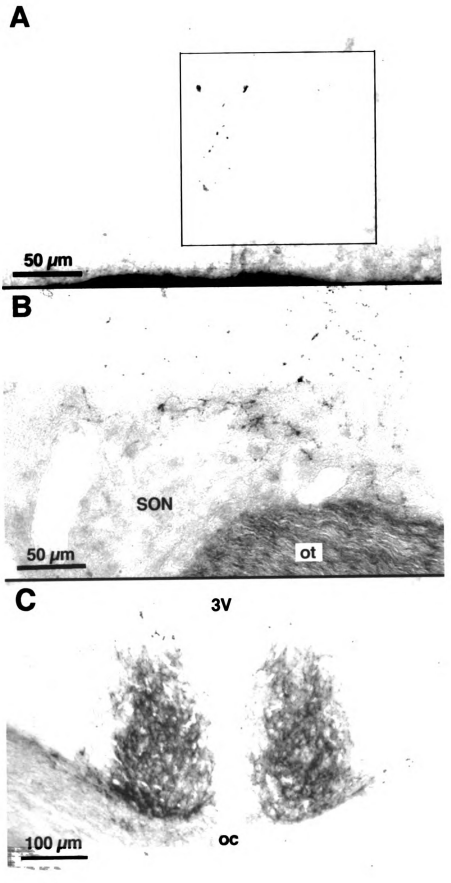
A
50 μm
B
SON
ot
50 μm
C
3V
100 μm
oc

postulated that, together with GABA, this peptide serves the inhibitory function ascribed to the VLPO (Sherin *et al.*, 1998). Third, the patterns of Fos expression indicates that the VLPO is sleep-active in *Arvicanthis* as well as in rats (Sherin *et al.*, 1996).

In *A. niloticus*, Fos expression within the VLPO increases at a time when the animals are inactive compared to when the animals are awake and active at the beginning of their dawn activity bout at ZT 23 (see Experiment 3). This increase in Fos expression during the inactive period seems to be restricted to the VLPO since time of perfusion did not affect Fos expression elsewhere in the preoptic area. However, these results most likely represent an underestimate of the amplitude of the daily rhythm of Fos in the VLPO of Nile grass rats because Fos expression in the VLPO is likely to decrease further after ZT23, as the animals become even more active and have spent more time without sleep. Furthermore, like other mammals, *Arvicanthis* presumably exhibit an increase in the amount of REM late in the sleep period, as SWS declines. Given that neuronal activity in the VLPO is thought to be involved specifically in SWS onset and maintenance (Sherin *et al.*, 1998; Sherin *et al.*, 1996), sampling of sleeping animals prior to ZT 20 may reveal even higher levels of VLPO Fos expression than were found in this study.

As described in the introduction, the VLPO is thought to send inhibitory projections to brain regions important in arousal and vigilance (Sherin *et al.*, 1998; Sherin *et al.*, 1996). The VLPO may also interact with other brain regions important in vigilance, such as the PVT. Fos expression in the middle region of the PVT increased at ZT 23, when the animals' activity increases and Fos expression in the VLPO was low. This supports the position that peak activity of the PVT and VLPO occur at different times in the sleep-wake cycle and leaves open the possibility that these two regions may have reciprocally inhibitory connections. Experiment 6 of this dissertation was designed in part to determine if the VLPO projects to the PVT in *A. niloticus*. However, functional studies ouside the scope of this dissertation are needed to determine if these connections are inhibitory.

For the most part, the functional and anatomical descriptions of *Arvicanthis* VLPO show it to be remarkably similar to the rat VLPO. However, one salient anatomical difference between the VLPO of rats and *Arvicanthis* is the degree to which retinal fibers project to that area. Retinal fibers were seen in apposition to Fos+ VLPO cells in the rat (Lu *et al.*, 1997), but in *A. niloticus*, only very sparse retinal projections were identified in the area in and around the VLPO (see Figure 15). The lack of labeling in the VLPO is not due to lack of

transport of the tracer as evidenced by labeling in the SCN as well as around the SON of both animals that receive CTβ injections.

Differential innervation of the VLPO by retinal fibers may be related to the discordant phase relationships between the light:dark cycle and the display of sleep in rats and *A. niloticus*. For example, light may promote sleep in rats, but not in diurnal species. Even after SCN lesions, nocturnal rats have longer sleep bouts during the light phase of the light:dark cycle (Mistlberger *et al.*, 1983). Further, the light:dark cycle has a powerful influence on the daily rhythms of feeding, drinking, and wheel running in rats with SCN lesions and fetal SCN grafts, whether or not the grafts restored free-running rhythms in these animals (Boer *et al.*, 1993). On the other hand, diurnal squirrel monkeys housed in constant light spend more time awake than their counterparts housed in a light-dark cycle (Wexler and Moore-Ede, 1985). These data demonstrate that light has direct effects on sleep and wakefulness, separate from the effect of light on circadian rhythms. The development of diurnality may involve not only a change in the phase relationship between the SCN and areas of the brain that control sleep, but also a change in the mechanisms that mediate the acute effects of light on these areas and on the display of sleep. Perhaps the absence of significant retinal projections to the

VLPO of *A. niloticus* reflects a lack of stimulation of sleep by light in this species. For example, in the same tissue used to examine retinal projections to the VLPO, no labeled fibers were seen in the PVT. The finding that *Arvicanthis* have fewer retinal projections to areas that are important in the control of the sleep/wake cycle (VLPO and PVT) suggests that diurnal animals' sleep cycles may be less affected by light than are nocturnal animals' sleep. Indeed, unlike the rat, diurnal chipmunks with SCN lesions do not show daily rhythms in activity when exposed to a light:dark cycle (Boer *et al.*, 1993; Sato and Kawamura, 1984b). The difference in the amount of retinal innervation to brain regions mediating sleep and arousal may account for this difference. Interestingly, in humans, few retniohypothalamic tract projections were seen rostral to the SCN, where the VLPO would be located (Dai *et al.*, 1998b).

In summary, these studies demonstrated that the VLPO of the diurnal *A. niloticus* increases its Fos expression during the rest phase of the cycle, when animals display behavioral indices of sleep. Thus, the VLPO of diurnal *Arvicanthis* is likely to serve the same function as in rats – modulating the onset and maintenance of SWS. The grass rat therefore appears to be an ideal animal model to compare how light, circadian, and homeostatic influences combine to affect sleep differently in diurnal and nocturnal species. The following study

uses *A. niloticus* to investigate how Fos expression changes over the light:dark cycle in the VLPO as well as other brain regions important in the sleep/wake cycle.

EXPERIMENT 5: Daily Rhythms in Fos expression in Brain Areas Related to the Sleep-Wake Cycle in the Diurnal Nile Grass Rat

The previous experiment demonstrated that the *Arvicanthis* VLPO contains a sleep-active cluster of cells similar to the rat VLPO. Because the VLPO is active during sleep, it should show a daily rhythm in activity similar to the sleep/wake pattern in *A. niloticus*. The study described below examines the Fos expression in the grass rat VLPO, as well as in the PVT, CMT, and TMN, over time points similar to those used in the experiment using laboratory rats (Experiment 1). Also, the Fos expression in histamine-containing cells was ascertained. It is predicted that these brain regions will show rhythms in Fos expression in *A. niloticus*, and that the rhythms will be out of phase with the rhythms seen in rats. If this prediction is confirmed, then it would support the hypothesis that differences in the sleep-wake cycle of nocturnal and diurnal animals are due to different patterns of activity in brain areas important in sleep and wakefulness.

Methods:

Animals. Twenty-four male *A. niloticus* were used in the following study. Animals were singly housed, and fed and watered *ad libitum* as described in Experiment 3. The animals were housed on a 12:12 light:dark cycle, with lights on at ZT 0.

Tissue Collection. The animals were perfused in pairs at 4 ZTs: ZT 0.5, ZT 5, ZT 13, and ZT 17, following an injection of Equithesin (1 ml, i.p.) in the animal room; at ZT 13 and 17, a light-tight hood was placed over the animals' heads in order to prevent light-induced Fos expression in the SCN and other brain areas. The animals were then perfused with PBS and PLP as described earlier (see Experiments 1 and 4) . Brains were postfixed for 24 hours and then transferred to 20% sucrose in PBS. The brains were sectioned at 30μm using a freezing microtome. The sections were divided into three sets and stored in cryoprotectant.

Fos and Histamine Immunocytochemistry. Every third section was processed for Fos immunocytochemistry (ICC) using a rabbit anti-fos primary antibody (Santa Cruz) as described in Experiment 1. Separately, the posterior half of the hypothalamus was subjected to double-label ICC for Fos and histamine. The standard protocol was used with some modifications. For Fos, the primary antiserum used was sheep anti-Fos (Cambridge, 1:1000) with normal donkey serum

(NDS), the secondary antiserum was donkey anti-sheep, and DAB-Ni was the chromagen. For histamine ICC, rabbit anti-histamine (Sigma, 1:1000) was used with NGS; the secondary antiserum was goat anti-rabbit, and DAB was the chromagen (3 min incubation for each chromagen). No immunostaining for histamine was detected after primary antibody deletion or preabsorbtion with histamine (100 μg/ml diluted serum; Sigma).

Microscopic Analysis. Brain regions were examined for Fos immunostaining using the same methods used in Experiment 1. The number of Fos+ cells in the VLPO was counted at 400X magnification using an optical grid (190 $\mu m)^2$. The PVT, CMT, and TMN were identified with the aid of the rat brain atlas (Paxinos and Watson, 1997). The PVT was divided into 3 subregions as described in Experiments 1 and 4, and the number of Fos+ cells was determined for each region at 250X magnification. The number of Fos+ cell in the CMT was determined at 250X magnification using an optical grid (300 $\mu m)^2$. The DTM was located in the posterior hypothalamus, on either side of the third ventricle; the number of Fos+ cells in one section containing the DTM was counted at 100X in an area of (120 $\mu m)^2$. The VTM was located caudal to the DTM, along the edge of the brain bilaterally in the posterior hypothalamus; the number of

Fos+ cells in a (150 μm)^2 grid was counted at 250X. This grid encompassed the magnocellular region of the VTM, which differed in size from the DTM. The data for each brain region were averaged to yield an average number of Fos+ cells per section. The data for each brain region were subjected to a one-way ANOVA, with the number of Fos+ cells per section as the dependent variable and the ZT as the independent variable; Fisher's PLSD was used for pairwise comparisons. Correlations between brain regions with respect to the number of Fos+ cells/section were also determined using Pearson's r. Differences and correlations were considered significant if $p<0.05$.

For the histamine double-label ICC, the number of histamine+ (hist+) cells as well as the number of hist+ cells containing Fos were counted in the lateral group of hist+ cells (including the VTM) using an Olympus BX 60 microscope at 400X. The percent of hist+ cells containing Fos was calculated for each animal. Because the data were expressed as percentages, they were subjected to an arc-sine transformation to normalize the distribution. The data were then subjected to a one-way ANOVA, with ZT as the independent variable and percent hist+ cells containing Fos as the dependent variable.

Results:

As shown in Figures 16, ZT significantly affected the number of Fos+ cells in the VLPO ($F_{(3,20)}$=3.486, p<0.05). The number of Fos+ cells at ZT 17 was significantly greater than the number of Fos+ cells at ZT 5 and ZT 13 (p<0.05; see Figure 17, top). As shown in Figure 16, Fos+ cell number varied significantly across time of day in the PVT as a whole ($F_{(3,20)}$=8.439, p<0.001). There were more Fos+ cells in the PVT at ZT 0.5 than at any other time point (p<0.05; see Figure 17, middle); More Fos+ cell were found in the PVT at ZT 5 than at ZT 13 (p<0.05). When the PVT subregions were analyzed, a significant rhythm of Fos expression was found in the middle PVT ($F_{(3,20)}$=4.605, p<0.05; see Figure 17) and posterior PVT ($F_{(3,20)}$=7.861, p<0.01), but not in the anterior PVT ($F_{(3,20)}$=1.782, p=0.183). A similar rhythm in Fos expression was seen in each PVT subdivision; the data for the PVT subdivisions were pooled and the data for the entire PVT Fos expression were used for the correlation analyses (see Table 3).

No significant differences in Fos+ cell number across the light:dark cycle were found in the CMT ($F_{(3,20)}$=1.251, p=0.318; see Figure 16). However, as shown in Table 3, a significant correlation was found between Fos+ cell number in the PVT and the CMT (r=0.794, p <0.0001). A significant rhythm in the number of Fos+

Figure 16. Fos+ cell number in the ventrolateral preoptic area (VLPO) of *A. niloticus* housed on a 12:12 light:dark cycle at different zeitgeber times (ZT; hours after lights-on). Fos+ cell number in the VLPO increased at ZT 17, when these animals are likely to be sleeping. Fos+ cell number in the paraventricular nucleus of the thalamus (PVT) showed a rhythm over the L:D cycle, with Fos expression peaking at ZT 0.5. There was no significant rhythm in Fos expression in the centromedial nucleus of the thalamus (CMT). A rhythm in Fos expression was seen in the ventral tuberomammillary nucleus (VTM), with Fos+ cell number lowest at ZT 17. No rhythm in Fos+ cell number was seen in the dorsal TMN (DTM). In all graphs, a. significantly different from ZT 0.5, b. significantly different from ZT 17, c. significantly different from ZT 5, ($p<0.05$).

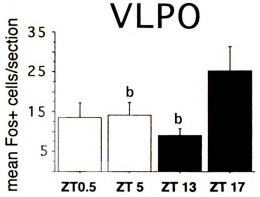
VLPO
mean Fos+ cells/section
35
25
15
5
b
b
ZT0.5
ZT 5
ZT 13
ZT 17

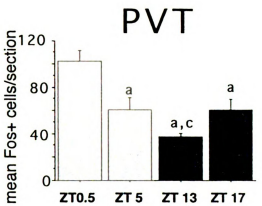
PVT
mean Fos+ cells/section
120
80
40
0
a
a,c
a
ZT0.5
ZT 5
ZT 13
ZT 17

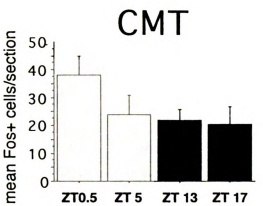
CMT
mean Fos+ cells/section
50
40
30
20
10
0
ZT0.5
ZT 5
ZT 13
ZT 17

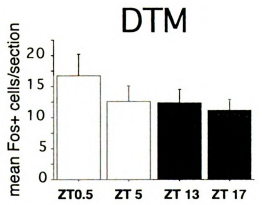
DTM
mean Fos+ cells/section
20
15
10
5
0
ZT0.5
ZT 5
ZT 13
ZT 17

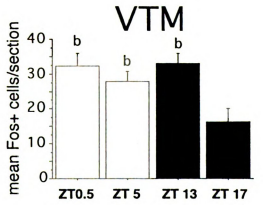
VTM
mean Fos+ cells/section
40
30
20
10
0
b
b
b
ZT0.5
ZT 5
ZT 13
ZT 17

Figure 17. Photomicrographs of Fos+ cells in the ventrolateral preoptic area (VLPO; top), paraventricular thalamic nucleus (PVT; middle), and centromedial thalamic nucleus (CMT; bottom) at different zeitgeber times (ZTs) in *Arvicanthis niloticus*. More Fos+ cells were seen in the VLPO at ZT 17 than at any other time point, including ZT 13 as shown here. The PVT contained more Fos+ cells at ZT 0.5 than ZT 13. Lastly, no significant rhythm in Fos expression was seen in the CMT. 3V = third ventricle, oc = optic chiasm.

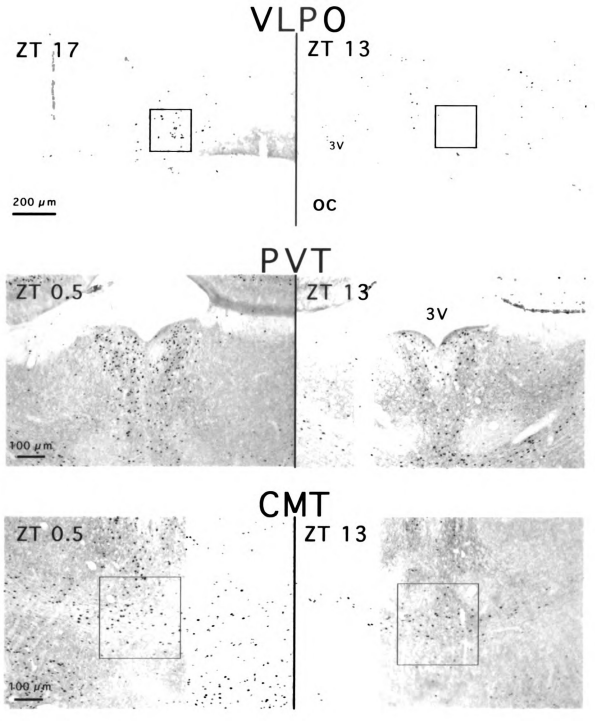
VLPO
ZT 17
ZT 13
3V
200 μm
OC
PVT
ZT 0.5
ZT 13
3V
100 μm
CMT
ZT 0.5
ZT 13
100 μm

Table 3

Correlations between Fos+ cell number in brain regions in *A. niloticus*

	VLPO	PVT	CMT	VTM	DTM
VLPO	---	0.281	0.252	-0.237	0.200
PVT	---	---	0.794**	0.168	0.370
CMT	---	---	---	0.414*	0.319
VTM	---	---	---	---	0.320
DTM	---	---	---	---	---

VLPO, ventrolateral preoptic area; PVT, paraventricular thalamic nucleus; CMT, centromedial thalamic nucleus; VTM, ventral tuberomammillary nucleus; DTM, dorsal tuberomammillary nucleus. *$p<0.05$, **$p<0.0001$

cells was found in the VTM ($F_{(3,20)}$=4.330, p<0.05), where Fos cell number at ZT 17 was less than any other time point (p <0.05; see Figures 18 and 16). No effect of ZT was found in the DTM ($F_{(3,19)}$=0.646, p=0.595). As shown in Table 3, Fos+ cell numbers in the CMT were also positively correlated with those for the VTM (r=0.414, p <0.05).

As shown in Figure 19 (top), some hist+ cells in and around the VTM contained Fos immunoreactivity. There was a significant rhythm in Fos expression within hist+ cells of the VTM ($F_{(3,18)}$=5.965, p<0.01). Specifically, more hist+ cells contained Fos at both ZT 0.5 and ZT 13 than at ZT 17; and more double labeling was seen at ZT 13 than at ZT 5 (p<0.05).

Discussion:

This study ascertained that the VLPO of the diurnal *A. niloticus* shows a significant rhythm in Fos expression in animals kept in a 12:12 light:dark cycle. Fos+ cell number increased in the middle of the night, at ZT 17. As shown in Experiment 3, *A. niloticus* are most likely to be sleeping in the middle of the dark phase. The pattern of Fos expression seen in the VLPO of *Arvicanthis* is therefore predictable from these animals' sleep patterns: at ZT 17, when VLPO Fos expression is high, grass rats are likely to be sleeping, whereas

Figure 18. Photomicrographs of Fos expression in the ventral (VTM) and dorsal (DTM) tuberomammillary nuclei in *Arvicanthis niloticus* at different zeitgeber times (ZTs). Fewer Fos+ cells were found in the VTM at ZT 17 than at any other time point. No rhythm in Fos expression was found in the DTM. Boxes represent areas analyzed in Experiment 5. 3V = third ventricle. Box over the VTM on the lateral edge of the brain $(150\mu m)^2$, box over the DTM near 3V = $(120\ \mu m)^2$.

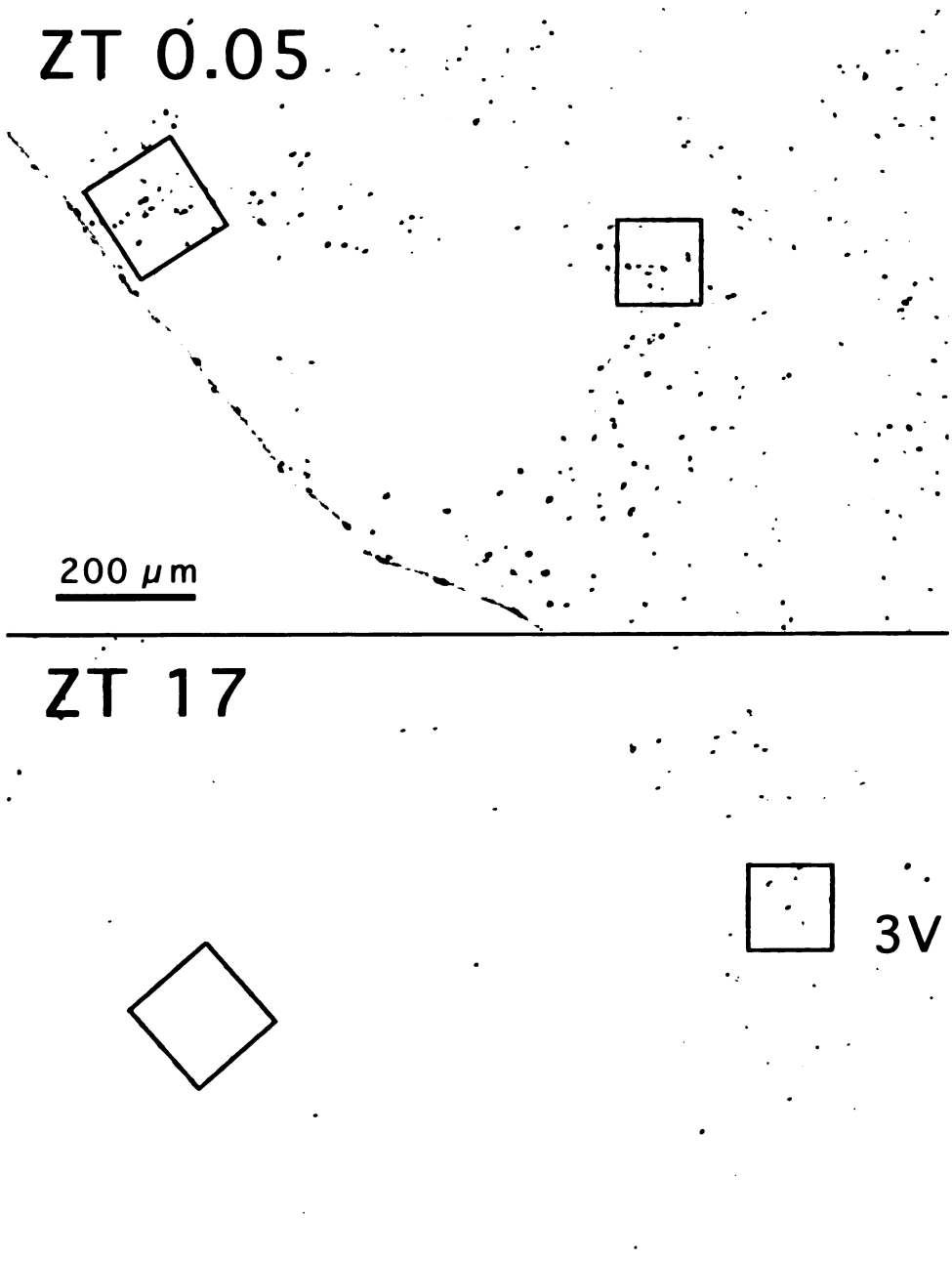
ZT 0.05
200 μm
ZT 17
3V

Figure 19. top: Photomicrograph of histamine-containing cells (hist+, beside asterisks) and Fos+ cells (arrows) in the ventral part of the tuberomammillary nucleus (VTM); many histamine-containing cells in the VTM were Fos+ (arrowheads). bottom: More hist+ cells in the VTM contained Fos at zeitgeber time (ZT) 0.5 and ZT 13 than at ZT 17; more double-labeled cells were also found at ZT 13 than ZT 5. The distribution of the proportions of hist+ cells containing Fos was normalized using the arcsin transformation. b. different from ZT 17. d. different from ZT 5.

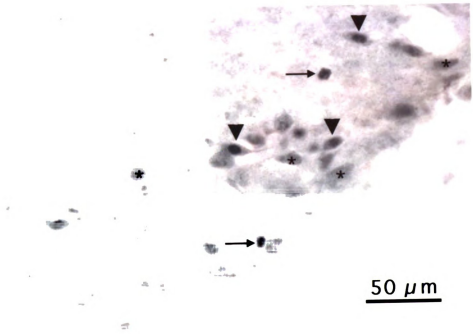
50 μm

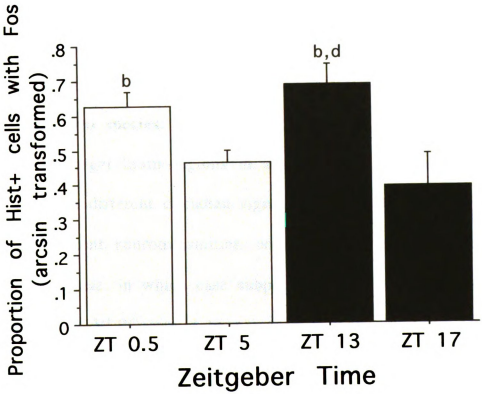
Proportion of Hist+ cells with Fos
(arcsin transformed)
.8
.7
.6
.5
.4
.3
.2
.1
0
b
b,d
ZT 0.5
ZT 5
ZT 13
ZT 17
Zeitgeber Time

they are unlikely to be sleeping when VLPO Fos expression is low, at ZT 0.5 - ZT 13. Taken together with data from Experiment 4, these results indicate that VLPO Fos expression increases throughout the middle and late night in *Arvicanthis*, and diminishes just prior to lights-on. The presence of a rhythm in the VLPO suggests that the circadian clock of the SCN influences the activity of the VLPO. However, given the presence of very few direct projections from the SCN to the VLPO in rats (Experiment 2), this circadian regulation is probably imposed via relay sites or via humoral rather than axonal SCN outputs.

The pattern of Fos expression seen in *Arvicanthis* differs considerably from the pattern seen in the rat VLPO (increased Fos at ZT 5 and ZT 13). Therefore, the circadian control of the VLPO differs between these two species. The critical difference in the circadian signal sent to target brain regions in diurnal and nocturnal animals may lie in (1) a different circadian signal emanating from the SCN, such as a different neurotransmitter, or (2) the same signal emitted at a different phase, in which case subpopulations of SCN cells projecting to the VLPO would be expected to have different patterns of activity over the circadian cycle in the two species. (3) There may also be an alteration of the circadian signal by an intermediary brain region. As described earlier (Experiment 2), the sPVHz, may play a

role in relaying the circadian signal to the VLPO. If this is the case, then the activity pattern of these sPVHz neurons should differ between species. Lastly (4), there may be differential responsiveness of target regions to similar circadian signals. If this is the case, then the process of modifying the timing of activity of a mammalian species over evolution (i.e., from nocturnal to diurnal, after a nocturnal bottleneck) would have involved a change in responsiveness of each individual SCN target region to a common signal.

This study also showed that the PVT of *Arvicanthis* displays a daily rhythm in Fos expression. For the most part, the pattern seen in the PVT is predictable from the activity pattern of this species: at the time of these animals' morning activity bout (ZT 0.5), Fos expression is highest in the PVT. The pattern seen during the dark phase, however, does not match expectations: Fos expression in the PVT does not increase at ZT 13, after these animals show a moderate activity peak, and it does not decrease at ZT 17, when they are likely to be sleeping and when Fos expression is increased in the VLPO. These observations suggest that the PVT may be more important in inducing wakefulness early in the light phase compared to the rest of the cycle. Other brain regions may be responsible for inducing wakefulness later in the day.

Although no rhythm was found in the DTM in grass rats, a significant rhythm in Fos expression was seen in the VTM, the region of the TMN shown to receive GABAergic and Galaninergic projections from the VLPO in rats (Sherin *et al.*, 1998). Fewer Fos+ cells were found in the VTM of *Arvicanthis* taken at ZT17 than at any other time point. Experiment 3 demonstrated that *Arvicanthis* are most likely to be sleeping in the middle of the night, when VTM Fos expression is lowest. Further, this pattern is the opposite as that seen in the VLPO, where Fos+ cell number was increased at ZT 17; given that the VTM and VLPO have mutually inhibitory connections (Sherin *et al.*, 1998), the decrease in Fos expression in the VTM at ZT 17 is not surprising. Since no rhythm in Fos expression was found in the rat TMN, the circadian modulation of Fos expression in the grass rat VTM may represent a species difference in the mechanism through which the circadian clock controls the activity cycle.

As previously described, evidence suggests that the TMN is more important in transitory, phasic events contributing to arousal than sustaining tonic activation of wakefulness in rats (Szymusiak *et al.*, 1989). The contribution of the TMN to the overall activity pattern may differ between species, however. The reduction in Fos expression in the VTM in *Arvicanthis* seen during the middle of the night (ZT 17) may reflect a circadian signal to the TMN in *Arvicanthis*

that is weak or absent in rats. Reduced activity in the TMN may facilitate the display of sleep in this diurnal species.

The importance of histamine in the peaks of locomotor activity in grass rats is supported by data from this experiment showing that Fos expression in histaminergic cells within the VTM peaks at ZT 0.5 and ZT 13. Therefore, histaminergic cells are most active at the times of the day when this species shows the strongest activity, at the light-dark transitions (see Experiment 3). This may contribute to the crepuscular nature of the *Arvicanthis* activity pattern. Further, since Fos expression in hist+ cells did not significantly decrease from ZT 0.5 to ZT 5 in grass rats, histamine may also promote wakefulness during the daytime and therefore contribute to the diurnal portion of its activity cycle. It is possible that the sudden change in lighting conditions startled the animals, inducing Fos expression in hist+ VTM cells at those times. However, the animals were raised under similar lighting conditions, allowing them to acclimate to the sudden change in lighting. Further, if stress caused the increase in Fos expression in hist+ VTM cells at the light:dark transitions, then the stress should have induced PVT Fos expression at both light:dark transitions, not at only ZT 0.5 (not ZT 13), as was found in this study.

Considering the combined patterns of Fos expression in the PVT and VTM, it is possible that, in *A. niloticus*, these two brain regions

contribute in distinct but complementary ways to the overall activity pattern of these animals. This introduces a possible difference between diurnal and nocturnal animals not previously considered – that species differences in activity patterns may involve differential contributions of distinct arousal systems to overall activity, and that the strength of circadian modulation (as opposed to only the pattern of modulation) of these arousal systems differ between species. Specifically, the circadian signal to the VTM may contribute more to wakefulness in *Arvicanthis* compared to rats.

No significant rhythm in Fos expression was found in the CMT of grass rats. This is in contrast to the significant pattern seen in the rat, and represents further evidence that wakefulness is supported by different brain arousal systems in the two species. Although no rhythm was seen in the CMT of *A. niloticus*, a significant positive correlation was seen between Fos expression in the PVT and CMT. Similar to the rat, since the PVT and CMT are activated together within the animal, this supports the assertion that these two brain regions both contribute to wakefulness. Additionally, there was a significant correlation between Fos expression in the CMT and VTM. Both the activity of intralaminar nuclei and posterior hypothalamic neural activity are associated with desynchronization of the EEG (Glenn and Steriade, 1982; Schwartz *et al.*, 1991). Together, the

activity of the CMT, PVT, and histaminergic nuclei may account for different components of arousal and wakefulness in this species.

Lastly, the possible effects of light on Fos expression in the VLPO and PVT must be taken into account when evaluating the data from these two species. For example, the presence of significant retinal projections to VLPO in the rat, nearly absent in *Arvicanthis*, implies that light may stimulate activity of the VLPO and contribute to its rhythmic expression of Fos in rats (Lu *et al.*, 1997), but not in *Arvicanthis*. Further, the presence of retinal projections in the rat PVT, a region that decreases Fos expression in the daytime, suggests that light may inhibit neuronal activity in the PVT. The absence of retinal projections to the PVT in *A. niloticus* implies that, contrary to the rat, light stimulation is not likely to directly contribute to activity in the PVT of this species. In rats, the light:dark cycle has a powerful effect on daily activity even in the absence of a circadian clock (Boer *et al.*, 1993). The present findings suggest that this effect of light may be absent or diminished in the diurnal rodent examined here (also see discussion in Experiment 4).

Thus far, it has been demonstrated that both nocturnal rats and diurnal *Arvicanthis* show rhythms in brain areas affecting sleep and wakefulness, and that these rhythms differ between the two species, often mirroring their activity patterns. The presence of a rhythm in

the PVT, a known target region of the SCN in rats, suggests that the SCN is important in the regulation of rhythmic Fos expression in this thalamic region. However, SCN projections to the PVT have yet to be documented in *Arvicanthis*. The next experiment first compares the profile of afferent input to the PVT in rats and *Arvicanthis*, with special attention paid to the SCN cells projecting to the PVT. Then, the phenotype of SCN neurons projecting to the SCN is compared in the two species.

EXPERIMENT 6: Suprachiasmatic Nucleus Projections to the Paraventricular Thalamic Nucleus in Rats and Nile Grass Rats

Previous experiments have revealed rhythms in Fos expression in the PVT in both rats and *A. niloticus* (see Experiments 1 and 5). It is therefore likely that the PVT receives circadian input from the SCN. Whereas the presence of SCN projections to the VLPO in rats is questionable, the existence of SCN projections to the PVT is undisputed (Watts *et al.*, 1987). However, no data have been collected on the projection patterns of the SCN in *Arvicanthis*. Therefore, the first aim of this study was to determine whether the SCN projects to the PVT in *A. niloticus* and, moreover, to compare the pattern of afferent input to the PVT between *Arvicanthis* and rat.

The SCN is a heterogeneous nucleus with numerous neuronal subpopulations, many of which can be identified by their peptide content (Inouye and Shibata, 1994). For example, many neurons in the SCNdm of the rat contain AVP, whereas the ventrolateral portion of the SCN (SCNvl) is characterized by cells containing vasoactive intestinal polypeptide (VIP) as well as gastrin releasing peptide (GRP) (Inouye and Shibata, 1994). It has been shown that the SCN exhibits a daily rhythm in the content and release of AVP, as well as AVP concentration in the CSF, which peaks in the light phase in rats

and other species, both nocturnal and diurnal (Cagampang *et al.*, 1994; Kalsbeek *et al.*, 1995; Noto *et al.*, 1983; Reppert *et al.*, 1987; Uhl and Reppert, 1986). In spite of these similarities in AVP rhythms in diurnal and nocturnal mammals, AVP neurons of the SCN may function differently in rats and *A. niloticus*. For example, recent data have shown that nocturnal rats show little colocalization of AVP and Fos in the SCN, whereas the diurnal *Arvicanthis* show a rhythm in Fos+ AVP cells which peaks in the light phase (Rose *et al.*, 1999). Since AVP neurons have been found to project to the PVT in rats (Watts and Swanson, 1987), it is possible that the regulation of target regions by vasopressinergic neurons in the SCN differs between species with different activity patterns.

Gastrin releasing peptide also shows a rhythm in the SCN of rats, peaking in the light phase of the cycle (Inouye and Shibata, 1994). The distribution of GRP+ cells within the SCN of grass rats is concentrated in the center of the nucleus, which differs from that seen in the rat. Also, whereas GRP+ cells often express Fos in rats (Romijn *et al.*, 1996), few GRP cells contain Fos in the *Arvicanthis* SCN (Katona *et al.*, 1998).

The different pattern of rhythmic expression of Fos in the PVT in rats and *Arvicanthis* may be due to the effect of different subsets of SCN neurons projecting to the PVT. Thus, the phenotype of PVT-

projecting cells, identified by peptide content, may differ between species. The second aim of the following study was therefore to compare the numbers AVP+ and GRP+ SCN neurons projecting to the PVT in rats and *Arvicanthis*.

Methods:

Animals. Thirty-five rats and thirteen *A. niloticus* were used in the following study. Animals were housed as described in Experiments 1 and 3, but were individually housed after surgery.

CTβ microinjection. In each animal, CTβ was microinjected into the PVT. The anterior PVT was targeted because it has been demonstrated that the SCN preferentially projects to the anterior portion of the PVT in rats (Watts *et al.*, 1987) and hamsters (Morin *et al.*, 1994). For rats, the standard protocol for stereotaxic microinjection was used (see Experiment 2), except that 20 nl CTβ was microinjected into the PVT using the following coordinates: AP −1.2 to −1.4 , ML ± 0.0, DV −5.1 to 5.3.

A. niloticus were injected with Nembutal (0.95 ml/kg) and the tops of the heads were shaved; small amounts of the inhalant anaesthetic metofane (methoxyflurane, Pitman-Moore) was also used. The animals were placed in the stereotaxic apparatus with the

bite bar at –5.0. An injection of Lidocaine (0.05 ml, s.c.) was given just under the skin on the skull, and artificial tears (the Butler Company) were applied to the eyes to prevent drying. An incision was made through the skin, and bregma was exposed. The following coordinates were used for the PVT in *Arvicanthis*: AP +0.8, ML ±0.0, DV –3.9 or –4.0. cholera toxin-β was then slowly injected into the PVT (20 nl), as described in Experiment 2. After surgery, gelfoam was placed on the skull, wounds were closed with autoclips, animals were given saline (0.5 ml, i.p.) and buprenex (0.1 ml, i.p.) to ease recovery; antiseptic ointment (Novalsan) was placed on the wound, and animals were placed alone in the cage which sat upon a heating pad until the animal awakened. The health of the animals was evaluated the morning after surgery.

Perfusion and Tissue Collection. Two days after surgery, animals were perfused. All *Arvicanthis* were perfused in the daytime. Rats were perfused at either ZT 5 or ZT 17. Animals were given an overdose of Nembutal (1.0 ml for *R.n.*, 0.5 ml for *A.n.*), and were then perfused as described earlier (Experiments 1 and 3). Brains were removed and postfixed in PLP for 4 hr (*R.n.*) or 2 hr (*A.n.*). All brains were sectioned into 30μm sections into 4 sets (*R.n.*) or 3 sets (*A.n.*). Sections were taken starting at the septal area and

extending through the hypothalamus to the rostral portion of the midbrain. Sections were stored in cryoprotectant for later use.

Immunocytochemistry. One set of sections was processed for CTβ-ICC as described in Experiment 2. Next, using the brains with the best PVT injections, double-label immunocytochemistry was performed for CTβ plus either GRP or AVP using the standard protocol with the following modifications. Brain sections were rinsed and incubated in the first blocking serum (NDS) followed by the first primary antiserum, rabbit anti-AVP or -GRP (1:10,000; Peninsula Laboratories, Inc.) for 1 (GRP) or 2 (AVP) nights. After rinsing, the tissue was incubated in the first secondary antiserum, biotinylated donkey anti-rabbit (1:500 for AVP; 1:400 for GRP; Jackson Laboratories). After the ABC incubation, sections were exposed to DAB for 2 min (AVP) or 5 min (GRP). The tissue was rinsed before being processed for CTβ-ICC (See experiment 2). The second chromagen used for CTβ immunostaining was SG (Vector Laboratories; blue stain). Sections were mounted onto gelatin-coated slides, dehydrated, and slides were affixed with coverslips.

Microscopy. First, the afferent projection patterns of the PVT in rats and *A. niloticus* were examined, with special attention paid to the SCN of both species; the brains containing the best PVT injections

were used. Second, the colocalization of CTβ with the peptides (AVP and GRP) was analyzed. Cellular peptide content and colocalization with CTβ were analyzed using camera lucida drawings of the SCN of 3 rats, as well as 3 Nile grass rats for GRP staining, and 8 Nile grass rats for AVP staining. Each section containing the SCN was drawn at 500X magnification (40X objective), and the locations of cells immunopositive for the peptide, CTβ, or both were indicated on the drawings. Only the cases where the SCN contained at least 25 CTβ+ cells were included in the analysis of peptide content. The numbers of double-labeled cells and CTβ+ cells were counted, and the percent of total CTβ+ cells containing each peptide was analyzed using a Mann-Whitney U (nonparametric) test to determine if there was a species difference in the percent of CTβ+ cells colocalized with each peptide.

Results:

The SCN of both rats and *Arvicanthis* contained retrogradely labeled CTβ+ neurons (Figures 19-22). The pattern of labeled cells in the rat SCN was similar to that described in Watts, *et al.* (1987), with labeled cells slightly more concentrated in the outer aspects of the SCN, including the sPVHz (Watts *et al.*, 1987), and in the dorsal

Figure 20. The injection sites within the paraventricular thalamic nucleus (PVT) in rats (n=3) used in comparisons with *Arvicanthis niloticus*. Brain sections are organized from rostral (top left) to caudal (bottom right). The PVT is shaded and the injections sites are outlined. 3V = third ventricle, sm = stria medullaris, f = fornix, IL = intralaminar thalamus, LD = lateral dorsal thalamus, Hb = habenula.

LD
Hb
IL
sm
t
3V

Figure 21. Pattern of CTβ+ retrogradely labeled neurons in the suprachiasmatic nucleus (SCN) of rats after injection of the tracer into the anterior paraventricular thalamic nucleus (PVT, see Figure 20) of rats. Brain sections are organized from rostral (upper left) to caudal (lower right). Cells containing CTβ were found throughout the SCN, as well as just dorsal to the SCN. 3V = third ventricle, oc = optic chiasm.

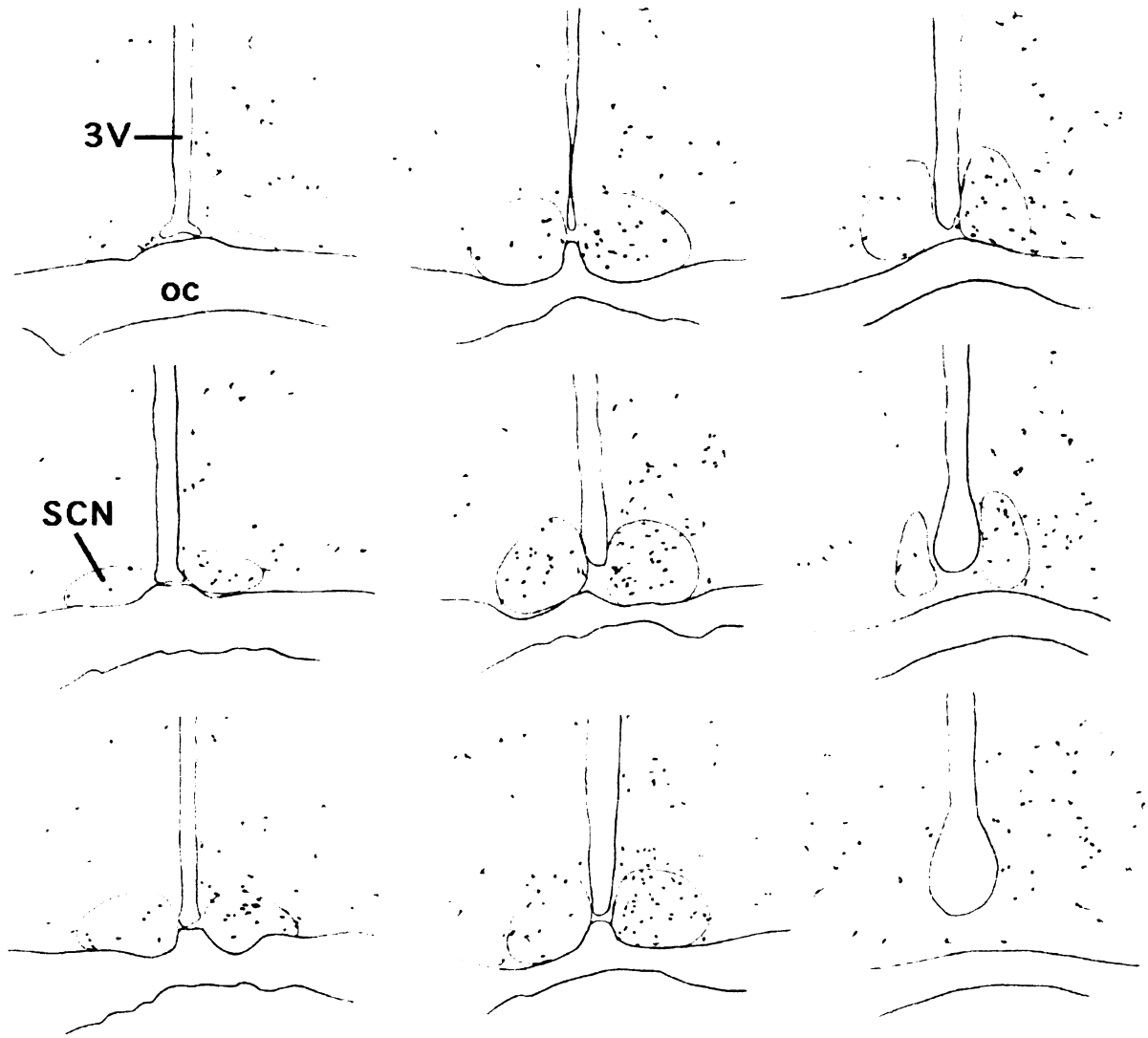
3V
OC
SCN

Figure 22. The injection sites within the paraventricular thalamic nucleus (PVT) in *Arvicanthis niloticus* (n=5) used in comparisons with the rat. Brain sections are organized from rostral (top left) to caudal (bottom right). The PVT is shaded and the injections sites are outlined. 3V = third ventricle, sm = stria medullaris, f = fornix, IL = intralaminar thalamus, LD = laterodorsal thalamus, Hb = habenula.

Figure 23. Pattern of CTβ+ retrogradely labeled neurons in the suprachiasmatic nucleus (SCN) of *Arvicanthis niloticus* after injection of the tracer into the anterior paraventricular thalamic nucleus (PVT, see Figure 22). Cells containing CTβ were found throughout the SCN, as well as just dorsal to the SCN. 3V = third ventricle, oc = optic chiasm.

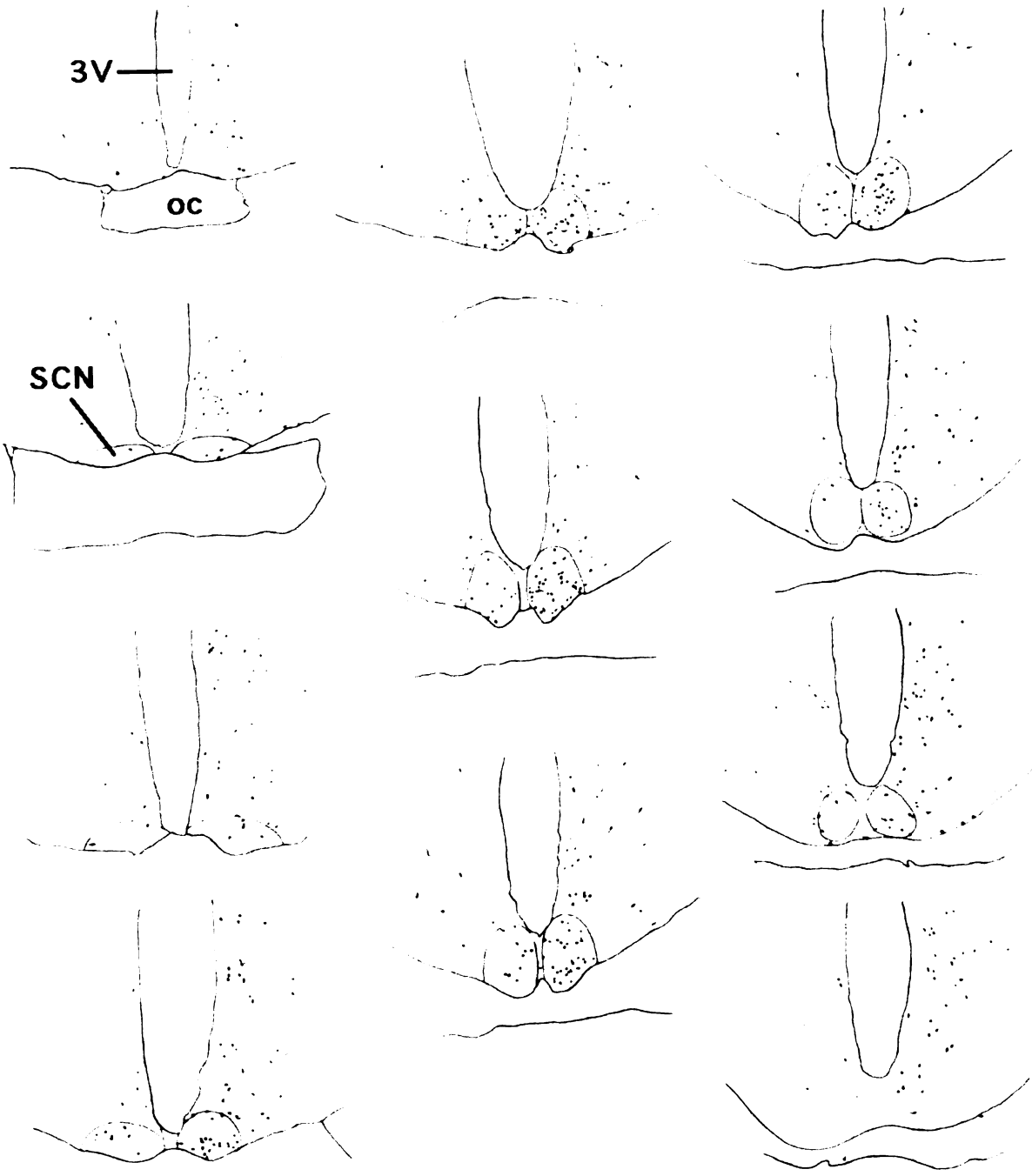
3V
OC
SCN

portion of the SCN in the rostral aspects of the nucleus (Figure 21). No such bias was observed in the labeling pattern in *A. niloticus*; in this species, PVT-projecting neurons were distributed more evenly throughout the SCN.

Vasopressinergic neurons were concentrated in the SCNdm in rats, but were distributed in a ring-like shape, avoiding the core of the SCN in *Arvicanthis*, as described in Rose, et al. (Rose *et al.*, 1999; see Figure 24). Many CTβ+ cells in the SCN were labeled for AVP (AVP+) in both rats and *Arvicanthis* (Figure 25; Table 4). However, no species difference was found in the percent of CTβ+ cells that were also AVP+ ($U=11.00$; $p = 0.838$). It should be noted that the percent of CTβ+ cells containing AVP followed a bimodal pattern, with two out of the 3 *Arvicanthis* with the most rostral PVT injections containing very few double-labeled cells in the SCN (1.790% of CTβ+ containing AVP; the third of the rostral injections was not an outlier) compared to more caudally placed injections.

Cells containing GRP (GRP+) in the SCN of rats were located in the SCNvl (Figure 24), but were concentrated in the middle (core) portion of the SCN in *Arvicanthis*. Interestingly, regions containing AVP and GRP were mutually exclusive in both species, with AVP+ cells forming a ring around GRP+ cells in the middle of the SCN in

Figure 24. Photomicrographs of the suprachiasmatic nucleus (SCN) of rats (*R.n.*, left column) and *Arvicanthis niloticus* (*A.n.*, right column) containing cells labeled with cholera toxin β (CTβ; blue), which project to the paraventricular thalamic nucleus (PVT). The photomicrographs on the top illustrate immunolabeling for arginine vasopressin (AVP; brown staining), which was concentrated in the dorsomedial portion of the SCN in rats and the outer aspects of the SCN in *A. niloticus*. Many CTβ+ cells were contained AVP in both rats and *A. niloticus*. The photomicrographs on the bottom illustrate gastrin releasing peptide (GRP; brown staining; left column) immunostaining in the SCN. Cells containing GRP were located in the ventrolateral aspects of the SCN in rats, but were concentrated in the center of the SCN in *A. niloticus*. Few CTβ+ cells contained GRP in either species. 3V = third ventricle, oc = optic chiasm.

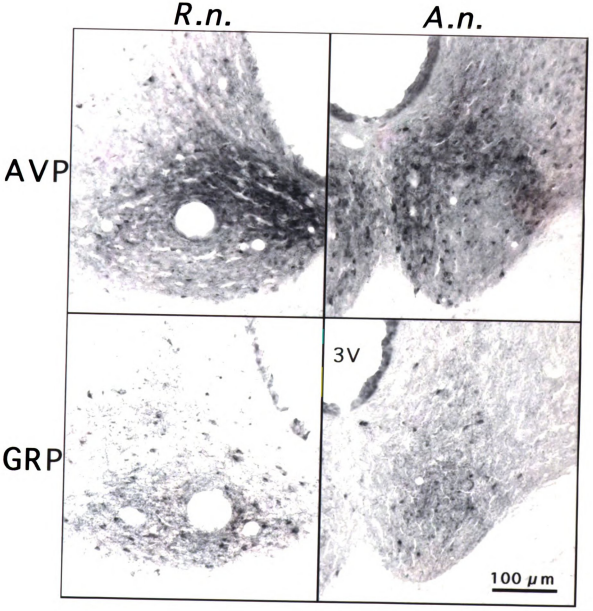
R.n.
A.n.
AVP
GRP
3V
100 μm

Figure 25. Photomicrographs of neurons in the suprachiasmatic nucleus of rats (A and B) and *Arvicanthis niloticus* (C). The SCN of both species contained cells that were retrogradely-labeled / cholera toxin-immunopositive (CTβ+; blue cells, indicated by arrows) projecting to the paraventricular thalamic nucleus (PVT). Many cells in the SCN contain vasopressin (AVP; brown staining; next to asterisks), and a portion of the CTβ+ cells in both species contain AVP (double-labeled cells indicated by arrowheads).

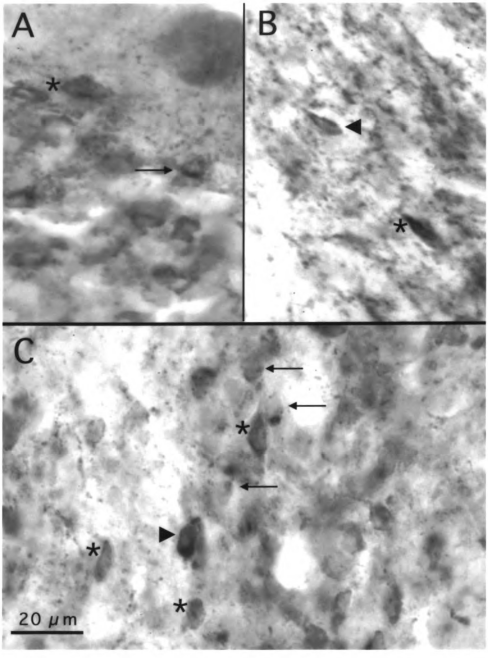
A
B
C
20 μm

Table 4

Peptide Content of SCN cells projecting to PVT
in rats and *A. niloticus*

Mean (±SEM) percent CTβ+ cells in SCN containing neuropeptides		
	AVP	GRP
Rattus Norvegicus (rat) n=	8.868% ±1.021 3	0.648% ± 0.341 3
Arvicathis niloticus (Nile grass rat) n=	6.464% ±1.404 8	0.749% ± 0.252 4

grass rats, and AVP in the SCNdm and GRP in the SCNvl in rats. The number of GRP+ cells in the SCN differed greatly within species (ranging from 93 to 300 in *R.n.*, and from 43 to 103 in *A.n.*). Very few CTβ cells in the SCN of either species contained GRP (Table 4), and no species difference was found (U=5.50; p = 0.860). The total number of cells containing CTβ after double labeling with GRP was 229.333 ± 115.609 in rats and 200.75 ± 63.700 in *A. niloticus*. In brain sections immunostained for both AVP and CTβ, 192.00 ± 92.049 CTβ+ cells were found in the SCN of rats, and 106.63 ±26.660 in *Arvicanthis*, indicating that fewer CTβ cells were detected in the sections labeled for AVP compared to GRP. Lastly, the PVT of rats and *Arvicanthis* contained fibers immunopositive for both AVP and GRP (Figure 26).

After successful injections of the PVT of rats (Figure 20), the distribution of CTβ+ cells in the rat outside the SCN was similar to that described in the literature (Cornwall and Phillipson, 1988). Many CTβ+ neurons were located in the most anterior and medial portion of the reticular thalamic nucleus (Rt), abutting the zona incerta, which also contained PVT-projecting cells. Neurons containing CTβ were found in the LS, BST, meA, and a few cells were

Figure 26. The paraventricular thalamus (PVT) of rats (left column) and *Arvicanthis niloticus* (right column) contained fibers immunopositive for vasopressin (AVP, top row) and gastrin releasing peptide (GRP; bottom row). Fibers are indicated by arrows. 3V = third ventricle.

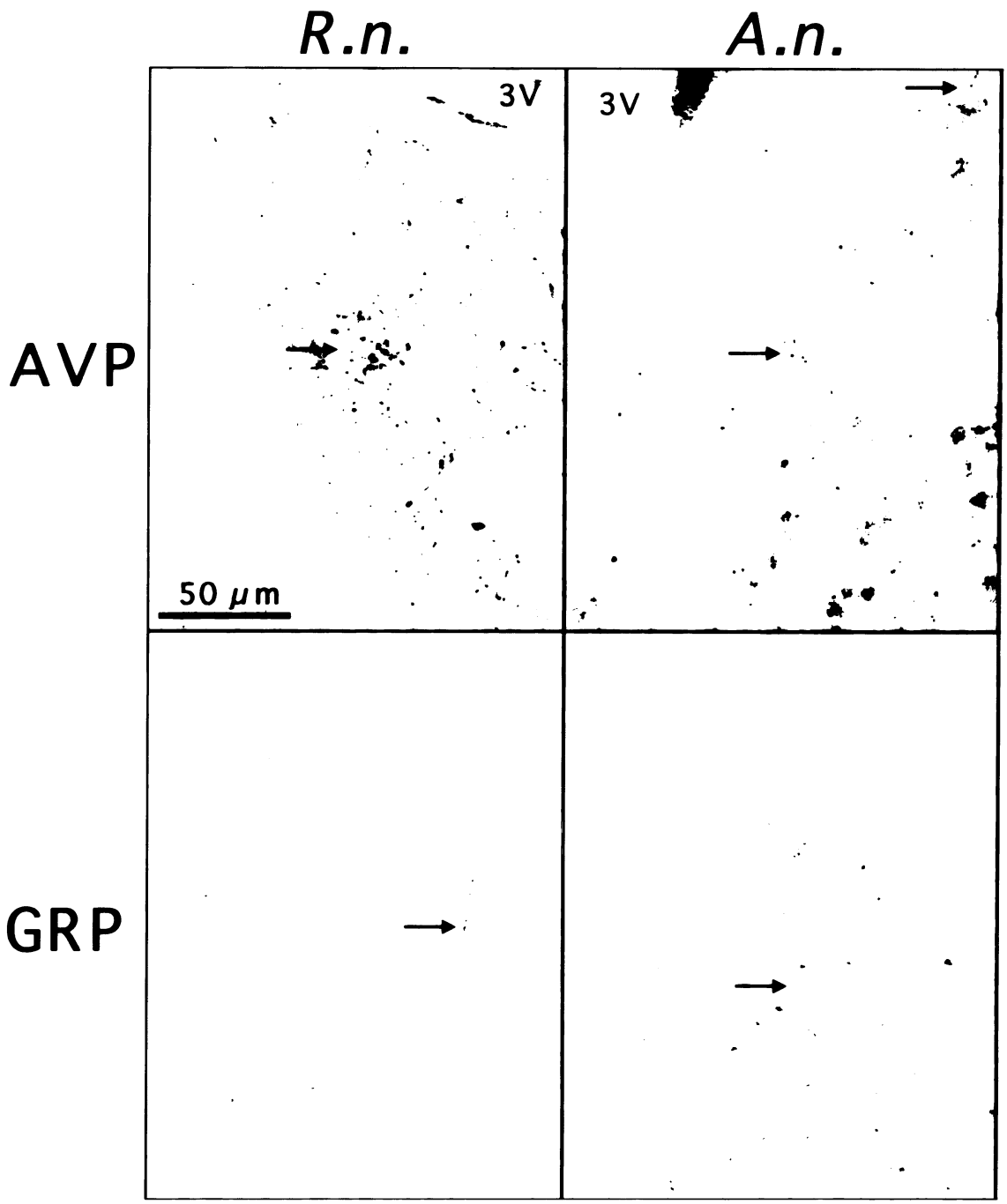
R.n.
A.n.
AVP
GRP
3V
3V
50 μm

located in the diagonal band. The MPS contained CTβ+ cells, as well as the mPO. Neurons projecting to the PVT were found in the VLPO; these cells were few in number, but consistently found in animals with successful PVT injections. Other hypothalamic nuclei also contained CTβ+ cells, including the PeV, AHA, DMN, VMH, posterior hypothalamus (PH), LH, and Arc, in and surrounding the TMN, and in the SUM; a few CTβ+ cells were found in the PVN. Although much of the brainstem was unavailable for analysis, the PAG was inspected and CTβ+ cells were found there. In the Nile grass rat, the PVT afferent projection pattern was similar to that on the rat, with CTβ+ cells found in the same regions including the VLPO. Compared to the rat, CTβ+ cells in *A. niloticus* tended to be more numerous in the nuclei of the diagonal band and less numerous in the meA. Labeled cells in the diagonal band of *A. niloticus* extended and merged with those of the LS.

Discussion:

These results are the first to document any SCN projections in a diurnal rodent, and more specifically, that the SCN sends projections to the PVT in *A. niloticus*, a diurnal rodent. A similar projection has also been documented in humans (Dai *et al.*, 1998). After a

retrograde tracer was injected into the PVT of *A. niloticus*, the pattern of retrograde labeling in the SCN differed slightly from that of rats; the bias toward the SCNdm typical of the rat was absent in the diurnal species (Figures 23, 24).

Many AVP+ SCN cells projected to the PVT in both species, and AVP+ fibers were identified in the PVT of both species (Figure 26). However, no difference was found in the number of AVP+ SCN cells that projected to the PVT between species. It should be noted that the AVP immunostaining may have obscured the identification of CTβ+ cells because many more CTβ+ cells were found in the SCN after immunolabeling for GRP compared to AVP. However, the reduction in CTβ+ cells associated with AVP staining was similar between species (36% in *R.n.*, 47% in *A.n.*). In contrast to AVP labeling, very few PVT-projecting SCN cells were GRP+ in either species. There were GRP+ fibers in the PVT of both species (Figure 26), but apparently most of these fibers do not originate in the SCN.

These results demonstrate that there is no species difference in the number of AVP+ or GRP+ SCN cells projecting to the PVT. Nonetheless, the activity patterns of at least AVP+ cells within the SCN may be different in these two species and this may influence the rhythm of Fos expression in the PVT. *Arvicanthis* show a rhythm of

Fos expression in AVP+ neurons of the SCN with a peak during the day. The same study showed that in rats, there is little or no colocalization of Fos and AVP in the SCN regardless of the sampling time (Rose *et al.*, 1999). Although nocturnal mice also show Fos expression in AVP+ cells, no rhythm in Fos/AVP colocalization has been demonstrated in this species (Castel *et al.*, 1997). Therefore, AVP+ SCN cells may project to the PVT in both species studies here, but the pattern of activity of these neurons may differ between species with different activity patterns. The rhythm of Fos expression seen in AVP+ cells of the *Arvicanthis* SCN may be a result of photic stimulation. Therefore, retinal projections may differentially affect peptidergic cell populations in the SCN of rats and *Arvicanthis*. This, together with the differential retinal innervation of the PVT described earlier, may contribute to species differences in the display of activity when animals are kept in a light:dark cycle.

It should be noted that the rats and *Arvicanthis* used in this study were perfused at different times of day. Given that some peptides within the SCN follow a circadian pattern (Inouye and Shibata, 1994), this may have affected whether or not a CTβ+, PVT-projecting SCN cell had a detectable amount of peptide. However, the

number of AVP+ cells have not been shown to vary over the light:dark cycle (Inouye and Shibata, 1994). Further, recent data have shown that the amount of peptide (AVP, GRP, or VIP) contained within cells of the SCN depends on the sleep state of the animal rather than the phase of the light:dark cycle *per se* (Schilling and Nurnberger, 1998). In the present study, the number of GRP+ SCN cells was highly variable in both species; and time of day could not account for this variability in GRP+ cell number. Even when many GRP+ cells were contained within an animal's SCN, few CTβ+ cells were found to contain GRP. Therefore, time of perfusion was not likely to bias the detection of peptide content in PVT-projecting SCN cells.

In both rats and *Arvicanthis*, the VLPO contains cells that project to the PVT. Although few CTβ+ cells are located in the VLPO, labeled cells were consistently found in animals with successful PVT injections. This is consistent with the anterograde labeling pattern after injection of the VLPO; fibers originating on the VLPO of rats were clearly present in the PVT, although the significance of this was not discussed by the author (Sherin *et al.*, 1998). Because the PVT both receives SCN input and projects to the VLPO, the PVT may relay circadian information to the VLPO and partially contribute to the

pattern of daily Fos expression seen in the VLPO. Further, Experiment 2 demonstrated that the rat PVT contains a small number of cells projecting to the VLPO. These data add to the functional model of sleep described in the introduction. The PVT and VLPO may have mutually inhibitory projections, which would partially account for the negative correlation seen between these areas with respect to Fos expression at different times of day (see Experiment 1).

GENERAL DISCUSSION

The experiments described in this dissertation have contributed to the development of a functional neuroanatomical model of the circadian control of sleep and wakefulness. Specifically, aspects of the circuitry through which the circadian clock may modulate sleep and arousal have been clarified. Further, the comparative approach of this work has identified similarities between diurnal and nocturnal animals, as well as striking species differences in the pattern of neural activity in brain regions important in the control of the sleep/wake cycle. The following discussion integrates this new information with the extensive literature on the neural regulation of sleep, as well as with the more limited literature on the neural correlates of species differences in the distribution of sleep and wakefulness across the day/night cycle. Before the comparative aspects of this work are discussed, though, the circadian modulation of brain regions integral in the sleep/wake cycle in the rat will be reviewed. In particular, the roles of the VLPO and the midline and intralaminar thalamic nuclei will be reevaluated in light of the present results.

Functional Neuronal Model of Sleep and Circadian Rhythms.

Role of the VLPO in the circadian modulation of the sleep/wake cycle. The results of Experiment 1 demonstrate the presence of daily rhythms in Fos expression in the VLPO, an area known to be involved in the homeostatic regulation of sleep (Sherin *et al.*, 1998; Sherin *et al.*, 1996). The VLPO regulates sleep and wakefulness via connections with brain regions important in arousal (TMN, raphe nuclei, LC, VTA, and cholinergic nuclei of the basal forebrain and pons). Although many of these anatomical pathways have been described in detail, most of the discussion concerning the functional features of these circuits has been limited to the putative inhibitory connections of the VLPO and the TMN (Sherin *et al.*, 1998; Stevens *et al.*, 1999). Data from Experiments 2 and 6 indicate that the PVT is likely to also be part of the circuitry by which the VLPO modulates sleep. The VLPO projects to the PVT and neural activity in the VLPO was negatively correlated with that of the midline thalamic nuclei (PVT and CMT; Experiment 1). Therefore, similar to what has been postulated for other outputs of the VLPO, control of wakefulness may involve inhibitory influences of the VLPO upon the PVT.

Although the role of the VLPO in the sleep/wake cycle is beginning to be elucidated, the mechanisms by which the SCN imposes a rhythm on VLPO activity have not yet been identified.

The evidence presented here indicates that the VLPO does not receive significant axonal input from the SCN in rats (Experiment 2). The SCN may affect VLPO neural activity by two other mechanisms. First, the SCN may indirectly modulate VLPO neuronal activity via a relay through an intermediate brain region. The sPVHz, an area of the hypothalamus that receives a large proportion of the SCN axonal output (Watts *et al.*, 1987), is a likely candidate for this role. It is also possible that the PVT, a recipient of numerous SCN projections (Experiment 6), contributes to the circadian modulation of the VLPO via direct projections to this region. Second, the SCN may impose a rhythm on VLPO cells though non-axonal outputs (Silver *et al.*, 1996). Fetal SCN grafts, that as a rule make very few connections with the host brain, restore both the circadian temperature rhythm and the sleep/wake cycle in rats with SCN lesions (Edgar *et al.*, 1992). These data are consistent with the claim that the SCN provides circadian control of the VLPO via a diffusible signal (however, see Stephan and Nunez, 1977). If that is the case, then elimination of any direct or multisynaptic neuronal projections from the SCN to the VLPO should not seriously diminish the rhythmic expression of Fos in the VLPO. Also, it is expected that SCN lesions will eliminate the VLPO rhythm in Fos expression, and that SCN transplants - even if encapsulated -

should restore the rhythm of Fos expression as well as the rhythmic display of sleep.

Roles of the midline and intralaminar thalamus in the modulation of the sleep/wake cycle. In rats, Fos expression in the CMT and PVT increases during the active phase (Experiment 1). The similarity between the daily profiles of Fos expression in the PVT and CMT implies that these two thalamic regions may serve a similar function in modulating daily arousal. The PVT is a rather large thalamic nucleus located between the ventral-most portion of the third ventricle and the medial intralaminar nuclei of the thalamus. With respect to Fos expression, the midline (e.g., PVT) and intralaminar nuclei (e.g., CMT) appear to form a continuous group of cells (see Figure 3); the daily patterns of Fos expression were similar in the two nuclei, and were consistently positively correlated (Experiments 1 and 5). Additionally, the PVT and intralaminar nuclei are often activated under the same conditions, such as during stress induced by exposure to noxious chemicals, immobilization, forced swimming, restraint, or pain (Cullinan *et al.*, 1995; Duncan *et al.*, 1996; Senba *et al.*, 1993). Therefore, some observations support the idea that these two nuclei form a single functional complex.

The conjecture that the PVT and intralaminar nuclei are part of a unitary midline thalamic system is at odds with data concerning

their projections and the developmental pattern of the thalamus. First, the PVT, but not the CMT, is considered part of the epithalamus, due to its embryologic origin (Jones, 1985). Second, the anatomical connections of the PVT and intralaminar nuclei differ markedly (Jones, 1985). The PVT receives projections from the hypothalamus, Rt, preoptic area, amygdala, PAG, LC, nucleus of the solitary tract, raphe nuclei, as well as dopaminergic, adrenergic, and medullary cholinergic nuclei (Cornwall and Phillipson, 1988; Otake and Ruggiero, 1995; Otake *et al.*, 1995; Phillipson and Bohn, 1994; Takada *et al.*, 1990, present studies). The PVT in turn sends axons primarily to the NAC, central amygdala, hypothalamus, hippocampus, and limbic cortical areas (Freedman and Cassell, 1994; Su and Bentivoglio, 1990; Wright and Groenewegen, 1995). In sharp contrast with the pattern of PVT connections, the intralaminar nuclei (which include the CMT) contain cells which relay information from the MRF to the cerebral cortex, as well as cells that receive projections from the cortex and send axons to the striatum (Berendse and Groenewegen, 1991; Glenn and Steriade, 1982; Jones and Laevitt, 1974; Ropert and Steriade, 1981; Steriade and Glenn, 1982). Further, the SCN has reciprocal connections with the PVT but not the CMT (present studies, Dai *et al.*, 1998; Moga *et al.*, 1995; Watts *et al.*, 1987). The only common input to the PVT and intralaminar nuclei is

the parabrachial nucleus (Bester *et al.*, 1997; Cornwall and Phillipson, 1988; Jones, 1985) and possibly the nucleus cuneiformis (Edwards and de Olmos, 1976; but see Cornwall and Phillipson, 1988; Otake and Ruggiero, 1995).

In a way, the similarity of the activity profiles of the intralaminar and midline thalamus may seem at odds with the divergent connection patterns of these two nuclear groups. However, an analysis of these connections suggests that the PVT and the intralaminar nuclei may serve separate but complementary functions with respect to wakefulness in mammals. Increased activity of intralaminar nuclei is important in wakefulness and vigilance because these cells relay information to the cerebral cortex and the dorsal striatum and are important in cortical desynchronization (Glenn and Steriade, 1982; Jones, 1985; Kinomura *et al.*, 1996). The PVT may serve a similar role by relaying information relevant to the vigilance state of the animal to limbic cortex and other "limbic" structures (i.e., hippocampus and amygdala), as well as to the ventral striatum (NAC). Like the MRF (which projects to the intralaminar nuclei), most brain regions projecting heavily to the PVT are also more active during wakefulness and after arousing stimuli (Aston-Jones and Bloom, 1981; Beck and Fibiger, 1995; Bester *et al.*, 1997; Cornwall and Phillipson, 1988; Cullinan *et al.*, 1995; Duncan *et al.*,

1996; Glenn and Steriade, 1982; Otake and Ruggiero, 1995; Otake *et al.*, 1995; Phillipson and Bohn, 1994; Ropert and Steriade, 1981; Senba *et al.*, 1993; Steriade and Glenn, 1982; Steriade *et al.*, 1982a; Takada *et al.*, 1990). Consequently, these two groups of thalamic nuclei (midline and intralaminar), may increase arousal and vigilance through parallel forebrain circuits.

Activation of the PVT is likely to affect the workings of the SCN pacemaker. Indeed, the PVT can be considered part of the circadian system, having reciprocal connections to the SCN as well as receiving afferent input from the IGL and the retina, both important in circadian regulation (Moga *et al.*, 1995; Otake *et al.*, 1995; Speh and Moore, 1992; Watts *et al.*, 1987, present results). Circadian rhythms, especially the locomotor activity rhythm, can be modulated (decreased in amplitude) by emotional states including stress (Amir and Stewart, 1998; Gorka *et al.*, 1996; Meerlo *et al.*, 1997). Because the PVT projects to the SCN and is affected by stress and fear, this brain region is well situated to affect SCN neural activity after stress or arousal.

Interestingly, there are striking similarities with respect to the origin of the neural inputs to the PVT and the VLPO. As demonstrated in these and other studies, the following brain regions project to both the VLPO and PVT in rats: BNST, LS, mPOA, MPA,

MeA; hypothalamic nuclei including DMH, the SCN or peri-SCN region, as well as the TMN and SUM; the parabrachial nucleus (PB), VTA, LC and raphe nuclei (Chou *et al.*, 1998; Cornwall and Phillipson, 1988; Morin *et al.*, 1994; Otake and Ruggiero, 1995; Otake *et al.*, 1995; Phillipson and Bohn, 1994; Sherin *et al.*, 1998; Sherin *et al.*, 1996; Takada *et al.*, 1990; Watts *et al.*, 1987, present results). These findings further support the idea that the PVT and VLPO are antagonistic components of a neuronal circuit that modulates sleep and wakefulness. If this is true, then activity in brain areas that project to both of these forebrain nuclei would be expected to have opposite effects on VLPO and PVT neural activity.

Taken together, the activity pattern and neural connections of the PVT implicate it in at least three aspects of the sleep/wake cycle. First, the PVT may affect wakefulness via the modulation of the same circuits as the VLPO. Second, the PVT may relay circadian signals to areas that control different aspects of wakefulness. For example, considering its projections to the NAC and its modulation of DA release there (Jones *et al.*, 1989), the activation of the PVT at night may increase the salience of rewarding stimuli during the active phase of the cycle. Third, the PVT inputs to the SCN may modulate the activity of the SCN based on the arousal state of the animal.

The presence of a rhythmic expression of Fos in the brain regions investigated here suggests that the circadian clock (and/or the light:dark cycle) modulates activity in these areas. However, unlike the VLPO, PVT, and TMN, all of which receive at least sparse input from the SCN, the CMT does not contain terminals from SCN neurons (Watts *et al.*, 1987). Neither does the CMT receive inputs from brain regions that may relay circadian signals, such as the sPVHz or the PVT (Jones, 1985). Therefore, the possible origin of a rhythm in Fos expression is less clear in the case of the CMT. The daily rhythm may be a result of the activity of indirect projections from the SCN to the pontine reticular formation (Mintz *et al.*, 1998). A second possibility is that the CMT receives input from a diffusible signal emanating from the SCN discussed above (Lehman *et al.*, 1995; Silver *et al.*, 1996).

Neural Activity in the Brain of Nocturnal and Diurnal Rodents.

One important contribution of these studies was the identification of a sleep-active region in the preoptic area of a diurnal species, *A. niloticus*. In this region, Fos expression increased during times of the night associated with the display of behavioral correlates of sleep in this diurnal rodent (Experiments 3, 4 and 5). In sharp contrast, VLPO Fos expression was low at night in the

nocturnal laboratory rat (Experiment 1). In general, five alternative explanations may account for the species difference in the phase of the rhythm in VLPO neuronal activity, and these alternatives are not necessarily mutually exclusive. First, the circadian signal from the SCN may differ between species (e.g., excitatory in one case and inhibitory in the other). Second, the signal may be the same but emitted at a different phase in nocturnal and diurnal animals. Third, the same signal may be interpreted differently by effector systems that control the overt expression of behavioral rhythms in these two species. Fourth, brain regions that serve as relays of SCN outputs, such as the sPVHz, may alter outgoing SCN signals in a species-specific fashion. In all these cases, the circadian signal from the SCN may be axonal, humoral, or both. Fifth, since all the rhythms in Fos expression were detected in animals housed under a light:dark cycle, the differences may be due to how the SCN or other brain regions are affected by light. The species difference in the VLPO serves as a good example of how circadian modulation of brain areas important in the control of sleep differs between diurnal and nocturnal species. Future work focusing on this brain area will serve to evaluate the possible interpretations of the data presented here.

The proposal that regions of the brain that serve to relay SCN signals function differently in diurnal and nocturnal species has

received some support. Specifically, species differences in the pattern of neural activity seen in the region of the sPVHz just outside the SCN have been reported. For example, the phases of rhythms in multiple unit activity (MUA) recorded from inside the SCN were different from the phases of rhythms recorded just outside the nucleus in rats (Inouye and Kawamura, 1979). In diurnal chipmunks, however, the phase of the neuronal activity rhythms was the same inside and outside the SCN (Sato and Kawamura, 1984a). Therefore, the activity patterns of neurons outside the SCN are out of phase with those of the SCN in nocturnal animals, but in phase with the display of behavioral activity. This supports the notion that the activity of an extra-SCN brain region such as the sPVHz may alter outgoing circadian signals from the SCN and therefore affect a species' activity pattern. Since some neurons of the sPVHz project to the VLPO (Experiment 2), this mechanism may be responsible for the species differences in VLPO Fos expression made evident by the results of Experiments 1, 4, and 5.

Recent data on the patterns of Fos expression in the SCN and sPVHz in rats and *Arvicanthis* support the likelihood of the sPVHZ modifying circadian signals originating from the SCN (Nunez *et al.*, in press). Although the rhythms in Fos expression in the SCN were similar between the two species, both showing peaks in the early

morning, the pattern seen in the sPVHz differed between species. Specifically, whereas the rhythmic Fos expression in the rat sPVHz resembled the SCN rhythm (namely, high in the early light phase and decreasing throughout the day and into the night), the *Arvicanthis* sPVHz showed a second peak in Fos expression in the middle of the dark period (ZT 17). Although this species difference in rhythmic Fos expression supports the proposition that the sPVHz may function as a modulator of outgoing circadian signals, the specific features of the rhythm do not correspond with those predicted from the results of electrophysiological studies (Inouye and Kawamura, 1979; Kurumiya and Kawamura, 1988; Sato and Kawamura, 1984a). From the data of MUA studies, the expectation was to see an increase in Fos expression in the sPVHz at night in the rats, not *Arvicanthis*, in order for it to correspond with rats' nocturnal display of activity (i.e., out of phase with peak SCN activity). The conclusion drawn from these data is that the sPVHz is not a simple "switch" where a change in neural activity can make an animal diurnal or nocturnal. Regardless, the species differences in sPVHz activity seem to contribute to the expression of either a diurnal or nocturnal behavioral pattern.

The species difference in the PVT Fos expresion pattern was not as notable as the difference found in the VLPO, with PVT Fos decreasing after the initial peak at lights-on (ZT 0.5) in *Arvicanthis*,

but high at both ZT 1 and ZT 17 in rats. Further, a significant rhythm was found in the CMT but not the TMN in rats, with the opposite being true for *Arvicanthis*. However, similar to the rat, the number of Fos+ cells in the PVT and CMT were positively correlated in grass rats (Experiments 1 and 5). Therefore, the PVT and CMT are likely to serve similar roles in wakefulness in the *Arvicanthis*, just as in the rat. Namely, these two thalamic regions most likely support wakefulness in both species through different but parallel arousal circuits.

For *A. niloticus*, the patterns of Fos expression seen in the PVT need to be evaluated taking into account the pattern of Fos expression seen in other regions that support wakefulness, such as the VTM. In *Arvicanthis*, Fos expression in the VTM remained high throughout the light phase and decreased in the middle of the dark phase (when VLPO Fos expression was high). Moreover, Fos expression within histamine-containing cells in the VTM of *A. niloticus* peaked at the light:dark transitions, when this species shows increased activity and little sleep. In rats, no significant rhythms in Fos expression were seen in brain regions rich in histamine. These results suggest that histamine may contribute more to daily arousal in diurnal Nile grass rats than in nocturnal rats. Indeed, the shift to diurnality may have involved more than just an

alteration of the circadian signal to SCN targets. Animals may have rhythmicity imposed through the combination of different *components* of wakefulness, or different arousal systems, and the strength of these components may differ between species. If, in fact, the histaminergic arousal system contributes more to the circadian rhythm of wakefulness in *A. niloticus*, then antihistamines are likely to decrease wakefulness more in the active period of *Arvicanthis* than rats.

Whereas activation of histaminergic systems may contribute to behavioral activation at dawn and dusk, neural activity in the PVT of *A. niloticus* was only elevated in association with the morning activity peak. If neural activity in the PVT contributes more to the morning activity peak compared to the evening activity peak in *Arvicanthis*, then one would predict that motivationally significant stimuli (i.e., food, sucrose, mates, drugs) would have more reward value when presented in the early light compared to the early dark period in Nile grass rats. Interestingly, most mating takes place in the period just before lights-on in *Arvicanthis* (McElhinny *et al.*, 1997), corresponding to their peak in PVT Fos expression (Experiment 5). To my knowledge, the idea that separate arousal systems have differential contributions to wakefulness in nocturnal and diurnal animals is new and therefore untested.

In summary, these studies have identified a group of structures in the brain where activity patterns correspond to different components of the sleep/wake cycle of rodents. Further, the activity patterns in many of these brain regions differ between nocturnal and diurnal rodents as predicted from their respective sleep/wake patterns. Species differences in the timing of wakefulness may reflect differences in how the circadian pacemaker interacts with areas of the brain that differentially support wakefulness and sleep. The results also indicate that differences in retinal projections may also influence the display of sleep and wakefulness across the day-night cycle. Finally, it seems likely that different aspects of wakefulness are mediated by different brain circuits that also show species-specific features.

APPENDIX: Notes on Methods

The immediate-early gene c-*fos* and its product (Fos) have been used as indicators of neuronal cell activation (Sagar *et al.*, 1988). Fos is a transcription factor that dimerizes with Jun and binds to the AP-1 promoter site to initiate gene transcription (Morgan and Curran, 1991). Many (but not all) neurons increase cellular Fos protein levels when they are activated. For example, neurons in the ventrolateral SCN increase levels of Fos when an animal is exposed to light at particular times of the day (Rea, 1992). The level of Fos protein peaks over 1 hr after c-*fos* mRNA levels are highest (Schwartz *et al.*, 1994), indicating that increases in Fos expression can be used as an index of neuronal activity occurring in the preceding hour. Fos can also be localized to specific cell populations. For example, in the rat SCN, neurons immunopositive for gastrin releasing peptide (GRP) are preferentially activated, as indexed by Fos immunoreactivity, after light stimulation (Earnest *et al.*, 1993; Earnest and Olschowka, 1993). In summary, localization of neurons expressing Fos can provide a great deal of information on the activation of specific neuronal groups under different environmental conditions.

Neuronal tract tracing is a common method used to describe the connectivity of brain regions. One commonly used retrograde tracer is horseradish peroxidase (HRP). More recently, the β subunit of cholera toxin (CTβ), either alone or conjugated to HRP, has been used as a retrograde tracer (Trojanowski *et al.*, 1981; Wan *et al.*, 1982). Unlike free HRP, CTβ uptake by the neuron does not depend on neuronal activity (Dumas *et al.*, 1979). Second, conjugates of HRP with CTβ substantially increase the sensitivity of labeling: labeling using the conjugate was not dependent on the amount of the conjugate used, unlike unconjugated HRP, and therefore a smaller volume of tracer was needed when the CTβ-HRP conjugate was used. Both of these differences appear to be due to the different mechanisms employed by the tracers (free HRP vs. CTβ). Cholera toxin binds to oligosaccharide "receptors" on the membrane surface, whereas HRP is internalized by fluid phase endocytosis at the terminal (Wan *et al.*, 1982). Due to this, labeling using CTβ does not appear to backfill cells in the same manner as HRP. Regardless, CTβ appears to be the superior neuronal tract tracer, and is used in the experiments described in this dissertation.

REFERENCES

Abe H, Honma S, Shinohara K, Honma K-I (1995) Circadian modulation in photic induction of Fos-like immunoreactivity in the suprachiasmatic nucleus cells of diurnal chipmunk, *Eutamias asiaticus*. *Journal of Comparative Physiology*, **176,** 159-167.

Allingham K, von Saldern C, Brennan PA, Distel H, Hudson R (1998) Endogenous expression of c-Fos in hypothalamic nuclei of neonatal rabbits coincides with their circadian pattern of suckling-associated arousal. *Brain Research*, **783,** 210-218.

Amir S, Stewart J (1998) Conditioned fear suppresses light-induced resetting of the circadian clock. *Neuroscience*, **86,** 345-351.

Armstrong, WE (1995) Hypothalamic supraoptic and paraventricular nuclei. In: The Rat Nervous System, 2nd ed. G. Paxinos, Ed.

Aston-Jones G, Bloom FE (1981) Activity of norepinephrine-containing locus coeruleus neurons in behaving rats anticipates fluctuations in the sleep-waking cycle. *The Journal of Neuroscience*, **1,** 876-886.

Beck CHM, Fibiger HC (1995) Conditioned fear-induced changes in behavior and in the expression of the immediate early gene *c-fos*: With and without diazepam treatment. *The Journal of Neuroscience*, **15,** 709-720.

Berendse HW, Groenewegen HJ (1991) Restricted cortical termination fields of the midline and intralaminar thalamic nuclei. *Neuroscience*, **42,** 73-102.

Bester H, Besson J-M, Bernard J-F (1997) Organization of efferent projections from the parabrachial area to the hypothalamus: A *Phaseolus Vulgaris*-leucoagglutinin study in the rat. *The Journal of Comparative Neurology*, **383,** 245-281.

Blanchong JA, McElhinny TM, Mahoney MM, Smale L (in press). Nocturnal and diurnal rhythms in the unstripped Nile rat, *Arvicanthis niloticus*. *Journal of Biological Rhythms*.

Boer GJ, Griffioen HA, Duindam H, van der Woude TP, Rietveld WJ (1993) Light/dark-induced effects on behavioral rhythms in suprachiasmatic nucleus-lesioned rats irrespective of the presence of functional suprachiasmatic nucleus brain implants. *Journal of Interdisciplinary Cycle Research*, **24,** 118-136.

Borbély AA, Neuhaus U (1979) Sleep deprivation: Effects on sleep and EEG in the rat. *Journal of Comparative Physiology A*, **133,** 71-87.

Bremer F (1975) Existence of a mutual tonic inhibitory interaction between the preoptic hypnogenic and the midbrain reticular formation. *Brain Research*, **96,** 71-75.

Brown M, Nunez AA (1989a) Vasopressin-deficient rats show a reduced amplitude of the circadian sleep rhythm. *Physiology & Behavior*, **46,** 759-762.

Brown MH, Nunez AA (1986) Hypothalamic circuits and circadian rhythms: Effects of knife cuts vary with their placement within the suprachiasmatic area. *Brain Research Bulletin*, **16,** 705-711.

Brown MH, Nunez AA (1989b) Vasopressin-deficient rats show a reduced amplitude of the circadian sleep rhythm. *Physiology and Behavior*, **46,** 759-762.

Cagampang FRA, Yang J, Nakayama Y, Fukuhara C, Inouye S-IT (1994) Circadian variation of arginine-vasopressin messenger RNA in the rat suprachiasmatic nucleus. *Molecular Brain Research*, **24,** 179-184.

Castel M, Belenky M, Cohen S, Wagner S, Schwartz WJ (1997) Light-induced c-Fos expression in the mouse suprachiasmatic nucleus: Immunoelectron microscopy reveals co-localization in multiple cell types. *European Journal of Neuroscience*, **9,** 1950-1960.

Chastrette N, Pfaff DW, Gibbs RB (1991) Effects of daytime and nighttime stress on Fos-like immunoreactivity in the paraventricular nucleus of the hypothalamus, the habenula, and the posterior paraventricular nucleus of the thalamus. *Brain Research*, **563,** 339-344.

Chou TC, Scammell T, Saper CB (1998) Afferents to the ventrolateral preoptic nucleus, 664.5. In: *Society for Neuroscience Abstracts*, Volume 2. Los Angeles, CA, pp. 1694.

Cornwall J, Phillipson OT (1988) Afferent projections to the dorsal thalamus of the rat as shown by retrograde lectin transport II. The midline nuclei. *Brain Research Bulletin*, **21,** 1470161.

Cui L-N, Saeb-Parsy K, Dyball REJ (1997) Neurones in the supraoptic nucleus of the rat are regulated by a projection from the suprachiasmatic nucleus. *Journal of Physiology*, **502,** 149-159.

Cullinan WE, Herman JP, Battaglia DF, Akil H, Watson SJ (1995) Pattern and time course of immediate early gene expression in rat brain following acute stress. *Neuroscience*, **64,** 477-505.

Dai J, Swaab DF, Van Dar Vliet J, Buijs RM (1989a) Postmortem tracing reveals the organization of hypothalamic projections of the suprachiasmatic nucleus in the human brain. *The Journal of Comparative Neurology,* **400,** 87-102.

Dai J, Van Der Vliet J, Swaab DF, Buijs RM (1998b) Human retinohypothalamic tract as revealed by in vivo postmortem tracing. *The Journal of Comparative Neurology,* **397,** 357-370.

Danguir J, Nicolaidis S (1980) Cortical activity and sleep in the rat lateral hypothalamic syndrome. *Brain Research*, **185,** 305-321.

Dijk D-J, Czeisler CA (1995) Contribution of the circadian pacemaker and the sleep homeostat to sleep propensity, sleep structure, electroencephalographic slow waves, and sleep spindle activity in humans. *The Journal of Neuroscience*, **15,** 3526-3538.

Dumas M, Schwab ME, Thoenen H (1979) Retrograde axonal transport of specific macromolecules as a tool for characterizing nerve terminal membranes. *Journal of Neurobiology*, **10,** 179-197.

Duncan GE, Knapp DJ, Breese GR (1996) Neuroanotomical characterization of Fos induction in rat behavioral models of anxiety. *Brain Research*, **713,** 79-91.

Earnest DJ, DiGiorgio S, Olschowka JA (1993) Light induces expression of fos-related proteins within gastrin-releasing peptide neurons in the rat suprachiasmatic nucleus. *Brain Research*, **627,** 205-209.

Earnest DJ, Olschowka JA (1993) Circadian regulation of c-*fos* expression in the suprachiasmatic pacemaker by light. *Journal of Biological Rhythms*, **8,** S65-S71.

Edgar DM, Dement WC, Fuller CA (1993) Effect of SCN lesions on sleep in squirrel monkeys: Evidence for opponent processes in sleep-wake regulation. *The Journal of Neuroscience*, **13,** 1065-1079.

Edgar DM, Ralph MR, Seidel WF, Lee LK, Dement WC (1992) Fetal SCN-transplants restore sleep-wake and body temperature circadian rhythms in SCN-lesioned rats. *Sleep Research*, **21,** 371.

Edwards SB, de Olmos JS (1976) Autoradiographic studies of the projections of the midbrain reticular formation: Ascending projections of nucleus cuneiformis. *The Journal of Comparative Neurology*, **165,** 417-432.

Ericson H, Blomqvist A, Kohler C (1991a) Origin of neuronal inputs to the region of the tuberomammillary nucleus of the rat brain. *The Journal of Comparative Neurology*, **311,** 45-64.

Ericson H, Köhler C, Blomqvist A (1991b) GABA-like immunoreactivity in the tuberomammillary nucleus: An electron microscopic study in the rat. *The Journal of Comparative Neurology*, **305,** 462-469.

Ericson H, Watanabe T, Kohler C (1987) Morphological analysis of the tuberomammillary nuclei in the rat brain: Delineation of subgroups with antibody against L-histidine decarboxylase as a marker. *The Journal of Comparative Neurology*, **263,** 1-24.

Freedman LD, Cassell MD (1994) Relationship of thalamic basal forebrain projection neurons to the peptidergic innervation of the midline thalamus. *The Journal of Comparative Neurology*, **348,** 321-342.

Friedman AH, Walker CA (1968) Circadian rhythms in rat mid-brain and caudate nucleus biogenic amine levels. *Journal of Physiology*, **197,** 77-85.

Friedman AH, Walker CA (1969) Rat brain amines, blood histamine and glucose levels in relationship to circadian changes in sleep induced by pentobarbitone sodium. *Journal of Physiology*, **202,** 133-146.

Gaus SE, Saper CB (1998) Efferent connections from the suprachiasmatic nucleus to the ventrolateral preoptic nucleus in the rat, 762.13. In: *Society for Neuroscience Abstracts*, Volume 2. Los Angeles, CA, p. 1920.

Glenn LL, Steriade M (1982) Discharge rate and excitability of cortically projecting intralaminar neurons during waking and sleep states. *The Journal of Neuroscience*, **2,** 1387-1404.

Gorka Z, Moryl E, Papp M (1996) Effect of chronic mild stress on circadian rhythms in the locomotor activity in rats. *Pharmacology Biochemistry and Behavior*, **54,** 229-234.

Gritti I, Mainville L, Jones BE (1994) Projections of GABAergic and cholinergic basal forbrain and GABAergic preoptic-anterior hypothalamic neurons to the posterior lateral hypothalamus of the rat. *The Journal of Comparative Neurology*, **339,** 251-268.

Illnerova H (1991) The suprachiasmatic nucleus and rhythmic pineal melatonin production. In: *Suprachiasmatic Nucleus: The Mind's Clock*. Edited by D. C. Klein, R. Y. Moore and S. M. Reppert. New York: Oxford University Press, pp. 197-216.

Iniguez C, Gayoso MJ, Carreres J (1985) A versatile and simple method for staining nervous tissue using Giemsa dye. *Journal of Neuroscience Methods*, **13,** 77-86.

Inouye S-I, Shibata S (1994) Neurochemical organization of circadian rhythms in the suprachiasmatic nucleus. *Neuroscience Research*, **20,** 109-130.

Inouye ST, Kawamura H (1979) Persistance of circadian rhythmicity in a mammalian hypothalamic "island" containing the

suprachiasmatic nucleus. *Proc. Natl. Acad. Sci. USA*, **76,** 5962-5966.

Itowi N, Yamatodani A, Kiyono S, Hiraiwa M, Wada H (1991) Effect of histamine depletion on the circadian amplitude of the sleep-wakefulness cycle. *Physiology & Behavior*, **49,** 643-646.

Johnson RF, Moore RY, Morin LP (1988a) Loss of entrainment and anatomical plasticity after lesions of the hamster retinohypothalamic tract. *Brain Research*, **460,** 279-313.

Johnson RF, Morin LP, Moore RY (1988b) Retinohypothalamic projections in the hamster and rat demonstrated using cholera toxin. *Brain Research*, **462,** 301-312.

Jones ED (1985) *The Thalamus*. New York: Plenum Press.

Jones EG, Laevitt RY (1974) Retrograde axonal transport and the demonstration of non-specific projections to the cerebral cortex and striatum from thalamic intralaminar nuclei in the rat, cat, and monkey. *The Journal of Comparative Neurology*, **154,** 349-378.

Jones MW, Kilpatrick IC, Phillipson OT (1989) Regulation of dopamine function in the nucleus accumbens of the rat by the thalamic paraventricular nucleus and adjacent midline nuclei. *Experimental Brain Research*, **76,** 572-580.

Kaitin K (1984) Preoptic area unit activity during sleep and wakefulness in the cat. *Experimental Neurology*, **83,** 347-357.

Kalivas PM (1982) Histamine-induced arousal in the conscious and penobarbital-pretreated rat. *The Journal of Pharmacology and Experimental Therapeutics*, **222,** 37-42.

Kalsbeek A, Bujis RM, Engelmann M, Wotjak CT, Landgraf R (1995) In vivo measurement of a diurnal variation in vasopressin release in the rat suprachiasmatic nucleus. *Brain Research*, **682,** 75-82.

Katona C, Rose R, Smale L (1998) The expression of Fos within the suprachiasmatic nucleus of the diurnal rodent *Arvicanthis niloticus*. *Brain Research*, **791,** 27-34.

Katona C, Smale L (1997) Wheel-running rhythms in *Arvicanthis niloticus*. *Physiology & Behavior*, **61,** 365-372.

Kinomura S, Larsson J, Guláa B, Roland PE (1996) Activation by attention of the human reticular formation and thalamic intralaminar nuclei. *Science*, **271,** 512-515.

Kiyono S, Seo ML, Shibagaki M, Watanabe T, Maeyama K, Wada H (1985) Effects of a-fluoromethylhistidine on sleep-waking parameters in rats. *Physiology & Behavior*, **34,** 615-617.

Klein DC, Moore RY, Reppert SM (1991) Suprachiasmatic Nucleus: The Mind's Clock. New York: Oxford University Press, pp. 467.

Kobayashi MR, Hopin IJ (1974) The effects of stress and environmental lighting on histamine in the rat brain. *Brain Research*, **74,** 356-359.

Kolb B, Dodic R, Whishaw IQ (1979) Effects of serial lateral hypothalamic destruction on feeding behavior, body weight, and neocortical and hippocampal EEG activity. *Experimental Neurology*, **66,** 263-276.

Krajnak K, Dickenson L, Lee TM (1997) The induction of Fos-like proteins in the suprachiasmatic nuclei and intergeniculate leaflet by light pulses in degus (*Octodon degus*) and rats. *Journal of Biological Rhythms*, **12,** 401-412.

Krilowicz BL, Szymusiak R, McGinty D (1994) Regulation of posterior lateral hypothalamic arousal related neuronal discharge by preoptic anterior hypothalamic warming. *Brain Research*, **668,** 30-38.

Kurumiya S, Kawamura H (1988) Circadian oscillation of the multiple unit activity in the guinea pig suprachiasmatic nucleus. *The Journal of Comparative Physiology*, **162,** 301-308.

Lehman MN, LeSauter J, Kim C, Berriman S, Tresco PA, Silver R (1995) How do fetal grafts of the suprachiasmatic nucleus communicate with the host brain? *Cell Transplantation*, **4,** 75-81.

LeSauter J, Lehman MN, Silver R (1996) Restoration of circadian rhythmicity by transplants of SCN "micropunches". *Journal of Biological Rhythms*, **11,** 163-171.

LeSauter J, Silver R (1994) Suprachiasmatic nucleus lesions abolish and fetal grafts restore circadian gnawing behavior in hamsters. *Restorative Neurology and Neuroscience*, **6,** 135-143.

Lin J-S, Hou Y, Sakai K, Jouvet M (1996) Histaminergic descending inputs to the mesopontine tegmentum and their role in the control of cortical activation and wakefulnes in the cat. *The Journal of Neuroscience*, **16,** 1523-1537.

Lin J-S, Sakai K, Vanni-Mercier G, Jouvet M (1989) A critical role of the posterior hypothalamus in the mechanisms of wakefulness determines by microinjection of muscimol in freely moving cats. *Brain Research*, **479,** 225-240.

Lin JS, Sakai K, Jouvet M (1994) Hypothalamo-preoptic histaminergic projections in sleep-wake control in the cat. *European Journal of Neuroscience*, **6,** 618-625.

Lineberry CG, Seigel J (1971) EEG synchronization, behavioral inhibition, and mesencephalic unit effects produced by stimulation of orbital cortex, basal forebrain and caudate nucleus. *Brain Research*, **34,** 143-161.

Lu J, Shiromani P, Saper C (1998) The effects of lesions of the ventrolateral preoptic nucleus (VLPO) on sleep, 664.4. In: *Society for Neuroscience Abstracts*, Volume 2. Los Angeles, CA, pp. 1694.

Lu J, Shiromani P, Saper CB (1997) Retinal projection to sleep-active c-*fos* area in the ventral lateral preoptic area. In: *27th Meeting of the Society for Neuroscience*. New Orleans, LA.

Lucas EA, Sterman MB (1975) Effect of a forebrain lesion on the polycyclic cycle and sleep-wake patterns in the cat. *Experimental Neurology*, **46,** 368-388.

Mallick BN, China GS, Sundaram KR, Singh B, Mohan Kumar M (1983) Activity of preoptic neurons during synchronization and desynchronization. *Experimental Neurology*, **81,** 586-597.

McElhinny TL, Smale L, Holekamp KE (1997) Patterns of body temperature, activity, and reproductive behavior in a tropical murid rodent, *Arvicanthis niloticus*. *Physiology & Behavior*, **62,** 91-96.

McGinty D, Alam MN, Szymusiak R (1997) Sleep deprivation increases the sleep-related discharge of sleep-active ventrolateral preoptic neurons. In: *27th meeting of the Society for Neuroscience*. New Orleans, LA.

McGinty DJ, Sterman MB (1968) Sleep suppression after basal forebrain lesions in the cat. *Science*, **160,** 1253-1255.

Meerlo P, van den Hoofdaker RH, Koolhaas JM, Daan S (1997) Stress-induced changes in circadian rhythms of body temperature and activity in rats are not caused by pacemaker changes. *Journal of Biological Rhythms*, **12,** 80-92.

Melander T, Hokfelt T, Rokaeus A (1986) Distribution of galanin like immunoreactivity in the rat central nervous system. *The Journal of Comparative Neurology*, **248,** 475-517.

Merchenthalter I, Lopez FJ, Negro-Vilar A (1993) Anatomy and physiology of central galanin-containing pathways. *Progress in Neurobiology*, **40,** 711-769.

Mintz EM, Price KM, Mickley NC, Albers HE (1998) Analysis of projections from the suprachiasmatic nucleus to the pontine reticular formation using pseudorabies virus, 762.14. In: *Society for Neuroscience Abstracts*, Volume 2. Los Angeles, CA, pp. 1920.

Mistlberger RE, Bergmann BM, Waldenar W, Rechtschaffen A (1983) Recovery sleep following sleep deprivation in intact and suprachiasmatic nuclei-lesioned rats. *Sleep*, **6,** 217-233.

Mochizuki T, Yamatodani A, Okakura K, Horii A, Inagaki N, Wada H (1992) Circadian rhythm of histamine release from the hypothalamus of freely moving rats. *Physiology & Behavior*, **51,** 391-394.

Moga MM, Weis RP, Moore RY (1995) Efferent projections of the paraventricular thalamic nucleus in the rat. *The Journal of Comparative Neurology*, **359,** 221-238.

Monti JM (1993) Involvement of histamine in the control of the waking state. *Life Sciences*, **53,** 1331-1338.

Monti JM, D'Angelo L, Jantos H, Pazos S (1988) Effects of a-fluoromethylhistidine on sleep and wakefulness in the rat. *Journal of Neural Transmission*, **72,** 141-145.

Monti JM, Jantos H, Leschke C, Elz S, Schunack W (1994) The selective histamine H1-receptor agonist 2-(3-trifluoromethylphenyl)histamine increases waking in the rat. *European Neuropsychopharmacology*, **4,** 459-462.

Monti JM, Jantos H, Ponzoni A, Monti D (1996) Sleep and waking during acute histamine H3 agonist BP 2.94 or H3 antagonist carboperamide (MR 16155) administration in rats. *Neuropsychopharmacology*, **15,** 31-35.

Morgan JI, Curran T (1991) Stimulus-transcription coupling in the nervous system: Involvement of the inducible proto-oncogenes *fos* and *jun*. *Annual Review of Neuroscience*, **14,** 421-51.

Morin LP, Goodless-Sanchez N, Smale L, Moore RY (1994) Projections of the suprachiasmatic nuclei, subparaventricular zone and retrochiasmatic area in the golden hamster. *Neuroscience*, **61,** 391-410.

Noto T, Hashimoto H, Doi Y, Nakajima T, Kato N (1983) Biorhythm of arginine-vasopressin in the paraventricular, supraoptic, and suprachiasmatic nuclei of rats. *Peptides*, **4,** 875-878.

Nuñez A (1996) Unit activity of rat basal forebrain neurons: Relationship to cortical activity. *Neuroscience*, **72,** 757-766.

Nunez AA, Bult A, McElhinny TL, Smale L (in press) Daily rhythms of Fos expression in hypothalamic targets of the suprachiasmatic nucleus in diurnal and nocturnal rodents. *Journal of Biological Rhythms*.

Ogawa Y, Kawamura H (1988) Increase of multiple unit activity during slow wave sleep in the cat preoptic area. *Brain Research Bulletin*, **20,** 897-902.

Oishi R, Itoh Y, Nishibori M, Saehi K (1987) Feeding-related circadian variation in *tele*-methylhistamine levels of mouse and rat brains. *Journal of Neurochemistry*, **49,** 541-547.

Orr E, Quay WB (1975a) Hypothalamic 24-hour rhythms in histamine, histidine decarboxylase and histamine-*N*-methyltransferase. *Endocrinology*, **96,** 941-945.

Orr EL, Quay WB (1975b) The effects of castration on histamine levels and 24-hour rhythm in the male rat hypothalamus. *Endocrinology*, **97,** 481-484.

Otake K, Ruggiero DA (1995) Monoamines and nitric oxide are employed by afferents engaged in midline thalamic regulation. *The Journal of Neuroscience*, **15,** 1891-1911.

Otake K, Ruggiero DA, Nakamura Y (1995) Adrenergic innervation of forebrain neurons that project to the paraventricular thalamic nucleus in the rat. *Brain Research*, **697,** 17-26.

Panula P, Pirvola U, Auvinen S, Airaksinen MS (1989) Histamine-immunoreactive nerve fibers in the rat brain. *Neuroscience*, **3,** 585-610.

Paré D, Smith Y, Parent A, Steriade M (1989) Neuronal activity of identified posterior hypothalamic neurons projecting to the brainstem peribrachial area of the cat. *Neuroscience Letters*, **107,** 145-150.

Paxinos G, Watson C (1997) *The Rat Brain in Stereotaxic Coordinates.* San Diego: Academic Press.

Peng Z-C, Grassi-Zucconi G, Bentivoglio M (1995) Fos-related protein expression in the midline paraventricular nucleus of the rat thalamus: Basal oscillation and relationship with limbic efferents. *Experimental Brain Research*, **104,** 21-29.

Pennartz CMA, Groenewegen HJ, Lopez de Silva FH (1994) The nucleus accumbens as a complex of functionally distinct

neuronal ensembles: An integration of behavioural, electrophysiological and anatomical data. *Progress in Neurobiology*, **42,** 719-761.

Philippu A, Prast H (1991) Patterns of histamine release in the brain. *Agents and Actions*, **33,** 124-125.

Phillipson OT, Bohn MC (1994) C1-3 adrenergic medullary neurones project to the paraventricular thalamic nucleus in the rat. *Neuroscience Letters*, **176,** 67-70.

Rea MA (1992) Different population of cells in the suprachiasmatic nuclei express c-*fos* in association with light0induced phase delays and advances of the free-running activity rhythms in hamsters. *Brain Research*, **579,** 107-112.

Reppert SM, Schwartz WJ, Uhl GR (1987) Arginine vasopressin: A novel peptide rhythm in cerbrospinal fluid. *TINS*, **10,** 76-80.

Roberts WW, Robinson TCL (1969) Relaxation and sleep induced by warming of preoptic region and anterior hypothalamus in cats. *Experimental Neurology*, **25,** 282-294.

Robinson BW, Mishkin M (1968) Alimentary responses to forebrain stimulation in monkeys. *Experimental Brain Research*, **4,** 330-366.

Romijn HR, Sluiter AA, Pool CW, Wortel J, Buijs RM (1996) Differences in colocalization between Fos and PHI, GRP, VIP and VP in neurons of the rat suprachiasmatic nucleus during the phase delay versus phase advance period of the night. *The Journal of Comparative Neurology*, **372,** 1-8.

Ropert N, Steriade M (1981) Input-output organization of midbrain reticular core. *Journal of Neurophysiology*, **46,** 17-31.

Rose S, Novak CM, Mahoney MM, Nunez AA, Smale L (1999) Fos expression within vasopressin-containing neurons in the suprachiasmatic nucleus of diurnal rodents compared to nocturnal rodents. *Journal of Biological Rhythms*, **14,** 37-46.

Rusak B, Meijer JH, Harrington ME (1989) Hamster circadian rhythms are phase-shifted by electrical stimulation of the geniculo-hypothalamic tract. *Brain Research*, **493,** 283-291.

Sagar SM, Sharp FR, Curran T (1988) Expression of c-*fos* protein in brain: Metabolic mapping at the cellular level. *Science*, **240,** 1328-1331.

Sallanon M, Denoyer M, Kitahama K, Aubert C, Gay N, Jouvet M (1989) Long-lasting insomnia induced by preoptic neuron lesions and its transient reversal by muscimol injection into the posterior hypothalamus in the cat. *Neuroscience*, **32,** 669-683.

Sato T, Kawamura H (1984a) Circadian rhythms in multiple unit activity inside and outside the suprachiasmatic nucleus in the diurnal chipmunk (*Eutamais sibiricus*). *Neuroscience Research*, **1,** 45-52.

Sato T, Kawamura H (1984b) Effects of bilateral suprachiasmatic nucleus lesions on the circadian rhythms in a diurnal rodent, the Siberian chipmunk (*Eutamias sibiticus*). *Journal of Comparative Physiology A*, **155,** 745-752.

Schilling J, Nurnberger F (1998) Dynamic changes in the immunoreactivity of neuropeptide systems of the suprachiasmatic nuclei in golden hamsters during the sleep-wake cycle. *Cell Tissue Research*, **294,** 233-241.

Schonrock B, Büsselberg D, Haas HL (1991) Properties of tuberomammillary histamine neurones and their response to galanin. *Agents and Actions*, **33,** 35-37.

Schwartz J-C, Arrang J-M, Garbarg M, Pollard H, Ruat M (1991) Histaminergic transmission in the mammalian brain. *Physiological Reviews*, **71,** 1-51.

Schwartz WJ, Davidsen LC, Smith CB (1980) *In vivo* metabolic activity of a putative circadian oscillator, the rat suprachiasmatic nucleus. *The Journal of Comparative Neurology*, **189,** 157-167.

Schwartz WJ, Reppert SM, Egan SM, Moore-Ede MC (1983) In vivo metabolic activity of the suprachiasmatic nuclei: A comparative study. *Brain Research*, **274,** 184-187.

Schwartz WJ, Takeuchi J, Shannon W, Davis EW, Aronin N (1994) Temporal regulation of light-induced Fos and Fos-like protein expression in the ventrolateral subdivision of the rat suprachiasmatic nucleus. *Neuroscience,* ***58,*** 573-583.

Senba E, Matsunaga K, Tohyama M, Noguchi K (1993) Stress-induced *c-fos* expression in the rat brain: Activation mechanism of sympathetic pathway. *Brain Research Bulletin,* **31,** 329-344.

Sherin JE, Elmquist JK, Torrealba F, Saper CB (1998) Innervation of histaminergic tuberomammillary neurons by GABAergic and galaninergic neurons in the ventrolateral preopic nucleus of the rat. *The Journal of Neuroscience,* **18,** 4701-4721.

Sherin JE, Shiromani PJ, McCarley RW, Saper CB (1996) Activation of ventrolateral preoptic neurons during sleep. *Science,* **271,** 216-219.

Shoham S, Teitelbaum P (1982) Subcortical waking and sleep during lateral hypothalamic "somnolence" in rats. *Physiology & Behavior,* **28,** 323-333.

Silver R, LeSauter J, Tresco PA, Lehman MN (1996) A diffusible coupling signal from the transplanted suprachiasmatic nucleus controlling circadian rhythms. *Nature,* **382,** 810-813.

Speh JC, Moore RY (1992) Retinal afferents as demonstrated with unconjugated cholera toxin. In: *Society for Neuroscience,* Volume 18. Anaheim, CA: Society for Neuroscience, pp. 876.

Stephan FK, Berkley KJ, Moss RL (1981) Efferent connections of the rat suprachiasmatic nucleus. *Neuroscience,* **6,** 2625-2641.

Stephan FK, Nunez AA (1977) Elimination of circadian rhythms in drinking, activity, sleep, and brain temperature by isolation of the suprachiasmatic nuclei. *Behavioral Biology,* **20,** 1-18.

Steriade M, Glenn LL (1982) Neocortical and caudate projections of intralaminar thalamic neurons and their synaptic excitation from midbrain reticular core. *Journal of Neurophysiology,* **48,** 352-371.

Steriade M, Oakson G, Ropert N (1982a) Firing rates and patterns of midbrain reticular neurons during steady and transitional states of the sleep-waking cycle. *Experimental Brain Research*, **46,** 37-51.

Steriade M, Parent A, Ropert N, Kitsikis A (1982b) Zona incerta and lateral hypothalamic afferents to the midbrain reticular core of cat - an HRP and electrophysiological study. *Brain Research*, **238,** 13-28.

Sterman MB, Clemente CD (1962a) Forebrain inhibitory mechanisms: Cortical synchronization induced by basal forebrain stimulation. *Experimental Neurology*, **6,** 91-102.

Sterman MB, Clemente CD (1962b) Forebrain inhibitory mechanisms: Sleep patterns induced by basal forebrain stimulation in the behaving cat. *Experimental Neurology*, **6,** 103-117.

Stevens DR, Kuramasu A, Haas HL (1999) GABA-B-receptor-mediated control of GABAergic inhibition in rat histamine neurons *in vitro*. *European Journal of Neuroscience*, **11,** 1148-1154.

Strogatz SH (1987) Circadian pacemaker interferes with sleep onset at specific times each day: Role in insomnia. *American Journal of Physiology*, **253,** R172-R178.

Su H-S, Bentivoglio M (1990) Thalamic midline cell populations projecting to the nucleus accumbens, amygdala, and hippocampus in the rat. *The Journal of Comparative Neurology*, **297,** 582-593.

Szymusiak R, Iriye T, McGinty D (1989) Sleep-waking discharge of neurons in the posterior lateral hypothalamic area of rats. *Brain Research Bulletin*, **23,** 111-120.

Szymusiak R, McGinty D (1986a) Sleep suppression following kainic acid-induced lesions of the basal forebrain. *Experimental Neurology*, **94,** 598-614.

Szymusiak R, McGinty D (1986b) Sleep-related neuronal discharge in the basal forebrain of cats. *Brain Research*, **370,** 82-92

Szymusiak R, McGinty D (1989) Effects of basal forebrain stimulation on the waking discharge of neurons in the midbrain reticular formation of cats. *Brain Research*, **498,** 355-359.

Szymusiak R, Satinoff E (1984) Ambient temperature-dependence of sleep disturbances produced by basal forebrain damage in rats. *Brain Research Bulletin*, **12,** 295-305.

Takada M, Campbell KJ, Moriizumi T, Hattori T (1990) On the origin of the dopaminergic innervation of the paraventricular thalamic nucleus. *Neuroscience Letters*, **115,** 33-36.

Tobler I, Borbely AA, Groos G (1983) The effect of sleep deprivation on sleep in rats with suprachiasmatic nucleus lesions. *Neuroscience Letters*, **42,** 49-54.

Trachsel L, Edgar DM, Seidel WF, Heller HC, Dement WC (1992) Sleep homeostasis in suprachiasmatic nuclei-lesioned rats: Effects of sleep deprivation and triazolam administration. *Brain Research*, **589,** 253-261.

Trachsel L, Tobler I, Borbely AA (1986) Sleep regulation in rats: effects of sleep deprivation, light, and circadian phase. *American Journal of Physiology*, **251,** R1037-R1044.

Trojanowski JQ, Gonatas JO, Gonatas NK (1981) Conjugates of horseradish peroxidase (HRP) with cholera toxin and wheat germ agglutinin are superior to free HRP as orthogradely transported markers. *Brain Research*, **223,** 381-385.

Uhl GR, Reppert SM (1986) Suprachiasmatic nucleus vasopressin messenger RNA: Circadian variation in normal and Brattleboro rats. *Science*, **323,** 390-393.

Wada H, Watanabe T, Yamatodani A, Maeyama K, Itoi N, Cacabelos R *et al.* (1985) Physiological functions of histamine in the brain. In: *Frontiers in Histamine Research*, Volume 51. Edited by C. R. Ganellin and J.-C. Schwartz. Oxford: Pergamon Press, pp. 225-235.

Wan X-CS, Trojanowski JQ, Gonatas JO (1982) Cholera toxin and wheat germ agglutinin conjugates as neuroanatomical probes: Their

uptake and clearance, transganglionic and retrograde transport and sensitivity. *Brain Research*, **243,** 215-224.

Watts AG, Swanson LW (1987) Efferent projections of the suprachiasmatic nucleus: II. Studies using retrograde transport of fluorescent dyes and simultaneous peptide immunohistochemistry in the rat. *The Journal of Comparative Neurology*, **258,** 230-252.

Watts AG, Swanson LW, Sanchez-Watts G (1987) Efferent projections of the suprachiasmatic nucleus: I. Studies using anterograde transport of *Phaseolus vulgaris* leucoagglutinin in the rat. *The Journal of Comparative Neurology*, **258,** 204-229.

Wexler DB, Moore-Ede MC (1985) Circadian sleep-wake cycle organization in squirrel monkeys. *American Journal of Physiology*, **248,** R353-R362.

Wright CI, Groenewegen HJ (1995) Patterns of convergence and segregation in the medial nucleus accumbens of the rat: Relationships of prefrontal cortical, midline thalamic, and basal amygdaloid afferents. *The Journal of Comparative Neurology*, **361,** 383-403.